#### Translational research from an Australasian perspective

George J. Dias

Department of Anatomy, University of Otago, New Zealand

Research performed in tertiary educational institutions has historically concentrated on the improvement of knowledge. This has been gradually changing over recent years where there is a movement for "translational research". Lately the research-funding environment has also been encouraging the enhancement of entrepreneurship with strong connections with the commercial sector. Universities have been setting up mechanisms to enable this change to become enterprising. This has led to the establishment of commercialisation and technology transfer offices that assist in protecting intellectual property arising from research and finding industry partners to commercialise this knowledge. Another function of these offices is to educate the academics as to the needs of the industry, identify and establish relationships with relavent industry partners, assist in securing traditional and non-traditional research funding, and finally support the pathway to commercialisation. In commercialisation, research discoveries are converted into products and services, generally via licensing or start-up ventures.

### Current status on research and development for biomedical application of biodegradable metals in Japan

A. Yamamoto

Research Center for Fnctional Materials, National Institute for Materials Research, Namiki 1-1, Tsukuba, Japan

First attempt of biomedical application of magnesium alloys in Japan was a cardiovascular stent by the group of Osaka University, Aoki, and AngesMG in 2005. However, the attempt was failed due to the lack of knowledge of Mg corrosion; application of noble metal insert into a Mg alloy tube for laser cutting of stent strut resulted in contamination of noble metal onto strut surface. This contamination of noble metal induced deteriorating corrosion of the Mg alloy stent at the implantation site in a rabbit artery. This negative result in the early stage of the development was interpreted as a large risk accompanying to the biomedical application of Mg alloys; therefore it suppressed the research and development of biomedical application of Mg alloy in Japan.

Several years later, Japan stent technology (JSTec) started the development of Mg alloy stent as a next project following to the development of new drug eluting stent made by cobalt-chromium alloy. Their attempt was forced to stop by the failure of first-in-man test of the new drug eluting stent<sup>3)</sup>. Their challenge on Mg alloy stent and related technologies were taken over by Japan medical device technology (JMDT). However, evaluation guidelines for biodegradable stents were publicized in 2016 under the supervision of Ministry of Health, Labour and Welfare and Ministry of Economy, Trade and Industry.

Recent success of Magmaris® by Biotronik indicates the risk in the development of Mg alloy implants can be acceptable, which collects Japanese companies and researchers' interest in this topic. Prof. Kawamura at Kumamoto University started a new project of developing a new magnesium alloy with long-period stacking ordered (LPSO) structure suitable for biodegradable stent application.

Orthopaedic/dental application of magnesium alloys is mainly carried out by the basic researches in universities due to their smaller market. In Tohoku University, the application of amorphous magnesium alloys as a bone prosthetic material is under investigatio. By the group of Tokyo Medical and Dental University and Olympus Corp., WE43 (Elektron SynerMag®) screws with/without anodization were implanted to the tibia of beagle

dogs. After 4 weeks of implantation, gas cavity formation and following bone absorption was observed for non-treated WE43 screws. Beside the degradation rare of Mg alloy implants, gas cavity formation depends on the implantation site of animals and humans. For the success of Mg alloy implants for bone tissue application, it is important to understand the biological factors influencing gas cavity formation and to establish an estimating method of gas cavity formation by Mg alloy implants.

In other fields, biodegradable clips for the closure of blood vessel and/or tubular organs were developed at Kobe University and forwarded to Dream Fastener Inc. Biodegradable airway stents and staplers stents are under the investigation by the group of AIST and Nagoya University<sup>11)</sup>.

### Cardiovascular stent and other applications in translation in China

Ke Yang

Institute of Metal Research, Chinese Academy of Science, China

Biodegradable magnesium alloys have been studied for more than 10 years in China, and one of the application targets was cardiovascular stent. There are at least three groups in China working on biodegradable magnesium alloy stents with support from companies. However great challenges still exist for reaching to the final target, from both the technological issues and the approval of CFDA. Other applications such as fixation of bone flap, stapler nail, etc., will also be briefly introduced.

### Current status and outlook on the clinical translation of biodegradable metals in South Korea

H-S Han<sup>1</sup>, H-C Jung<sup>2</sup>, Y-C Kim<sup>3</sup>, H-K Seok<sup>3\*</sup>

<sup>1</sup> <u>Nuffield Department of Orthopaedics, Rheumatology and Musculoskeletal Sciences</u>, University of Oxford, Oxford, U.K. <sup>2</sup> <u>R&D Division</u>, U&i Corporation, Uijeongbu, South Korea <sup>3</sup> <u>Center for Biomaterials</u>, Korea Institute of Science and Technology, Seoul, South Korea

INTRODUCTION: The concept of bone replacement has been dominant in the development of metallic implants and the biodegradable metals with the potential to stimulate bone formation have recently captured the attention of scientists. Among these metals, magnesium alloy is an attractive biodegradable material with unique set of properties. The corrosion of magnesium is accompanied by hydrogen evolution and a local increase in pH, which impose constraints on many potential biomedical applications. We have overcome these limitations and created a road map to the next generation of metallic biodegradable implant materials with the addition of completely biocompatible elements.

**METHODS:** Along with the addition of Ca, which is a biocompatible element that plays major in bone formation and remodeling, excellent material properties were achieved through the in-house built special mechanical extrusion machine. The state of the art method to synchronize the corrosion potentials of two constituent phases (Mg + Mg2Ca) with the selective doping of Zn into Mg2Ca was developed to control the corrosion rate. Furthermore, mechanical extrusion broke the connectivity of the Mg2Ca phases, which prevented continuous corrosion and the formation of a galvanic circuit that caused severe corrosion of the Mg-Ca alloy. Animal studies confirmed the large reduction in hydrogen evolution and revealed good tissue compatibility with increased bone deposition around the newly developed Mg alloy implants. Newly developed set of K-RESOMET implants have the mechanical strength, ability to stimulate bone growth and controlled slow degradation rate to be considered as an ideal candidate for biodegradable implant applications.

**RESULTS:** With all the extensive in vivo experience using developed magnesium alloy material over the past 5 years, we were able to receive an approval from Korea Food and Drug Administration (KFDA) for the first human clinical trial of orthopedic biodegradable metallic implant devices in Korea. Working closely with major hospitals in Korea, we have performed several hundreds of cases of small bone fixation screws in

the past two years and have received approval for sale in Korea.



Fig. 1: Developed prototypes of the K-RESOMET implants.

**DISCUSSION & CONCLUSIONS:** Working closely with the professionals from across the globe, these new materials are being tested and designed specifically for the application in clinical settings. The synergy provided from the top medical science researchers will allow the safe and precise deployment of new generation of biodegradable implant material in clinical field.

**ACKNOWLEDGEMENTS:** This research was supported by Korea Ministry of Health and Welfare (2M34410) and TRC Project (2V05400).

### The clinical translation of biodegradable JDBM Mg alloy for bone implants: Current status and the road ahead

G. Yuan

Shanghai Jiao Tong University, China

In recent years, biodegradable magnesium alloys emerge as a new class of biomaterials for medical devices. Deploying biodegradable magnesiumbased materials not only avoids a second surgery to remove bone implant but also circumvents the long-term foreign body response of permanent bone implants. However, these materials are often subjected to an uncontrollable degradation and rapid structural failure due to a localized and too rapid corrosion process. The patented Mg-Nd-Zn-Zr-based alloy (JDBM) has been developed in Shanghai Jiao Tong University. China in 2010. The alloy exhibits lower biodegradation rate and homogeneous nanophasic degradation pattern as compared to other biodegradable Mg alloys. The in vitro cytotoxicity tests using various types of cells indicate excellent biocompatibility of JDBM. The in vivo long-term assessment via implantation of JDBM screws in different animal models have also been performed. The results confirmed the uniform degradation mode in vivo. excellent biocompatibility and high mechanical properties. Although the fundamental research on JDBM has made great progress in material innovation and preclinical testing. The bottleneck is their translation from research to clinical trial. The clinical trial license is very difficult to be achieved in China, especially for the novel and innovative biodegradable Mg-based biomaterials. In the past several years, our group devote ourselves to the clinical translation of JDBM. The lecture will introduce the route map toward the clinical applications of bone implants, including the establishment of the company group, determination of the business mode, funding raise, and related animal experiments what we have done for applying the clinical trial license.

### A primer on the design and mechanical testing of orthopaedic fixation devices in translational medicine

B. Nowak

Department of Mechanical Engineering, University of Canterbury, New Zealand

State-of-the-art engineering approaches and advances orthopaedic materials offer in sophisticated design tools and a wide variety of biocompatible materials that can be potentially applied at the design stage of interface fixation devices. Moreover. various manufacturing techniques are now available (e.g. 3D printing of titanium) that have greatly increased possibilities. Consequently, the increased options in design also have led to greater complexity and functionality of interface devices (e.g. press fit screws, expandable screws and smart devices containing shape memory alloys).

Internet fixation devices have become the gold standard in the orthopaedic treatment of both trauma and degenerative diseases. However, the aseptic loosening of implants at the bone-implant interface is still a problem and requires improvements in interface fixation devices. Despite advances, optimally designed fixation devices are difficult to achieve due to bone being a complex, non-linear and non-uniform material that may alter its mechanical properties due to various clinical factors (e.g. osteoporosis). Additionally, the structure of bone undergoes constant changes (e.g. remodelling and bone formation) that leads to changeable mechanical properties of bone.

In this work, we attempt to present what has been learnt from orthopaedic implant device industry and how might this be best applied to the bench-tobedside translation of biodegradable metals? Biodegradable metals when compared to standard orthopaedic materials (e.g. titanium, titanium alloys) can offer lower postoperative treatment costs by minimising the number of revision surgeries. The evolution in materials testing will be discussed in terms of improving the design of fixation devices. For example, the use of synthetic bone materials in place in cadaveric testing is becoming more popular for assessing the mechanical performance of devices. Standardized testing procedures such as screw pull-up tests are being replaced by customized techniques mimicking the loadings in vivo that act on the interface fixation devices. In short, the medical device market still seeks an interface fixation device with an optimal design that leads to improved mechanical performance of the boneimplant interface and reduced patient recovery time, leading to potential new uses of biodegradable metals.

### Nonsense in Science: Impressions from a reviewers everyday life

N Hort<sup>1</sup>, H. Dieringa<sup>1</sup>, F. Feyerabend<sup>1</sup>, P Maier<sup>2</sup>, C. Vogt<sup>3</sup>

<sup>1</sup> Magnesium Innovation Centre, Helmholtz-Zentrum Geesthacht, Geesthacht, Germany
<sup>2</sup> University of Applied Sciences Stralsund, Stralsund, Germany
<sup>3</sup> Institute of Analytical Chemistry, Leibniz University Hannover, Hannover, Germany

**INTRODUCTION:** Publish or perish is the slogan everybody knows. Important findings are summarized in a paper, submitted to a journal and distributed to reviewers. The aim is that your statistics in publishing show that you are competitive: the more publications, the better. But normally reviewers do not accept a paper immediately as it is. They have questions, comments, critical remarks and alterations are necessary or the paper gets rejected. Even if there are comments that do not fit to the content or which are sometimes relevant, the reviewer is right in the first place. And considering reviewers ideas during design of experiments, data evaluation and presentation might improve the chances of acceptance. However, the co-authors of this paper represent more than fifty years of experience in reviewing. We will present examples of things that have to be regarded as no-go, wrong design of experiments, bias, sloppy work etc which should be avoided in a serious paper.

STRUCTURE OF THE DOCUMENT: Introduction and Experimental are two important chapters in reporting research. In the introduction often papers are cited to justify the described research. And often these references are a few decades old. Does this mean that no research has been done since then? No, often this is only a make-believe rather than a true statement. After all, primary sources should be cited.

The experimental section is the heart of most papers. Everything has to be described in the necessary accuracy. But often the important details are missing: "We performed XRD measurements." No start/end angle, no step size/time, no database mentioned which was used to evaluate data. Basically the experimental has to provide a recipe that enables others to repeat the experiment identically in another laboratory. This is also the idea behind "round robin" experiments, which need extensive and accurate planning. Another example is the choice of solutions - e.g. for simulated body fluid (SBF) there is a variety of formulations for different environments available, but this dependence on a specific environment is often disregarded.

**PRESENTATION OF DATA:** Fig. 1 shows an example how perception is influenced by the presentation of data. Fig. 1a seems to show large differences between the five different beams and this is how Excel automatically formats it. But here only a small fraction is presented. If the full scale of the x-axis would be used, the differences would appear much less or even negligible, see Fig. 1b. And as long scatter is not given, the information in this figure is questionable.

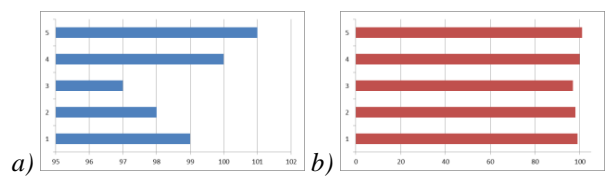


Fig. 1: Arousing wrong perception: a) seems to show significant differences but this is not represented by the same data and a full scalex-axis in b)

Even with statistics wrong perception can be evoked easily. For e.g. a weight change values like  $200\pm20 \mu g$ ,  $170\pm10 \mu g$ ,  $90\pm10 \mu g$ ,  $170\pm30 \mu g$  can be found in literature. An even decadic is given for the mean as well as for the standard deviation (SD). This can happen. But it is like a win in the lottery. From the mathematics calculating the SD it is almost impossible to have no digits. This can only be achieved by rounding. Measured values are often not even decadic numbers. Therefore it is also unlikely to have even decadic mean values. But if e.g. a weight change is measured in mg, rounded to the full number and then given in µg, decadic values can be reached. But still the SD would be a value with decimal places. However, this pretends a non-existing accuracy and should be regarded as data manipulation.

**SELECTION OF RESULTS:** In papers dealing with alloy development the authors often prepare numerous alloys. When it comes to results, a selection of presented data is often made. So far this is ok. But in most cases only selected data are shown and it is not clear why these data have been selected. This needs a proper explanation for the readers, and of course firstly for the reviewer.

### **Casting: theory and reality**

N. Hort<sup>1</sup>, B. Wiese<sup>1</sup>, F. Witte<sup>2</sup>, P. Maier<sup>3</sup>

<sup>1</sup> Helmholtz-Zentrum Geesthacht, Geesthacht, Germany. <sup>2</sup> Charité, Berlin, Germany. <sup>3</sup> University of Applied Sciences Stralsund, Stralsund, Germany.

**INTRODUCTION:** In most cases, melting and casting are the first steps to produce components or feedstock material from metals and alloys for a certain application. This sounds easy and in principle, it is. However, certain aspects do not allow a full reproducibility to 100 %, segregations occur, heat transfer can vary and homogeneity of microstructure cannot be guaranteed etc. 1

**MELTING:** In theory, melting metals and alloys is easy: put them into a mould, heat it up until everything is molten! In practice, the way materials are molten depends on the material itself. E.g., Mg and its alloys need melt protection. Therefore, protective gases, fluxes or a melting environment has to used to avoid ignition and burning.

In practice, metals and alloys may react with tools, with constituents from the environment and burn-off/pick-up may occur due to interactions of the base material and alloying elements with crucibles, tools, fluxes, environment etc. For Mg alloys containing rare earth metals (RE) it is known that around 10 wt.% of RE disappear due to burn-off3. In addition, gases may be picked up by the melt it-self and there is also evidence that larger amounts of H2 can be incorporated into the melt and the solid.

Finally yet importantly, Fe based materials are used in the production of pure Mg, processing of alloys and as tools in cast shops. Therefore, the pick-up of Fe during melt processing is an issue and the amount of Fe in a casting depends on the time of melt exposure to Fe moulds and tools. Even if there are solutions to bind the Fe in intermetallic phases this is often not applicable due to defined compositions and the impact that intermetallic particles have on properties.

**SOLIDIFICATION:** Phase diagrams (which represent the equilibrium and often not reality) can be used to design alloys as they provide information on the existence of phase with respect to composition and temperature. They also can be used to estimate the amount of segregation and which phases will exist in the final microstructure (=reality). Segregations are an enrichment of alloying elements from the grain boundary towards the grain boundary. Fig. 1a shows an example. The blue colour represents Y and its enrichment as described can be observed. The red colour represents Nd and its intermetallic phases, which form at the eutectic

temperature in the end of solidification and can therefore be found on grain boundaries. These microstructural features have impact on the property profile of the cast material. Additionally dirt, particles and gas are driven by the solidifying material ahead of the solidification front and will concentrate finally in the centre of the casting.

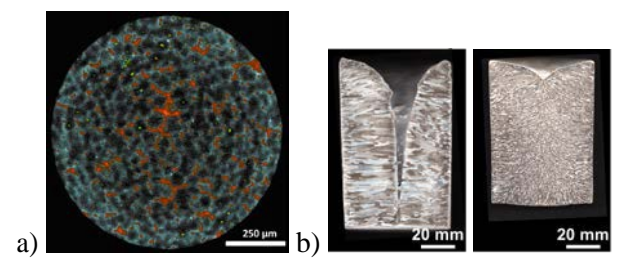


Fig. 1: a) SRµCT, segregations and intermetallic phases in WE43, b) blowholes in a cylindrical casting

During solidification, the materials undergo a phase transition from liquid to solid. This is accompanied with a change in volume as the density of a solid material is higher than that of the liquid: the material shrinks. As long as melt can feed into interstices between growing dendrites, the process works fine. But if feeding is blocked, porosity occurs or blowholes build up in upper part of castings (Fig. 1b). Therefore, casting defects exists and may deteriorate properties.

CAST SHOP TECHNOLOGY: Different cast shop technologies result in different microstructures with respect to the differences in geometries of moulds and accordingly different cooling conditions. In Mg technologies normally protective gases are in use where e.g. air, N<sub>2</sub>, Ar, CO<sub>2</sub> are used as carrier gases together with SF<sub>6</sub> to protect the melt. Fluxes (combinations of fluorides and chlorides) are also in use.

### Synchrotron-diffraction and -tomography in alloy development

D. Tolnai, T. Subroto, R.H. Buzolin, S. Gavras, N.Hort

Magnesium Innovation Center, Helmholtz-Zentrum Geesthacht, Geesthacht, Germany

**INTRODUCTION:** Magnesium alloys possess properties that entitle them as the future material of choice in vital key technologies. Their light weight and excellent specific strength makes them attractive for the transportation and energy sectors. Furthermore their in vivo corrosion properties unequivocally qualify particular Mg alloys to be used as smart materials in the field of biodegradable implant development. applications require a specific property profile, which can be obtained through the optimization of processing and microstructure design. The internal architecture of the phases, their volume fraction and spatial distribution influences the macroscopic thermo-mechanical behaviour of the material. Therefore understanding of the sequence of phaseformation and phase-evolution during solidification is the first step towards microstructure engineering of these alloys.

METHODS: The combination of *in situ* synchrotron-diffraction (DESY) and –tomography (PSI) was utilized to study the solidification of Mg5Nd5Zn. The molten samples were cooled until reaching the fully solid state, using different cooling rates; 50 K/min and 100 K/min for the diffraction experiments and 5 K/min for the tomographic tests, respectively. In the diffraction experiments the Debye-Scherrer patterns were recorded continuously during cooling. The results of both characterisation techniques were used to completely describe the microstructure evolution of the alloy during solidification from a compositional and architectural viewpoint as well.

**RESULTS:** The evolution of the phases during solidification was elucidated by synchrotron diffraction (Fig. 1/a). First □-Mg dendrites solidify at a temperature of 637 °C followed by the Mg<sub>3</sub>(Nd,Zn) phase at 598.°C. The solidification ends with the formation of Mg50Nd8Zn42 at 469 °C. The general trend of solidification was confirmed by DTA measurements; however there is a temperature offset originating by the temperature measurement at the synchrotron experiment. The evolution of the internal architecture of the alloy during solidification could be followed shortly after coherency, which occurs at 537.5 °C, until solidification is fully completed at 500 °C as shown in Fig. 1/b. The interconnectivity of the dendrites is very high through the observation of the solidification, since the proper reconstruction

of the tomographic data becomes possible as the dendrites remain stable in the liquid. The volume fraction of the  $\alpha$ -Mg dendrites increases while the interdendritic liquid fraction decreases as the solidification proceeds. Pores and shrinkage holes can only be detected at the fully solid state as the liquid freezes and the feeding becomes insufficient.

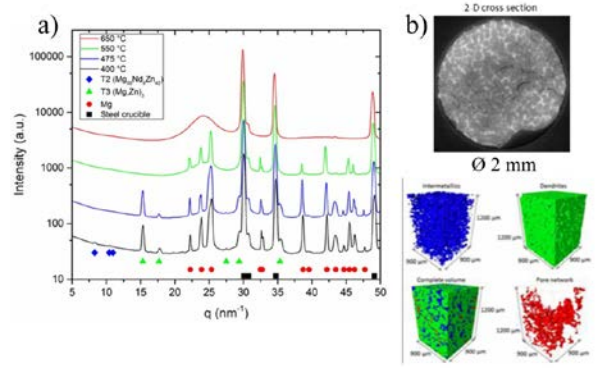


Fig. 1: a) X-ray line profiles, b) 3D structure of the internal phases, acquired during solidification of Mg5Nd5Zn

DISCUSSION & CONCLUSIONS: The *in situ* synchrotron-diffraction and -tomography are uniquely able to assist in solidification studies of multiphase alloys. In the case of Mg5Nd5Zn, the solidification sequence was determined. The phases were identified based on diffraction, complemented by SEM and TEM investigations. The results contradict those of thermodynamic simulations and can be used to re-evaluate the existing databases. The tomographic results have shown the structural changes and how the internal architecture of the material develops during solidification.

**ACKNOWLEDGEMENTS:** The authors acknowledge the Deutsche Forschungsgemeinschaft for the funding in the framework of the proposals TO817/4-1 and ME4487/1-1.

### Additive manufacturing of magnesium alloys

L Jauer<sup>1</sup>, M Kimm<sup>2</sup>, W Meiners<sup>1</sup>, RJ Santos Batista<sup>1</sup>, N Labude<sup>3</sup>, M Bienert<sup>3</sup>, S Neuß<sup>3,4</sup>, B Lethaus<sup>5</sup>, M Müther<sup>6</sup>, A Kopp<sup>6</sup>, C Ptock<sup>6</sup>, JH Schleifenbaum<sup>1,7</sup>

<sup>1</sup> Fraunhofer Institute for Laser Technology ILT, Aachen, Germany <sup>2</sup> Chair for Laser Technology, RWTH Aachen University, Germany <sup>3</sup> Institute of Pathology, RWTH Aachen University, Germany <sup>4</sup> Helmholtz Institute for Biomedical Engineering - Biointerface Group, RWTH Aachen University, Germany <sup>5</sup> Department of Cranio-Maxillofacial Surgery, RWTH Aachen University, Germany <sup>6</sup> Meotec, Germany <sup>7</sup> Digital Additive Production, RWTH Aachen University, Germany

INTRODUCTION: Additive Manufacturing (AM) also known as 3D printing enable economic manufacture of individualized and complex parts. Therefore, AM is widely used for manufacturing patient-specific bone and joint prostheses and implants with designed interconnected porosity. Especially the latter is of great interest when it comes to manufacturing biodegradable implants. Scaffold-like structures allow for significant reduction of bulk material, full vascularization of the implant and the ingrowth of newly formed bone.

**METHODS:** The AM technology used in this study is laser-powder bed fusion (L-PBF). L-PBF uses focused laser radiation to melt thin layers of powder material according to a sliced CAD model and builds complex parts layer by layer. To demonstrate the feasibility to build complex shaped individualized implants a patient specific implant with interconnected porosity is designed. Therefore, a mandible defect is virtually created from a human skull CAD model. For integrating interconnected porosity, an octahedral unit cell structure is created in the Software Rhino. Using the Rhino plugins Grasshopper and Intralattice the unit cell is duplicated, a slight gradient by means of varying strut and pore size is applied. The structure and shape of the octahedral unit cells is then adapted to the defect surface contours via cell deformation. Therefore trimming of the lattice structure could be avoided, resulting in a homogeneous boundary contour. Furthermore the surface of the lattice struts and nodes are smoothed. To build this demonstrator WE43 powder from MSE (Clausthal, Germany) is used which is sieved to a particle size of 25-63 µm before L-PBF processing. The L-PBF machine setup is the same as in L. Jauer et. al. (2015). After build-up the demonstrator is cleaned from sintered powder by glass bead blasting. For further surface smoothing it is then etched for 30 s with 10% nitric acid and rinsed with ethanol.

**RESULTS:** Fig. 1 shows the CAD model of the demonstrator with interconnected porosity (left) and the demonstrator after L-PBF and post-processing (right). The CAD model features a total porosity of approx. 80% by design.



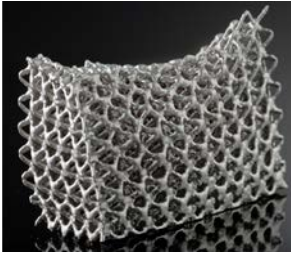


Fig. 1: demonstrator for a patient specific implant with interconnected porosity for a mandible defect with a length of approx. 34 mm; left: CAD model; right: photograph of AM demonstrator made from biodegradable WE43 magnesium alloy after post-processing

**DISCUSSION & CONCLUSIONS:** This study shows the feasibility to design and build complex shaped individualized implants with interconnected pore structure out of biodegradable magnesium alloys by AM with high detail resolution and dimensional accuracy. Future work will focus on a surface treatment by plasma electrolytic oxidation to compensate for the high initial corrosion caused by the large total surface area. Afterwards, the corrosion performance and the mechanical strength of scaffolds depending on strut and pore size will be assessed.

**ACKNOWLEDGEMENTS:** This work was funded by the European Regional Development Fund (ERDF).

### Customizing the microstructure in three-dimensional Mg structures

R Marek<sup>1</sup>, F Wohlfender<sup>1,2</sup>, B Wiese<sup>3</sup>, M de Wild<sup>1</sup>

<sup>1</sup> <u>University of Applied Sciences Northwestern Switzerland</u>, School of Life Sciences, Institute for Medical and Analytical Technologies, Muttenz, CH. <sup>2</sup> <u>University of Basel</u>, Swiss Nano Institute, Basel, CH. <sup>3</sup> <u>Helmholtz-Zentrum Geesthacht</u>, Zentrum für Material- und Küstenforschung GmbH, DE.

**INTRODUCTION:** 3D printing of degradable Mg implants opens new clinical possibilities. Besides the geometry and the chemistry, the microstructure is an important factor influencing the corrosion rate. It is known for Selective Laser Melting (SLM) that process parameters have an effect on the grain structure. We propose to use SLM for the production of implants with directed degradation by controlling the grain structure.

**METHODS:** A mandible plate (5 x 0.5 x 0.2 cm) and simple cubes (a = 5 mm) were designed with SolidWorks CAD software (Version 13). Two freeform objects were applied from thingiverse.com. A modified SLM system (Realizer 100, MCP Realizer, Germany) with a 100 W fiber laser was used to additively manufacture the three-dimensional objects layerby-layer under a protecting Ar atmosphere. xyhatching strategy of laser trajectories in consecutive layers was applied, see arrows in Fig. 2a. Details can be found in F. Wohlfender et al. (2016). AZ91 powder (SFM SA, Switzerland, particle size  $D_{10}$  39.7 µm,  $D_{50}$  59.0 µm,  $D_{90}$ 92.4 µm) was used as a starting material. The microstructure was metallographically investigated after grinding, polishing and etching with HNO<sub>3</sub>/ethanol for 10 sec using a SEM (TM-3030Plus, Hitachi, Japan) and light microscope (Olympus BX61, Stream Motion 1.8 software). Grain size was determined by quantifying linear intercepts of grain boundaries along 700 µm lines.



Fig. 1: Freeform magnesium AZ91 structures, produced by Selective Laser Melting.

**RESULTS:** Figure 1 shows the produced freeform shapes (left) and the mandible plate (right). Due to its fine design and the low specific weight of Mg, this bone implant weighs only 0.62 g. Four distinct regions were determined in metallographic sections of SLM cubes (Fig. 2a), each consisting of typical grain sizes, see table 1. Interestingly, the

microstructure is influenced by the laser trajectories (heat-affected zone in regions ②, ③ & ④) and the smallest grains are found where the starting laser induces the maximal energy and thus the highest temperature (region ①). A decoration with Mg particles is observed at the boundary. The corrosion of such cubes is heterogeneous and can be attributed to the different grain sizes.

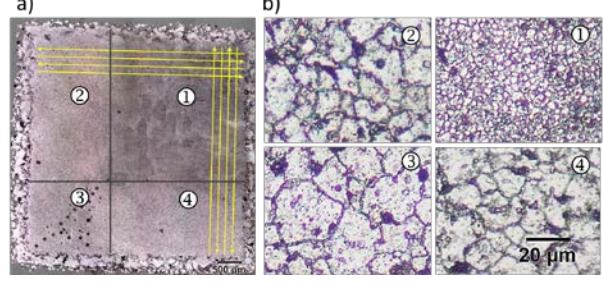


Fig. 2: Light microscopic images of SLM-Mg microsection a) overview incl. laser trajectories, b) details of regions  $\mathbb{O}$  -  $\mathbb{G}$ .

Table 1. Region-dependent grain size.

Region	Average grain size [µm]
1	$3.5 \pm 1.0$
2	$12.0 \pm 0.4$
3	$15.1 \pm 2.4$
4	$9.7 \pm 0.5$

**DISCUSSION & CONCLUSIONS:** SLM allows the fabrication of complex-shaped Mg structures. During the laser process, the solidification rate and thus the grain size and phases can be locally influenced due to different heat extraction. The SLM scanning strategy therefore could be used to locally control mechanical and corrosion properties, e.g. for prospective implants with directed degradation.

**ACKNOWLEDGEMENTS:** This project was supported by the *stiftung***fhnw**.

#### Influence of extrusion parameters on Mg-10Gd

J Harmuth, B Wiese, J Bohlen, T Ebel, R Willumeit-Römer

Helmholtz-Centre Geesthacht (HZG), Germany

**INTRODUCTION:** The application of an implant defines the requirements for a material, e.g. biocompatibility, homogeneous corrosion and mechanical properties. The effects of a variation of extrusion parameters on the microstructure evolution and mechanical properties of Mg-10Gd alloy are presented in this work. The whole process chain is situated in-house at HZG thus enabling precise control of processing parameters.

**METHODS:** The binary Mg-10wt.%Gd alloy was prepared by permanent direct chill casting in a resistance furnace. Pure Mg was molten in the furnace at 710 °C, followed by the addition of pure Gd. The melt was stirred at 250 rpm for 15 min and poured into preheated moulds. After placing the mould in a holding furnace at 650 °C for 2 min the mould was slowly immersed into a water bath for a direct solidification of the ingot.

Ingots were machined to cylinders of 150 mm length and 50 mm diameter and homogenized at 525 °C for 8 h prior to extrusion. Round bars with a diameter of 10 mm were produced by indirect extrusion (ratio 1:25). Ingots were pre-heated to the respective extrusion temperatures for 1 h prior to extrusion. Nine combinations of extrusion parameters were chosen with varied temperature (350, 400, 450 °C) and speed (0.75, 1.50, 3.00 m/min).

Microstructural analysis was carried out on longitudinal sections of the round profiles using optical microscopy. Grain sizes were determined by counting line intersections with grain boundaries on polished surfaces. Vickers hardness was determined with a load of 5 kg and a dwell time of 30 s. Uniaxial tensile testing at room temperature was applied to characterize the mechanical properties of the extruded bars using samples with a diameter of 5 mm and a gauge length of 25 mm. All tests were performed on a universal testing machine at a constant strain rate of  $10^{-3}$  s<sup>-1</sup>.

**RESULTS:** Microstructure evolution is exemplarily shown in Fig.1. An increase in extrusion temperature and/or speed leads to an increase in grain size and a decrease in hardness. Grain size in general is ranging from 5 to 27  $\mu$ m for the given parameter variations.

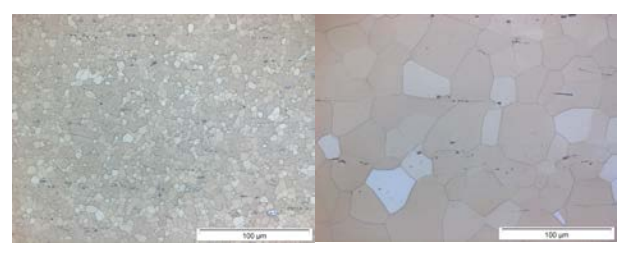
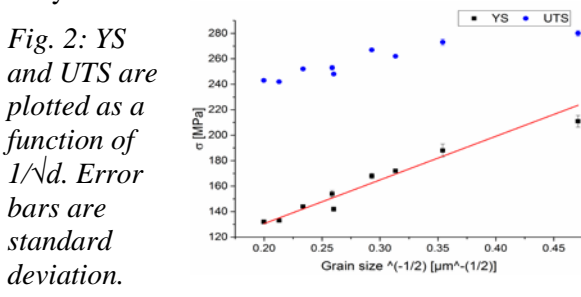


Fig.1: Left: 0.75 m/min @ 350°C, grain size 5  $\mu$ m; right: 3.00 m/min @ 450°C, grain size 27  $\mu$ m.

The grain size strengthening effect is visualized using the Hall-Petch relation (1) where d is the average grain size,  $\sigma$  the yield strength (YS) and k and  $\sigma_0$  are material specific parameters.

$$\sigma = k / \sqrt{d + \sigma_0} \tag{1}$$

The relationship between grain size and YS and ultimate tensile strength (UTS) is presented in Fig. 2. The linear fit in YS is obtained by the method of least squares and represents the form of equation (1). A direct relation between microstructure and mechanical properties can be concluded. The determined k value of  $343 \pm 33$  MPa  $\mu m^{-1/2}$  is comparable to existing studies for Mg-Gd and indirect extruded Mg alloys.



**DISCUSSION & CONCLUSIONS:** Tailoring of mechanical properties depending on extrusion parameters is feasible. Grain size strengthening effect can be confirmed for as extruded Mg-10Gd.

### Post-processing and plasma electrolytic oxidation coating of additive manufactured magnesium scaffolds

M Müther<sup>1</sup>, A Kopp<sup>1</sup>, C Ptock<sup>1</sup>, L Jauer<sup>2</sup>, N Labude<sup>3</sup>, M Bienert<sup>3</sup>, S Neuß-Stein<sup>3</sup>, B Lethaus<sup>4</sup>, JH Schleifenbaum<sup>5</sup>

1 Meotec GmbH & Co. KG, Aachen, Germany 2 Fraunhofer Institute for Laser Technology ILT, Aachen, Germany 3 Institute of Pathology, RWTH Aachen University, Germany 4 Department of Cranio-Maxillofacial Surgery, RWTH Aachen University, Germany 5 Digital Additive Production, RWTH Aachen University, Germany

**INTRODUCTION:** Additive manufacturing (AM) of patient specific implants is a promising field for future bone implants. Especially the production of bio-degradable magnesium implants, enhancing bone ingrowth through a porous structure is aimed at by AM. Using this processing routine, problems of after treatment by means of cleaning as well as controlling the degradation behaviour are still to be solved.

METHODS: The AM technology used in this study is laser-powder bed fusion (L-PBF). L-PBF specimens with strut diameters varying between 300 and 500 µm and pore diameters between 500 and 800 µm are produced using WE43 powder. To avoid contamination by non-biocompatible materials, glass bead blasting of the specimens is excluded from the post-processing routine, which includes the following steps. First ultrasonic cleaning in ethanol is used to remove any lose or slightly sintered powder. Following, a variation of acid etching as well as electrochemical etching is studied for removing of strongly sintered powder particles and surface smoothing. Parameters varied in the process are type of acid, acid concentration, time and if required electric current. Acids used are Nitric, phosphoric and picric. To guarantee even material removal on the outer and inner porous structure, specimens are continuously moved for acid flow. Finally, a plasma electrolytic oxidation (PEO) surface coating, as explained in O. Jung et al. (2015), is added to the specimens for improvement of degradation behaviour as shown in O. Jung et al. (2015). Specimens are contacted through a thread to apply the electric current, when using electrochemical etching and PEO-coating

**RESULTS:** Figure 1 shows the results of post-processing. Removal of sintered powder in the inner structure is achieved and the former CAD contour is approximated by opening all inner pores of the specimen. A PEO-coating is successfully applied, including all inner contours while creating a typical PEO ceramic and smoothening the etched surface.

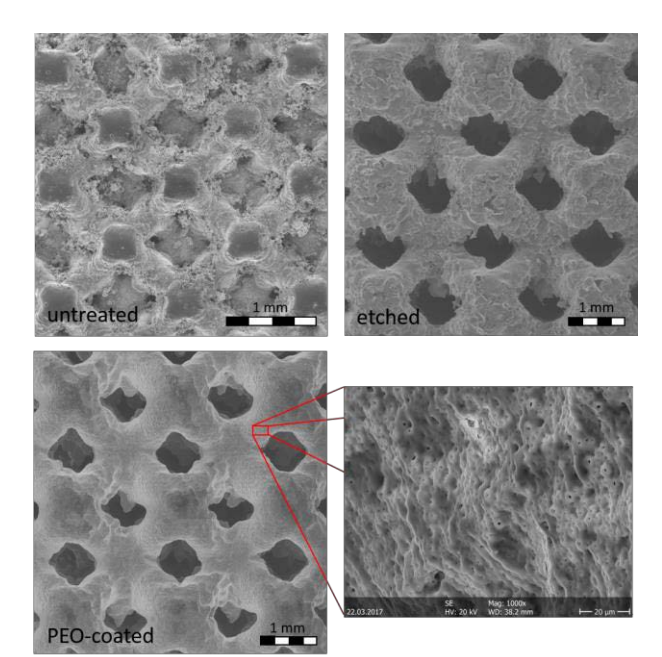


Fig. 1: Images of porous L-PBF -produced specimens without post-processing (1), acid-etched (2) and acid-etched plus PEO-coated (3,4).

**DISCUSSION & CONCLUSIONS:** This study shows the feasibility of post-processing and PEO-coating complex inner contours containing pore diameters of down to 500 μm made from biodegradable magnesium without the use of bioincompatible blast material. Ongoing research will focus on optimizing surface quality, geometrical accuracy and adjusting PEO-surface thickness regarding degradation behaviour.

**ACKNOWLEDGEMENTS:** This work was funded by the European Regional Development Fund (ERDF) and the Ministry of Economy, Energy and Industry of North Rhine-Westphalia.

# Mg as reinforcement of PLA films produced by colloidal techniques for improving biomaterial properties

A. Ferrandez<sup>1,2</sup>, M Lieblich<sup>1</sup>, B.Ferrari<sup>2</sup>, R. Benavente<sup>3</sup>, JL Gonzalez-Carrasco<sup>1,4</sup>

<sup>1</sup> <u>CENIM-CSIC</u>, Spain, <sup>2</sup> <u>ICV-CSIC</u>, Spain, <sup>3</sup> <u>ICTP-CSIC</u>, Spain, <sup>4</sup> <u>CIBER-BBN</u>, Spain

**INTRODUCTION:** Mg used as reinforcement of a polymeric matrix has already shown its ability to improve important biomaterial's properties (Young modulus, creep strength, bioactivity, less biofilm formation). Moreover, degradation of composites occurs without changing physiological pH values and with a slow production of hydrogen due to the protective nature of polylactic acid (PLA). Formerly, PLA/Mg composites were prepared by thermoplastic routes, which have the drawback of degrading the polymer during processing. Colloidal techniques, on the contrary, have the advantage of producing homogeneous blends at room temperature. Further shaping of the biomaterial would require additional processing. In the case of films, if this processing is tape casting the use of high temperatures is again avoided.

**METHODS:** PLA polymer was dissolved in THF and mixed with a colloidal suspension of Mg particles  $< 100 \, \mu m$  stabilized by PEI or CTAB, in proportion of 0 to 50% mass. The tapes were formed and left to dry at room temperature for 24 hours and then at 60 °C for 24 h. Characterization of films was performed by DSC, TGA, SEM, mechanical tests, etc. Degradation in PBS was followed through pH, H<sub>2</sub> release and weight loss.

**RESULTS:** The backscattered electron images of *Figure 1* show, as an example, cross sections of the films prepared with 10 and 50% mass of Mg. It is seen that the polymer covers every magnesium particle and that one side of the film presents more roughness than the other.

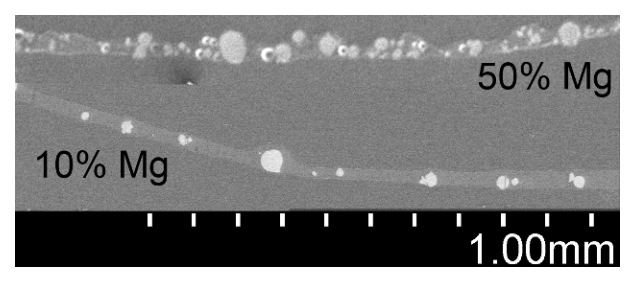


Fig. 1: PLA/Mg composite film cross-sections containing 10 and 50% mass of Mg particles (SEM image).

The TGA results, *Figure 2*, show that no solvent coming from the processing route has been retained

and that the presence of Mg shifts the degradation of PLA to lower temperatures. This is not a problem because the composite matrix does not lose properties until at least 160°C.

Mechanical tests indicate a higher Young modulus of composites with respect to the monolitic polymeric matrix. Hydrogen is released at a slow rate and pH value of the PBS solution is preserved.

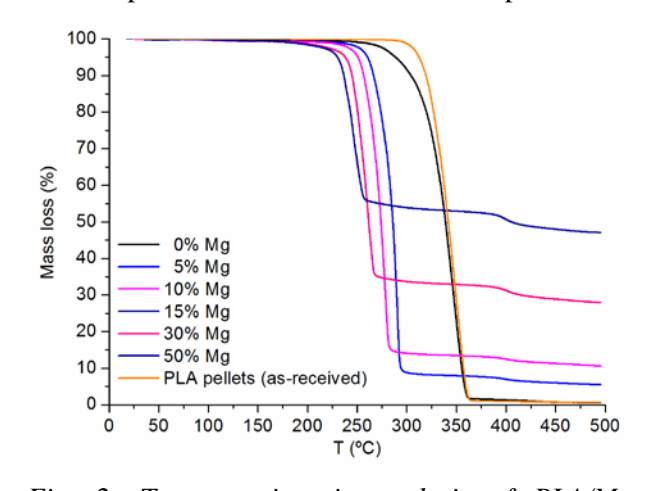


Fig. 2: Termogravimetric analysis of PLA/Mg films containing up to 50% mass of Mg particles.

**DISCUSSION & CONCLUSIONS:** Tape casting results in a successful processing route to obtain sound composite films formed by combinations of PLA and Mg. These films may find applications in the biomedical field for example as wound dressings or grafts.

ACKNOWLEDGEMENTS: MAT2015-63974-C4-1 and MAT2016-79869-C2-1-P (MINECO), MULTIMAT Challenge: S2013/MIT-2862 (CM).

# Manufacturing and Assessment of high strength Mg-Nd-Gd-Zr-Zn alloy implant prototypes and test specimen, using PM (Powder Metallurgy) methods

M. Wolff<sup>1</sup>, M. Luczak<sup>1</sup>, J. G. Schaper<sup>1</sup>, B. Wiese<sup>1</sup>, T. Ebel<sup>1</sup>, R. Willumeit-Römer<sup>1</sup>, T. Klassen<sup>2</sup> 1<u>Helmholtz-Zentrum Geesthacht</u> 2Helmut Schmidt Universität, Hamburg

INTRODUCTION: Current Mg-based biometal research focusses on substitution of low strength biodegradable polymer-based implants (fig. 1) which are at present in clinical usage. These implants are produced using plastic injection moulding technique. The same shaping technique can be applied for production of Mg-based implants by metal injection moulding (MIM) (fig. 2-5). Using a commercial available Mg-alloy powder, suture anchor screw implant prototypes and test specimens showing 161 MPa of ultimate tensile strength (UTS) were manufactured.

**METHODS:** Mg-Nd-Gd-Zr-Zn alloy powder and, for reference, cast material (Magnesium Elektron, UK) was used for this investigation. Test specimen production was done using press and sinter (P+S)technique as well as MIM (Arburg, Germany). Sintering was performed using a hot wall furnace (MUT, Jena, Germany) at 643-646 °C for 2-32 h argon under atmosphere. Additional treatments T4 (545°C, 5h) and T6 (200°C, 20h) were applied on part of the sintered and cast material. Degradation testing were performed in a semi static test setup using DMEM + 10% FBS for a 7 day screening. The microstructure was studied using SEM and EDX (TESCAN) and analySYS pro software. The Archimedes method was used to determine porosity and density.

**RESULTS:** Suture anchor screw prototypes as shown in Fig. 2-5 and tensile test specimens were successfully produced using MIM. The MIM tensile test specimens sintered at 644 °C for 2 h showed UTS of 161±5.5 MPa, YS of 120±11 MPa and elongation at fracture of 3.36±0.7 %. Specimens produced by P+S-technique achieved UTS of 188±4 MPa, YS of 118±6.5 MPa and elongation at fracture of 5±1.2 %. Biodegradation tests disclosed pitting corrosion of the as sintered material but not of the cast reference material. Impurities could not be found by EDX. Sintered specimens obtained a near dense condition showing  $0.74 \pm 0.05$  % residual porosity and 2.7mm/a corrosion rate whereas the reference cast material obtain 0.11 mm/a, only; both in the T4 condition.

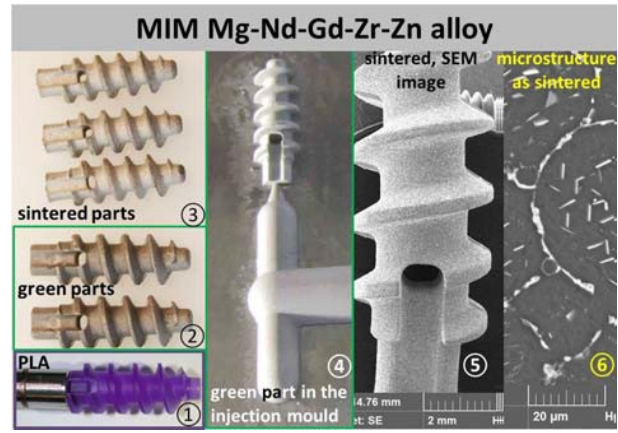


Fig. ①: Suture anchor screw made of PLDLA by injection moulding technique (Courtesy: ConMed). Fig.②-⑤: Suture anchor screw made by MIM of Mg-Nd-Gd-Zr-Zn alloy in green condition (Fig.②) and sintered condition (Fig.③) [consider shrinkage between parts in Fig. 2 & 3]. Fig.④: PLA as well as MIM-Mg parts are made in the same mould.

Fig. (5): SEM image of the as sintered screw. Fig. (6): Microstructure of the as sintered material showing secondary phases onto ancient particle boundaries (roundish) and needle shape secondary phases inside of the particles/grains.

properties of the P+S and MIM processed Mg alloy identify a high strength, ready to use material. The biodegradation tests disclose differences between cast processed material and sintered powder which have to be checked carefully in further experiments to explain and understand the discrepancy. Possible explanations might be impurity pick up during sintering (crucible setup and material) or inhomogeneous secondary phase formation which can act as galvanic couple, changing degradation behaviour.

## Photo-chemical etching as a new tool for fabricating magnesium biodegradable stents

V Shanov<sup>1,2</sup>, T Tiasha<sup>2</sup>, P Kandala<sup>2</sup>, G Zhang<sup>2</sup>, P Salunke<sup>2</sup>, V Chaswal<sup>2</sup>, P Roy-Chaudhury<sup>3</sup>, D Celdran<sup>3</sup>, B Campos<sup>4</sup>, M Schulz<sup>2</sup>, Z Yin<sup>2</sup>, Y Yun<sup>5</sup>, J Wang<sup>5</sup>, Y Koo<sup>5</sup>, W Wagner<sup>6</sup>, X Gu<sup>6</sup>, A D'Amore<sup>6</sup>

Department of BCEE, University of Cincinnati, Cincinnati, OH, USA. Department of MME, University of Cincinnati, Cincinnati, OH, USA. College of Medicine, University of Arizona, Tucson, AZ, USA. College of Medicine, University of Cincinnati, Cincinnati, OH, USA.
 Chemical, Biological and Bioengineering Department, NCAT State University, NC, USA.
 McGowan Institute for Regenerative Medicine, University of Pittsburgh, Pittsburgh, PA, USA

INTRODUCTION: Magnesium is a promising material for medical implants due to its biocompatibility and the ability to resorb in body. Manufacturing stents by laser cutting has become the industrial standard. However, this expensive approach reveals some issues, including surface oxidation, thermal stress, charged dross sticking everywhere, slow material removal even with femtosecond lasers, need of expensive Mg tubing and multiple post-treatment. All this motivated us to employ photo-chemical etching for fabricating of Mg stents and to test them in vitro and in vivo.

**METHODS:** The starting material was rectangular sheet of magnesium alloy AZ31 with thickness of 250 microns, purchased from Goodfellow. The photochemical etching method transfers a pattern of the stent onto the sheet, followed by chemical etching. Finally, etched sheets with desired dimensions are rolled to cylinders and laser welded along the side seam. This inexpensive process does not generate residual stress in the material during processing and no post-treatment of the stent after manufacturing is required. For fabricating helical stents, two-dimensional Mg ribbons with selected dimensions were photo-chemically etched with a desired pattern. The spiral shape was formed by simple winding on a guiding rod which determined the stent diameter. No welding is required for the helical design and the dimensions of the device can be varied.

**RESULTS:** Figure 1 displays pictures of photochemically etched AZ31 stents fabricated in 2 designs: cylindrical and helical. The corrosion properties of the stents have been studied in vitro using static and dynamic (DMEM fluid) flow. The effect of flow shear stress was evaluated and corrosion protective polymer coatings were proposed. The helical stent was successfully tested in a porcine ex vivo model exposed to static and dynamic flow. Balloon expanded helical stents were studied in a homemade flow visualization

system and the obtained initial data suggested a swirling flow caused by the stent. Preliminary in vivo tests of the photo-chemically etched Mg stents have been conducted using a pig model in an arteriovenous fistula environment.

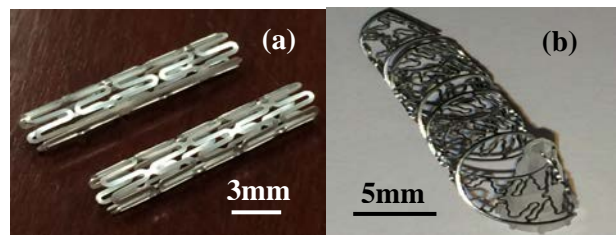


Fig. 1: Pictures of photo-chemically etched AZ31 stents: (a) cylindrical stent; (b) helical stent.

DISCUSSION & CONCLUSIONS: Photochemical etching is a robust approach for fabrication of Mg biodegradable stents, which can lower their price down to about \$100. It overcomes some limitations of the laser cutting approach and allows fabricating stents with any size and pattern. The Mg helical stent reveals a different mode of expansion compared to the cylindrical stent, which allows expanding 2 times beyond its initial diameter and is expected eventually to preserve the spiral laminar blood flow. In vitro and in vivo studies of Mg photo-chemically etched stents provided promising preliminary data for vascular applications of these devices.

**ACKNOWLEDGEMENTS:** This research was funded by NSF through the ERC Grant No. NSF EEC-0812348.

### Preparation and properties of MAO/Zn-modified calcium phosphate coatings on magnesium alloys for orthopedic applications

Bingbing Yan<sup>1</sup>, Lei Chang<sup>1\*</sup>, Jun Wang<sup>1\*</sup>, Liguo Wang<sup>1</sup>, Shijie Zhu<sup>1</sup>, Shaokang Guan<sup>1\*</sup>

<sup>1</sup>School of Materials Science and Engineering, Zhengzhou University, Henan, China

INTRODUCTION: As a degradable metal, magnesium alloys exhibit several advantages, biocompatibility including improving enhancing bone formation in vivo. However, the poor corrosion resistance of magnesium alloys may lead to the implant failure on the fracture site. Therefore, it is necessary to improve the corrosion resistance of magnesium alloys, while maintaining good biocompatibility. In this study, the MAO/Zncalcium phosphate modified coating synthesised on the surface of Mg-Zn-Ca alloys by means of micro-arc oxidation (MAO) technique combined with dual-pulse electrodeposition technique.

METHODS: The bulk material was cut into specimens with the dimension of 25×10×4 mm<sup>3</sup>, followed by polishing and ultrasonic cleaning. MAO technique was first applied to generate a porous base layer with the electrolytic solution of Na<sub>3</sub>PO<sub>4</sub> • 12H<sub>2</sub>O, NaOH and glycerine; and subsequently, a degradable Zn-modified calcium phosphate coating was produced on the top layer by means of the dual-pulse electrodeposition technique. The morphology, elementary composition and phase composition of asdeposited MAO/Zn-modified coatings analysed by SEM, EDX, XRD, FTIR and XPS. The effect of coatings on in vitro degradation behaviours was studied via immersing specimen in simulated body fluid at 37°C. The effect of coatings on in vitro degradation behaviours was studied via immersing specimen in simulated body fluid at 37°C. Electrochemical tests besides hydrogen evolution and weight loss measurement were performed.

**RESULTS:** According to Fig.1(a), it could be MAO/Zn-modified calcium observed that phosphate coatings were composed of long strip shape crystals. The EDX results revealed that the ratio of Ca and Zn to P was to be 1.52:1, indicating the nature of Ca deficiency. Based on the XRD results, coatings mainly contained biodegradable nonstoichiometric parascholzite, as shown in Potentiodynamic Fig.1(b). polarization electrochemical impedance spectroscopy results suggested that coatings exhibited better corrosion resistance than uncoated specimens as well as MAO coatings, as shown in Fig.2. In addition, coatings

were highly hydrophilic and the thickness was around  $16\mu m$ , which would be favourable for initial cell adhesion and spreading of osteoblast.

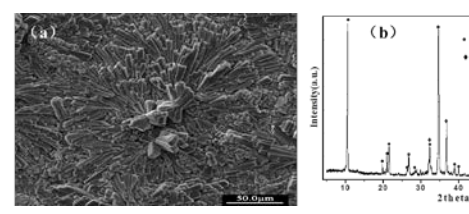


Fig. 1: The surface morphologies of the Znmodified calcium phosphate coating (a) and the XRD pattern of coating (b).

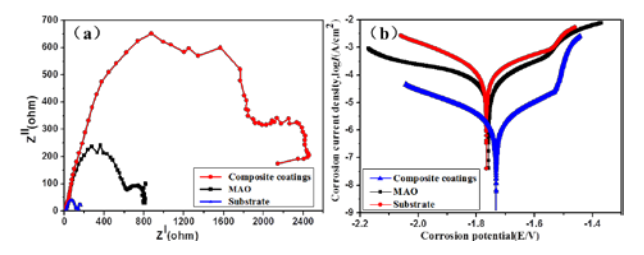


Fig. 2: Potentiodynamic polarization curves (a), EIS spectra (b) of samples tested in SBF.

**DISCUSSION & CONCLUSIONS:** In the present study, a MAO/Zn-modified calcium phosphate coating was successfully synthesised on Mg-Zn-Ca alloys with improved in vitro corrosion resistance. The effects of composite coatings on corrosion resistance and biocompatibility will be further investigated by long-term immersion tests as well as in vitro cell culture study, of which the results shall shed a light in the research of magnesium-based orthopaedic implants.

ACKNOWLEDGEMENTS: Authors are grateful for the financial support of the National Key Technology R&D Program of China (No. 2015AA033603), National Natural Science Foundation of China (No.51601169), and Major Science and Technology Project of Henan Province (No. 141100310900).

## Corrosion of heat-treated and MAO coated Mg-1.2Zn-0.5Ca-0.5Mn: A candidate alloy for bioresorbable skeletal fixation

D Dean<sup>1</sup>, H Ibrahim<sup>2</sup>, AD Klarner<sup>3</sup>, AA Luo<sup>3</sup>, I Valerio<sup>1</sup>, R Skoracki<sup>1</sup>, M Miller<sup>1</sup>, M Elahinia<sup>2</sup>

<sup>1</sup>Department of Plastic Surgery, <sup>3</sup>Department of Materials Science and Engineering, The Ohio State University, Columbus, OH USA. <sup>2</sup>Department of Mechanical, Industrial and Manufacturing Engineering, University of Toledo, Toledo, OH USA.

INTRODUCTION: Standard of care skeletal fixation devices use Ti-6Al-4V (Surgical Grade 5 titanium). In most cases these devices are left permanently in the body and may then alter the bone's loading pattern causing concentrations or stress shielding. The former can lead to device failure and the latter can lead to bone resorption due to lack of loading. Other problems that can occur over the long term with permanent fixation hardware are formation, infection, and/or irritation of adjacent soft tissues. We have determined that the alloy Mg-1.2Zn-0.5Ca-0.5Mn biocompatible (wt.%) is likely to reliably resorb following the healing of a reconstructed skeletal segment if it is formed with sufficient strength. We hypothesize that heat treatment can be used to bring about the strength that is needed and that Micro Arc Oxidation (MAO) coating may significantly delay corrosion. Our goal is to delay corrosion that would weaken the fixation hardware until 4-6 months.

**METHODS:** We heat-treated Mg-1.2Zn-0.5Ca-0.5Mn cylindrical coupons to achieve sufficient mechanical strength and corrosion resistance. The Mg alloy coupons were solution-treated at 510 °C for 3 hours then quenched in water. The solution-treated samples were then artificially-aged in an oil bath for 3 hours. Next, these coupons were coated with a composite ceramic layer composed of Mg oxide (MgO) and entrapped calcium phosphate nano particles of β–TCP and HA (1:1 ratio) via MAO. Finally, the specimens were placed in simulated body fluid (SBF) solution for 3, 7, 14, 21, and 28 days (N=3 at each time point).

**RESULTS:** MAO-coated coupons show pitting and pores (Fig. 1), a common observation following MAO coating with  $\beta$ -TCP and HA nano particles. It is assumed that these particles were entrapped in the sintered structure forming a composite coating. The immersion test results (Fig. 2) show that the MAO-coated coupons corroded more slowly than heat-treated coupons which themselves had a lower corrosion rate than the ascast coupons.

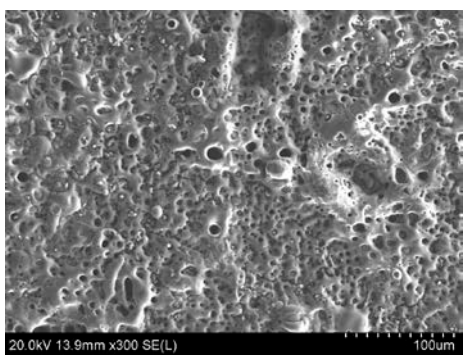


Fig. 1: Surface morphology of the MAO-coated Mg alloy showing pitting and microporosity.

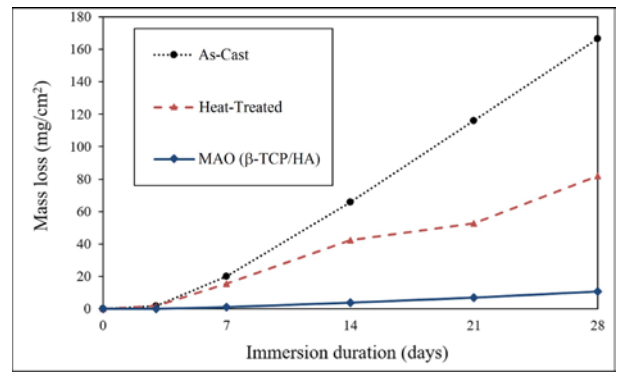


Fig. 2: Mass loss obtained after immersion of the as-cast, heat-treated, and MAO-coated Mg coupons in SBF solution at 7.4 pH and 37 °C for 3, 7, 14, 21 and 28 days (N=3 at each time point).

**DISCUSSION & CONCLUSIONS:** Heat treatment strengthened and reduced corrosion of the Mg alloy coupons. Ceramic coating produced via MAO resulted in further slowing of corrosion. The use of heat treatment followed by MAO coating may be beneficial for the fabrication of Mg-1.2Zn-0.5Ca-0.5Mn skeletal fixation devices with predictable resorption rates.

**ACKNOWLEDGEMENTS:** This work has been partially supported by Third Frontier (State of Ohio) TVSF grant #15-791.

### Surface modification by glass ceramic coatings of magnesium alloys: surface and electrochemical performance in vitro

S Omar<sup>1</sup>, E Martinez Campos<sup>2</sup>, Y Castro<sup>3</sup>, A Duran<sup>3</sup>, J Ballarre<sup>1</sup>, S Cere<sup>1</sup>

<sup>1</sup> INTEMA, University of Mar del Plata, Argentina. <sup>2</sup> Instituto de Estudios Biofuncionales, Universidad Complutense de Madrid, Madrid, Spain. <sup>3</sup> Instituto de Cerámica y Vidrio (C.S.I.C.), Campus de Cantoblanco, 28049 Madrid, Spain.

**INTRODUCTION:** Surface modification of metallic materials is the approach for developing functional properties assure to biocompatibility, enhance tissue acceptance, and/ or inhibit corrosion rate. In this work, surface modification of two commercial magnesium alloys is presented. The alloys were coated with 58S glass coating by sol-gel, with organic precursors such as silicon and phosphate alcoxydes and calcium lactate with the aim of inducing new bone formation by the bioactive glass together with the deceleration of the corrosion rate and hence the hydrogen evolution.

**METHODS:** AZ31B (Al 3%, Zn 1%, Mn 0.2%) and AZ91D (Al 9%, Zn 1%, Fe 0.005%, Mn 0.33%, Ni 0.002%) were used as substrates. Plane samples were polished until 2500 grit SiC paper and cleaned prior to coat. 58S glass (60 mol% SiO<sub>2</sub>, 36 mol% CaO, 4 mol% P<sub>2</sub>O<sub>5</sub>) was prepared by sol-gel method using tetramethyl orthosilicate, methyltriethoxysilane, triethyl phosphite calcium L-lactate hydrate as precursors, HNO<sub>3</sub> 1N as catalyser, ethylene glycol to improve the alkoxide condensation degree and methanol to dissolve the calcium lactate. Micro-Raman assays were performed to analyze deposits composition (Invia Reflex Confocal, Renishaw RM 2000, UK) with a 785 nm wavelength laser. Electrochemical assays were performed to determine degree of degradation of the coating and the Mg alloy. Hank Buffered Salt Solution (HBSS) at 37 °C was used as electrolyte. Coated samples were seeded with C2C12-GFP mouse autofluorescent pre-myoblast cell line. Cells were incubated at 37 °C with 5% CO<sub>2</sub>. C2C12-GFP cells were seeded on the materials with a density of  $3 \times 10^4$  cells per cm<sup>2</sup>. This cell line was evaluated by fluorescence microscopy (FITC filter  $\lambda ex/\lambda em = 490/525$  nm) at 72 and 168 h to determine cell adhesion and growing on the material.

**RESULTS:** coatings thickness were  $1.2 \pm 0.1$  and  $0.9 \pm 0.2$  µm for AZ31 and AZ91 respectively. Polarization curves and EIS results show that the coatings applied onto AZ31 although are thicker than the ones applied on AZ91 present more defects since the total impedance of the former is

lower than for the AZ91 and also the corrosion density current for coated AZ91 is lower after immersion (Figure 1). This fact is observed in the very early stages of immersion and also after 17 days of immersion. By Raman spectroscopy, magnesium hydroxide, Mg-Al hydrocalcites (Mg and Al hydroxy-carbonate), apatite and hydroxylcarbonate apatite can be detected on the surface after 72 h immersion<sup>1</sup>. Cell culture show that AZ31 alloys both blank and coated showed preliminary good adhesion but then a possible cytotoxic effect is observed. Both AZ91 blank and coated samples showed good cytocompatibility, cell adhesion and proliferation.

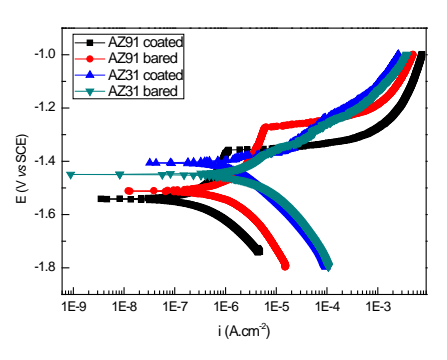


Fig. 1: polarization curves for coated samples after 17 days of immersion in HBSS at 37 °C.

DISCUSSION & CONCLUSIONS: Coatings applied onto the Mg alloys shown to be biocompatible in vitro (in the sense of apatite like deposit) but cytocompatibility only proceed for the samples using AZ91 as substrate. This is probably associated to the higher corrosion rate that the AZ31 experiments both coated and bare and the modification of the local alkalinisation that the media experiments.

**ACKNOWLEDGEMENTS** The support from the CONICET, PIP 752; and Universidad Nacional de Mar del Plata (Project 15G/449) is acknowledged.

### Magnetron sputtered Fe-FeMn composites for biodegradable Implants

T Jurgeleit<sup>1</sup>, LK Jessen<sup>1</sup>, E Quandt<sup>1</sup>, C Zamponi<sup>1</sup>

<sup>1</sup>Chair for Inorganic Functional Materials, Institute for Materials Science, Faculty of Engineering, University of Kiel, Germany

**INTRODUCTION:** The goal for Fe based biodegradable materials is either to accelerate the degradation rate or enhance the strength in comparison to pure Fe. One of the most promising is alloying element is Mn. FeMn alloys with high Mn contents were found to show promising mechanical properties, furthermore, the FeMn  $\gamma$ -phase shows antiferromagnetic behaviour which is beneficial with respect to possible MRI examinations. In previous work it was shown that magnetron sputtering is a suitable method to produce micro patterned, freestanding Fe based devices, showing a high mechanical strength due to their characteristic microstructure.

**METHODS:** Structured freestanding Fe-FeMn multilayer composites of different layer sequences were fabricated via magnetron sputtering and UVlithography. The foils were annealed under reducing atmosphere in order to adjust their microstructure. The microstructure was investigated by STEM, SEM, EDX and XRD analysis. For the determination of the mechanical properties uniaxial tensile tests were performed. Electrochemical polarization in buffered Hanks solution at 37 °C was used to measure the corrosion rates. The magnetic properties were measured by a vibrating sample magnetometer.

**RESULTS:** The as-deposited foils showed clearly separated layers (Fig.1) consisting of  $\alpha$ -Fe and  $\gamma$ -FeMn phases. While the γ phase showed a very fine- and isometric-grained crystalline structure, the α-Fe phase showed a more columnar grain growth. Thus by varying the layer thicknesses it was possible to tailor the initial grain sizes of the α-Fe phase. Depending on the annealing parameters the layer structures were partially kept higher intact. At temperatures, homogeneous microstructure and an increased amount of γ-FeMn phase were observed. The annealed foils showed a high tensile strength (845.2 MPa-1117.2 MPa) and maximum strain values (15 %-21 %) that are considered to be sufficient for the envisaged applications. Depending on the layer and annealing parameters it was even possible to tailor the yield strength (667.8 MPa-837.65 MPa). The corrosion rates laid in-between pure Fe and FeMn30. The foils showed a significant smaller magnetisation than pure Fe.

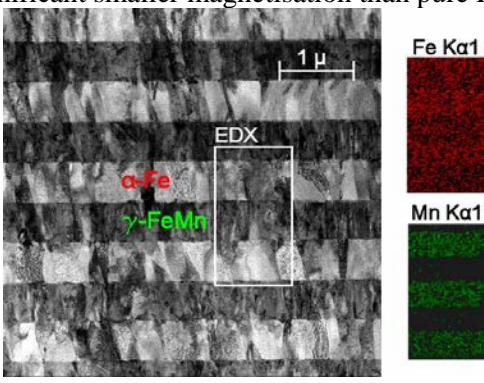


Fig. 1: STEM image and elemental mapping of an as deposited Fe-FeMn multilayer composite film.

**DISCUSSION & CONCLUSIONS:** It was shown that the method is suitable to fabricate FeMn based foils showing a strength by a factor of three higher than the sputtered pure Fe and even higher than sputtered FeMn30. The values can be attributed to the initially fine grained structure and a hardening due to α-Fe precipitates. Even the higher corrosion rate can be explained by the formation of these precipitates as they can act as local element and hence accelerate the degradation. Due to the stabilisation of the antiferromagnetic y phase during annealing a decrease in the magnetization is observed. The presented method offers a large number of process variables to tailor the microstructure. Therefore, it is a promising approach to optimize the material properties with respect to the intended use as biodegradable implants.

**ACKNOWLEDGEMENTS:** Funding via DFG is gratefully acknowledged.

### Effect of cold rolling on the degradation behaviour of a Fe-16Mn-0.7C twinning induced plasticity steel

Sergio Loffredo<sup>1,2,3</sup>, Carlo Paternoster<sup>1</sup>, Nicolas Giguère<sup>3</sup>, Maurizio Vedani<sup>2</sup>, Diego Mantovani<sup>1</sup>

<sup>1</sup><u>Lab. Biomaterials and Bioengineering</u>, CRC-I, Dept. Min-Met-Mat Engineering & CHU de

Québec Research Center, Laval University, Quebec City, Canada <sup>2</sup><u>Dept. of Mechanical</u>

Engineering, Politecnico di Milano, Italy <sup>3</sup>Quebec Metallurgy Center, Trois-Rivières, Canada

INTRODUCTION: Biodegradable metals for cardiovascular stents require a combination of strength, ductility and degradation behaviour which is difficult to achieve. A magnesium-based cardiovascular scaffold obtained the CE mark in 2016, since clinical trials showed that the device degraded effectively and safely in 12 months. However, this implant is significantly bigger than its non-degradable counterparts. Iron-based alloys provide superior mechanical properties, but their degradation proceeds too slowly. Twinning induced plasticity (TWIP) steels possess performances similar to those of Co-Cr alloys, while they are susceptible to corrosion in Cl-rich environments. Since such steels change their microstructure when plastically deformed, it is important to evaluate whether this variable can modify their degradation behaviour.

METHODS: Fe-16Mn-0.7C alloy was melted in an induction melting furnace with a liquid argon protection system starting from pure Fe (> 99.9%), pure Mn (> 99.7%) and pure graphite. Solution heat treatment was performed at 1100°C for 12 hours in an inert atmosphere furnace, followed by Ar-assisted high pressure quenching. 12.5 mm thick billets were hot rolled to reduce their thickness. Cold rolling was performed to induce different degrees of plastic deformation inside the material. The chosen reduction ratios were 10% (named CR10), 25% (CR25) and 50% (CR50). Annealing at 800°C for 15 minutes followed by water quenching (CRA) was performed on some sheets in order to have a fully recrystallized which served as reference Annealed pure iron was used as control.

Static immersion tests were carried out to evaluate the degradation rate (DR) of the alloy in the aforementioned conditions. Hanks' modified salt solution was used as corrosion medium (pH = 7.4  $\pm$  0.1), while all tests were carried out in a cell culture incubator (T = 37  $\pm$  1°C, 5% CO<sub>2</sub> atmosphere) to better simulate the arterial environment. Test duration was set at 14 days.

**RESULTS:** Deformation at different reduction ratios modified the microstructure of the alloys.

The number and density of twins increased with increasing deformation. When annealing was performed, full recrystallization was achieved, having equiaxed grains with no twins present inside them. Static immersion tests showed that the degradation rate of the alloy is at least 2 times higher with respect to that of pure iron. DR was seen to increase with increasing amount of induced plastic deformation. Moreover, the annealed state showed the highest DR among the four studied states.

**DISCUSSION & CONCLUSIONS:** Fe-16Mn-0.7C alloy was produced by casting and deformed by cold rolling. Static immersion tests showed an increase in DR compared with pure iron. DR increased with increasing deformation, while the annealed state shows the highest DR. This may be due to the different microstructures of the alloy originating from their different thermo-mechanical treatment history.

**ACKNOWLEDGEMENTS:** This research was funded by the Natural Sciences and Engineering Research Council of Canada.

## Ethylene oxide and gamma irradiation: applicable sterilization techniques for Mg alloys for biomedical applications

S Johnston <sup>1</sup>, MS Dargusch <sup>1</sup>, A Atrens <sup>1</sup>

<sup>1</sup> The University of Queensland, Materials Engineering, School of Mechanical and Mining Engineering, Brisbane, Qld 4072, Australia

INTRODUCTION: Sterilization of medical devices and instruments is a vital part of infection control during surgery. However, sterilization techniques are often quite harsh, and can negatively impact material properties<sup>1</sup>. It is essential to select an appropriate sterilization technique, which does not negatively influence key material properties. For magnesium (Mg) implants, corrosion resistance is arguably the most significant material property, and is almost certainly the most sensitive. To safeguard the success of Mg medical devices, applicable sterilization techniques must be determined.

**METHODS:** Three sterilized conditions were evaluated using five magnesium alloys. The five magnesium alloys were: HP-Mg, AZ91, ZE41, XHP-Mg and ZX00. The three sterilized conditions were: sterilized with ethylene oxide (EO), sterilized with gamma irradiation (GI) and a non-sterilized control group.

Corrosion assessment was via an *in vitro* immersion test conducted in CO<sub>2</sub>-bicarbonate buffered Hanks' solution maintained at ~37 °C and a pH of ~7.4. Corrosion was measured via mass loss and hydrogen evolution. Two-way analysis of variance (ANOVA) with replication was used to determine the significance of any results. Statistical significance was defined as a probability of  $p \le 0.05$ ).

**RESULTS:** Figure 1 presents the corrosion rates measured by mass loss  $(P_m)$  for the five alloys, and the three sterilized conditions. The sterilization condition caused little difference in the corrosion rate for each alloy. This was supported by the results of the ANVOA, presented in table 1. There was a significant difference between the corrosion rates of the materials (as was expected). However, there was no significant difference between the sterilized groups. There was also no interaction between the two variables (sterilized condition and material), indicating that this result was consistent for the five alloys. These results were also consistent for the hydrogen evolution data.

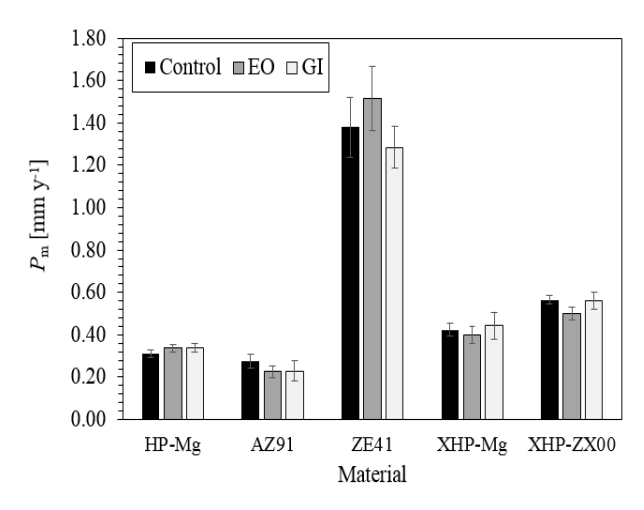


Fig. 1: Corrosion rates from mass loss  $(P_m)$  of the three sterilization groups and the five alloys.

*Table 1. Two-way ANOVA (with replication)* 

Corrosion Rate	Source of Variation	Degrees of Freedom	p value
	Material	4	<< 0.01
$P_{ m m}$	Sterilization Condition	2	0.85
	Interaction (Material x Sterilization)	8	0.55

**DISCUSSION & CONCLUSIONS:** Sterilization with either EO or GI did not significantly influence the corrosion of a range of Mg alloys. This result supports the use of either of these techniques for use on Mg medical implants and devices.

**ACKNOWLEDGEMENTS:** The authors thank Cherilyn Hoe (UQ), Peter Uggowitzer (ETH, Zurich), Martina Cihova (ETH, Zurich) & Jörg Löffler (ETH, Zurich).

# Effect of Equal Channel Angular Pressing (ECAP) on microstructure, mechanical properties and degradation of a Mg-Ag alloy

J Horky<sup>1</sup>, K Bryła<sup>2</sup>, M Krystian<sup>1</sup>, L Lityńska-Dobrzyńska<sup>3</sup>, B Mingler<sup>1</sup>

1 <u>AIT Austrian Institute of Technology GmbH</u>, Center for Health & Bioresources, Biomedical Systems, Wr. Neustadt, AT. 2 <u>Institute of Technology</u>, Pedagogical University of Cracow, Kraków, PL. 3 <u>Institute of Metallurgy and Material Science</u>, Polish Academy of Sciences, Kraków, PL.

**INTRODUCTION:** Mg alloys for biodegradable medical implants have to combine a high strength with a proper degradation rate. The strength can be increased by alloying as well as by grain refinement. This study investigates a Mg-Ag alloy with antibacterial properties due to the Ag content and explores the effect of grain refinement by ECAP on strength and degradation.

METHODS: Mg-4wt% Ag was investigated in ascast condition as well as after a homogenization heat treatment at 440°C for 16h followed by water quenching. ECAP was done on homogenized samples using a special double-ECAP tool with three channels and two points of intersection with different angles. The first pass was conducted at 370°C, followed by a second one at 330°C. Mechanical properties were investigated by compression tests. Microstructural examinations were performed by light microscopy as well as by scanning and transmission electron microscopy. Degradation was studied over a period of three weeks by measuring the hydrogen evolution of samples immersed in simulated body fluid (SBF27 from [3] with TRIS-HCl buffer) at 36°C. The medium was changed every week.

**RESULTS:** The microstructure of as-cast Mg-4Ag consists of large grains (350 µm average diameter) and a dendritic structure with micron-sized Ag-rich precipitates. The homogenization heat treatment leads to a dissolution of the dendritic structure and the formation of a solid solution without changing the grain size. Thereby, the compressive strength increases by 31% (from 219 MPa to 288 MPa), whereas the compressive yield strength remains nearly constant at about 50 MPa. ECAP processing leads to a strong reduction of grain size (25 µm after 1 pass and 15 µm after 2 passes) and a further increase in ultimate compressive strength (5% and 13% after 1 and 2 passes, respectively) and an even larger increase in compressive yield strength (13% after 1 pass and 37% after 2 passes). Concerning the degradation behaviour (see figure 1 & table 1), as-cast Mg-4Ag shows a very high degradation rate and the sample completely dissolved before the end of the test.

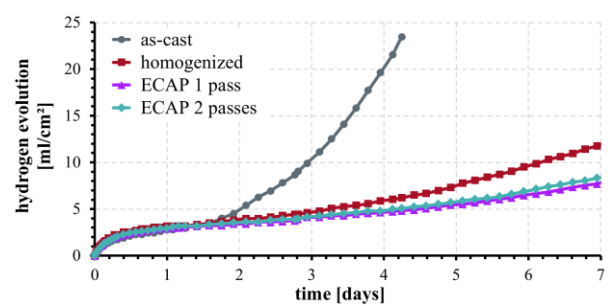


Fig. 1: H2 evolution of Mg-4Ag during the first week of degradation in SBF.

The homogenization drastically decreases the degradation rate and subsequent ECAP processing has no significant effect on the degradation properties.

Table 1. Degradation rate of Mg-4Ag after different periods of immersion in SBF. The values are obtained by interpolation and derivation of the H2 evolution data.

Degradation rate [mm/year]				
time	as-cast	homog-	ECAP	ECAP
[days]		enized	1 pass	2
				passes
3	16.5	2.8	1.8	1.9
10		3.6	3.0	2.8
17		5.1	5.0	4.5

**DISCUSSION & CONCLUSIONS:** Homogenization and dissolution of Ag-rich precipitates of as-cast Mg-4Ag dramatically decrease the degradation rate due to reduction of micro-galvanic coupling. Moreover, the mechanical properties are increased. Subsequent ECAP processing further increases the compressive strength by means of grain boundary strengthening while the desirable low degradation rate remains.

**ACKNOWLEDGEMENTS:** Financial support by the FFG funded RSA '*HighPerformBioMat*' is acknowledged.

### Multi-parameter instability of Zn-Mg alloy wires

AJ Griebel<sup>1</sup>, JE Schaffer<sup>1</sup>, C Galligan,<sup>1,2</sup> PK Bowen,<sup>2</sup> J Goldman,<sup>3</sup> and JW Drelich<sup>2</sup>

<sup>1</sup> Research & Development, Fort Wayne Metals, Fort Wayne, IN, USA. <sup>2</sup>Department of Materials Science and Engineering, <sup>3</sup>Department of Biomedical Engineering, Michigan Technological University, Houghton, MI 49931, USA

INTRODUCTION: Zinc-based alloys have generated significant interest as absorbable metals for medical applications in recent years. The most attractive property is the corrosion rate, which appear ideal for vascular stents. However, the strength of pure Zn is prohibitively low. The addition of alloying elements such as Mg have been shown to increase its strength. Zn-Mg microalloy wires do have appropriate degradation and improved strength (data to be submitted), but instabilities complicate their use.

**METHODS:** Three low-alloyed Zn-Mg binary alloys were prepared by vacuum induction melting. Compositions were measured by ICP-OES to be (in wt%) Zn-0.08Mg, Zn-0.005Mg, and Zn-0.002Mg. Ingots were machined to Ø50 mm and extruded at 150°C to Ø13 mm. Extruded rods were cold drawn to a diameter of 0.25 mm. 99.99% Zn wire was produced as a reference.

To assess effects of shelf-aging, wires were tensile tested at room temperature (RT) at various time points (0, 1, 10 days after drawing). Additionally, wires were tested at three strain rates (.000167s<sup>-1</sup>, .0033s<sup>-1</sup>, and .0167s<sup>-1</sup>) 10 days after drawing. Finally, select wires were tensile tested at both RT (22°C) and body temperature (37°C) to inform *in vivo* behaviour.

**RESULTS:** Zn08Mg and Zn005Mg show significant room-temperature aging (Fig. 1), while Zn002Mg and 99.99Zn do not.

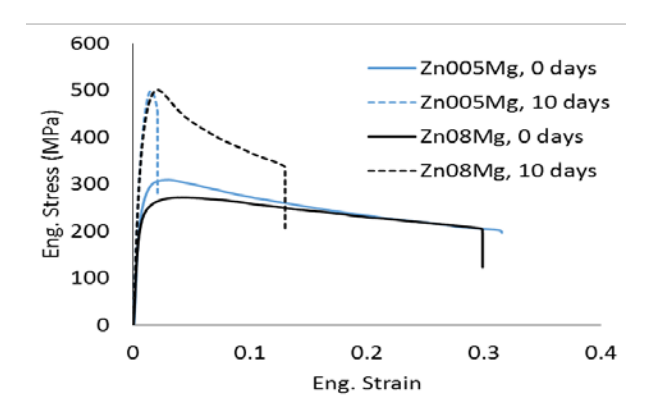


Fig. 1: Zn005Mg and Zn08Mg wires show significant property change after 10 days at RT.

All wires showed a high dependence on strain rate (Zn08Mg stored for 10 days shown in Fig. 2). Testing at 37°C showed reduced strength but higher elongation than RT (Fig. 3).

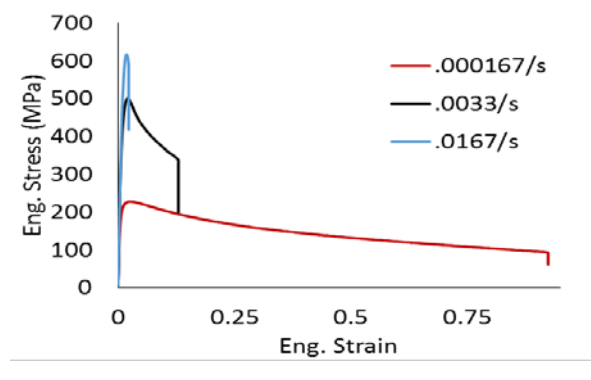


Fig. 2: Zn08Mg wire tensile properties show a high dependency on strain rate.

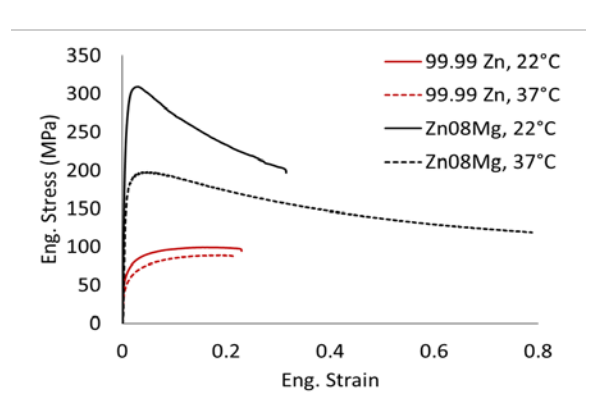


Fig. 3: Testing wires at 37°C (dashed lines) vs 22°C (solid) results in significant property shifts.

**DISCUSSION & CONCLUSIONS:** While Zn-Mg alloys offer unique corrosion and mechanical properties, significant work remains to address the room-temperature instability. For all Zn-based wire, device-appropriate strain rates and test temperatures must be used.

**ACKNOWLEDGEMENTS:** U.S. NIH-NHLBI (#1R15HL129199-01) and U.S. NIH-NIBIB (#5R21 EB 019118-02).

#### **Evaluation of different fatigue criteria for biomedical devices**

F Berti<sup>1</sup>, D Allegretti<sup>1</sup>, G Pennati<sup>1</sup>, F Migliavacca<sup>1</sup>, L Petrini<sup>2</sup>

<sup>1</sup>Department of Chemistry, Materials and Chemical Engineering, Politecnico of Milano (Italy) <sup>2</sup>Department of Civil and Environmental Engineering, Politecnico di Milano (Italy)

**INTRODUCTION:** Vascular stents are nowadays gold standard for the treatment of atherosclerotic diseases. They are commonly made of stainless steel, cobalt-chrome and more recently nickel-titanium allovs (NiTi) while with the advent of regenerative medicine, absorbable magnesium stents are being investigated as an alternative for permanent ones. FDA normative requires among others fatigue tests for a device approval, to guarantee an appropriate performance once deployed. Stent fatigue analysis need some considerations: the device is first crimped on a catheter, introducing plastic strains altering the overall response once implanted, and the pulsatile load introduces a multiaxial state of stress due to the complex geometry. Finite element analyses are commonly used for the study of fatigue behaviour of stents. Damage parameters commonly used in the fatigue analysis are first principal stress/strain, valid for proportional loadings. However, criteria based on critical plane could give results that are more reliable for these non-proportional loadings. This study proposes a coupled experimentalnumerical methodology able to evaluate fatigue performance of NiTi stents in different loading conditions. Hence, a validation of the correct prediction has been obtained through a comparison with experimental tests. This could be extended to other material stents, such as magnesium based ones.

**METHODS:** NiTi mechanical properties (static and fatigue) were experimentally studied through tensile tests on multi dog-bone shape wires specimens. Stents with different geometry and made with the same material were subjected to axial fatigue tests. The stent FE model was created and used to simulate the durability tests thanks to the implicit solver ANSYS Mechanical APDL. Fatigue criteria for non-proportional solicitations based on critical plane were selected and used to predict fatigue results.

**RESULTS:** The FE results for every case have been analysed in terms mean and amplitude equivalent strain in the most critical zone and risk of fracture through a constant life diagram. An example of loading condition for one stent is

showed in Figure 1 in terms of Brown-Miller and Fatemi-Socie fatigue criteria.

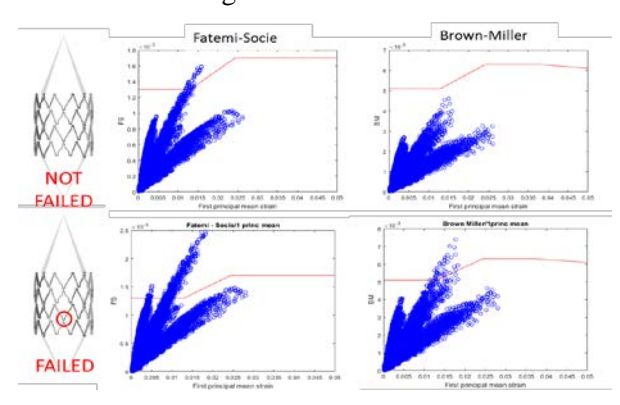


Fig.1 Results of fatigue criteria for one stent

DISCUSSION & CONCLUSIONS: The comparison highlights that all the fatigue criteria give the same critical zone, in agreement with the place where experimental fractures occurred. However, they provide different results in terms of failure risks. The experimental results, even if still preliminary, give indication of the predictivity goodness of Brown-Miller criterion among others for NiTi stents. This experimental and numerical approach for fatigue endurance prediction in complex devices, is extendable also to resorbable magnesium stents.

# Microstructure, mechanical and electrochemical performance of a biodegradable Mg-2Zn-0.2Mn-0.5Ca/2HA nanocomposite

Y. Huang<sup>1</sup>, M. Razavi<sup>2</sup>

1 BCAST, Inst. of Materials & Manufacturing, Brunel University London, Uxbridge, UB8 3PH UK. 2National Dept. of Radiology, School of Medicine, Stanford University, California 94304 USA

**INTRODUCTION:** Adding hydroxyapatite (HA) into Mg alloy has been demonstrated to enhance corrosion resistance with respect to biomedical applications. However, Mg/HA composites exhibit inconsistent electrochemical performance and poor mechanical properties, particularly with high HA contents and large HA particle size. At Brunel, investigations have been carried out to study the effect of particle size, distribution and fabrication route on the performance of Mg/HA composites. This paper describes the characterization of microstructure, mechanical and electrochemical Mg/HA nanocomposite. performance of an METHODS: A 99.9wt% pure Mg-2Zn-0.2Mn-0.5Ca (wt%) alloy was used as matrix. Spherical HA particles of 20-50nm in diameter were mixed into the alloy melt with the help of a high shear rotor-stator device at 670-680°C. The mixture was cast into cylindrical ingots of f60×120mm. The ascast ingots were then extruded at 350°C into bars of a 15×15mm cross-section. Selected extrusion bars were isochronally annealed for 1h at 300, 350 and 400°C. Mechanical properties were tested by compression tests following ASTM-E9. Electrochemical properties were tested by static polarization in Hank's solution at 37°C. Immersion tests for measuring corrosion rate were conducted in the same solution at 37°C for various times, using a WE-3 immersion oscillator.

**RESULTS & DISCUSSION:** Presented are the results for an Mg/HA nanocomposite with 2% HA. High shear mixing produced a globally uniform distribution of HA particles in the Mg matrix (Fig. 1a) with a fine grain structure (Fig. 1b). Extrusion

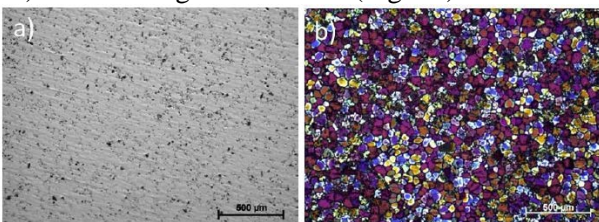


Fig. 1: Optical micrographs showing a) particle distribution; b) grain structure.

resulted in microstructural elongation and further refinement (Fig. 2a). Fully recrystallized equiaxed grain structure developed after annealing (Fig. 2b).

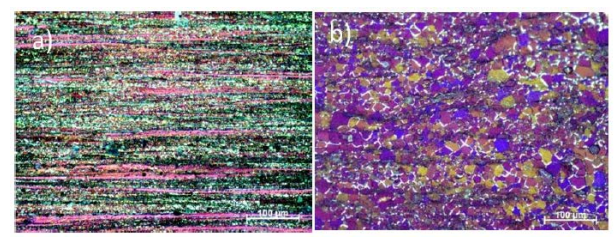


Fig. 2: Optical micrographs showing the microstructure after a) extrusion, b) annealing at  $350^{\circ}$ C for 1 h.

The annealed material exhibited excellent ductility while extruded showed yield strength as high as ~238MPa with reasonably good ductility of ~12% uniform reduction (Fig. 3), which are adequate for biomedical use.

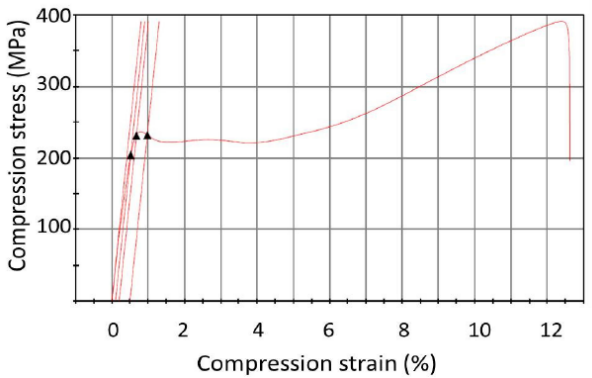


Fig. 3: Compression stress-strain curve of extruded Mg-2Zn-0.2Mn-0.5Ca/2HA composite. Extruded & annealed samples exhibited increased open circuit potential, reduced corrosion current and corrosion rate, compared to those for the ascast and matrix. The experimental results are given in Table 1. Overall, both mechanical properties and corrosion resistance of the Mg-2Zn-0.2Mn-0.5Ca/2HA nanocomposite were satisfactory.

Table 1. Selected results of polarization and 7 days immersion tests.

Sample	Potential	Current	Corrosion rate
	(V)	$(mA/cm^2)$	(mg/cm <sup>2</sup> /h)
As-cast	-1.51	17.8	26.8×10 <sup>-2</sup>
Extruded	-1.45	11.7	$7.6 \times 10^{-2}$
Annealed@350	-1.45	8.7	$3.1 \times 10^{-2}$
Extru-Matrix	1.54	13.9	23.2×10 <sup>-2</sup>

**ACKNOWLEDGEMENTS:** This work was supported by the MeDe Innovation, the EPSRC Centre for Innovative Manufacturing in Medical Devices [grant number EP/K029592/1].

### Corrosion mechanisms on magnesium samples for ophthalmological devices

M Ferroni<sup>1</sup>, MG Cereda<sup>2</sup>, F Boschetti<sup>1</sup>

INTRODUCTION: Wet age-related macular degeneration and diabetic macular edema are two of the main causes of vision loss in developed countries. Millions of people suffer of these chronical pathologies worldwide and they are treated by intravitreal injections of specific drugs. A device able to release preset bolus of drug would be an optimal solution to avoid the collateral effects of treatments. In this context, magnesium or its alloys can be a promising biomaterial, considering its bioresorbable nature in biological fluids and the biocompatibility of its corrosion products. Our work seeks to understand the corrosion mechanisms acting on magnesium samples, considering the peculiar characteristics of the ocular behavior. The implemented method consists in a combined numerical and experimental approach.

METHODS: We developed a numerical model of the fluid-dynamics inside the posterior chamber, where clinicians inject the drug. We identified two kinds of boundary conditions: i) the physiological milieu around the vitreous body and ii) the ocular saccades. In parallel, we simulated the insertion of a layer of magnesium to evaluate the shear stress field acting on the free surfaces. Then, corrosion tests on pure magnesium samples were done using a custom experimental set-up for 24 hours. The experimental flux was set to recreate on the upper surface of specimens the same shear stress field evaluated by the simulations (Figure 1).

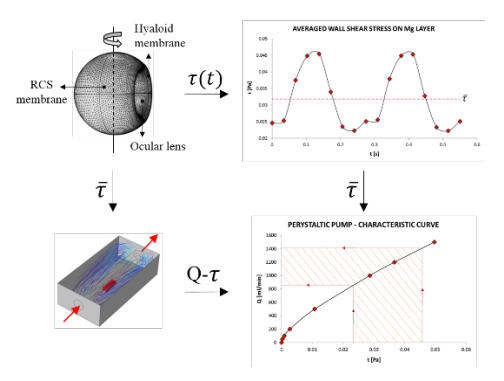


Fig. 1: Scheme of the numerical approach.

Thus, we implemented a numerical model able to optimize the flow rates of the experimental set-up, using a Nelder-Mead optimization method. Before and after the corrosion tests, morphology and

profile of all the specimens were evaluated and compared using a field emission scanning electron microscope (SEM, S360, Cambridge Instruments) and a 3D laser confocal microscope (LEXT OLS4000, Olympus), for the evaluation of the corrosion mechanisms.

**RESULTS:** The shear stress profile follows the sinusoidal trend of the saccades, with an averaged value of 0.032 Pa in the range between 0.023 and 0.046 Pa, which correspond to flow rates between 870 and 1410 ml/min. Figure 2 shows the morphology and the profile before the corrosion tests. Some localizations, randomly placed along regular and flat areas, can be noticed (Figure 2.B).

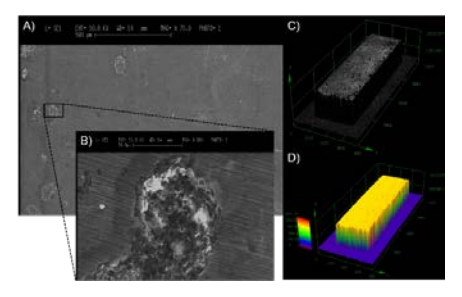


Fig. 2: A) SEM image of a standard surface. B) Zoom of a localization. C) Map of intensity. D) 3D profile of heights from LEXT.

proposed is able to recreate the ocular fluid-dynamic conditions and analyse the consequent corrosion on magnesium samples. Results show shear stress values less than 0.1 Pa that generate controlled and uniform corrosion when tested invitro. Some pre-existing localizations influence the final corrosion pattern. Maps from LEXT allow us to evaluate the local decrease of the sample heights and the correspondent corrosion rates in a physiologic ocular environment.

**ACKNOWLEDGEMENTS:** The magnesium samples were kindly provided by National Engineering Research Center of Light Alloy Net Forming, Shanghai Jiao Tong University, China.

<sup>&</sup>lt;sup>1</sup> Department of Chemistry, Materials and Chemical Engineering, Politecnico di Milano, Italy

<sup>&</sup>lt;sup>2</sup> Department of Biomedical and clinical science, Sacco Hospital, University of Milan, Italy

### Influence of solution heat treatment on corrosion morphology of Mg4Gd wire

P Maier<sup>1</sup>, H Schöning<sup>1</sup>, M Bechly<sup>1</sup>, G Szakács<sup>2</sup>, N Hort<sup>2</sup>

1 University of Applied Sciences Stralsund, Stralsund, Germany. 2Helmholtz-Zentrum Geesthacht, Magnesium Innovation Center, Geesthacht, Germany

**INTRODUCTION:** The interest on Mg wires for biomedical applications is increasing. Its drawing process is meanwhile well established. A recent study has shown that a post solution heat treatment (T4) after wire drawing improves the remaining mechanical properties of a warm drawn Mg4Gd wire after corrosion by immersion. Fig. 1 shows exemplary the improvement in stress corrosion. The improvement is based on less harmful sizes and shapes of corrosion pits and their smaller amount after T4. This study presents additional information using the corrosion rates and pitting factors as a function of time to describe the corrosion and its morphology.

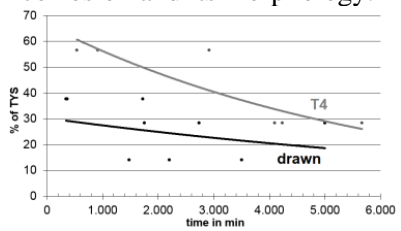


Fig. 1: T4 on SCC: stresstime to rupture curves, T4: TYS 130 MPa, asdrawn: TYS of 260 MPa [1]

The importance of the corrosion morphology is described in Maier et al. (2016, 2017). Briefly it should be pointed out, that pits increase stress intensity by notch effects when an additional mechanical loading is applied.

METHODS: T4 was done at 500°C for 6h after wire drawing, like described in [1]. Immersion test were done in Ringer solution up to 3 days in 37°C (3 wires, length of 30mm, 500ml electrolyte). The corrosion rate (CR) was calculated by using mass loss, the pitting factor (PF) is calculated by dividing the deepest corrosion pit, taken from micrographs, by the average corrosion from CR.

**RESULTS:** Fig. 2 shows SEM images the wires after corrosion and the cross-section micrographs cutting a corrosion pit. The number of corrosion pits (subsurface) and its depth decrease by T4.

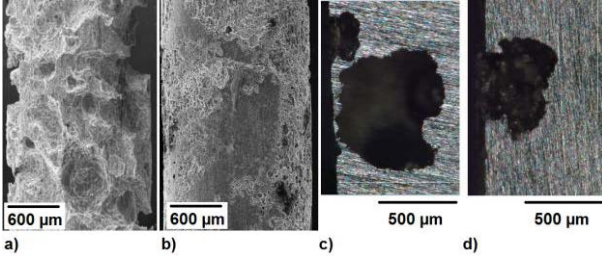


Fig. 2: Mg4Gd wire: SEM image of as-drawn (a) and heat treated (b) wire, micrographs with pits of as-drawn (c) and heat treated (d) wire, all after 1 day

The chart in Fig. 3a shows that the CR decreases

by applying T4 and as a function of time. After 3 days a reasonable CR of ~1.5 mm/year is reached. Figure 3b shows a rather strong increase in depth of corrosion pits for the as-drawn condition and only a small increase in pit depth for the T4 system (left). The resulting pitting factors are very high for these wires: up to 70 (right). Because of its dependence on the CR, which is discussed below, there is no trend in development of PF over time.

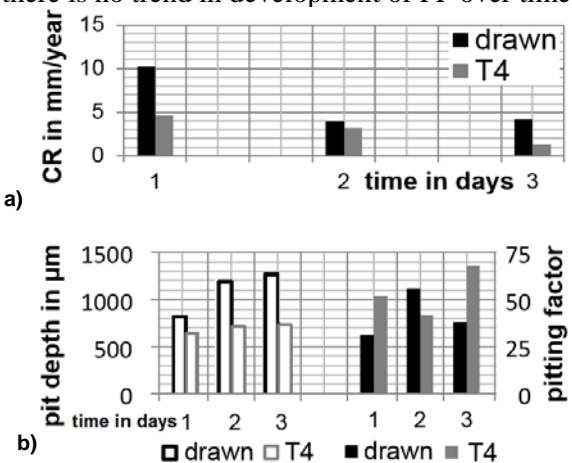


Fig. 3: Mean corrosion rate CR (a), pit depth and pitting factor (b) of as-drawn and heat treated wire

**DISCUSSION & CONCLUSIONS:** The PF in the as-drawn condition reaches its maximum after 2 days. Even the pits are growing towards 3 days, the PF decreases due to the stabilisation in CR. The PF of the T4 condition shows the highest value after 3 days. Here the pits do not grow, but the mean CR reaches the smallest value. With this the improvement in remaining strength seen in [1] does not only depend on the PF, but also on the actual pit depth (smaller in T4) and number of pits. There are less pits in the T4 condition, which keeps the remaining load bearing area higher. It can be summarized that T4 acts positive. However, the PF is far too high. The better understanding of process parameters during wire drawing, the better control of the grain size by recrystallization and surface quality improvement should be applied.

## Surface treatments, sandblasting and ultrasonication, for modification of the biodegradation behavior of pure iron

JC Zhou<sup>1</sup>, YY Yang<sup>1</sup>, M Frank<sup>1</sup>, S Virtanen<sup>1</sup>

<sup>1</sup> Institute for Surface Science and Corrosion, Department of Materials Science and Engineering, University of Erlangen-Nuremberg, Erlangen, Germany

INTRODUCTION: Iron-based materials have significant attention in terms biodegradable materials, because of their excellent mechanical properties and stable biodegradation process. However, the slow degradation rate of iron-based materials does not match the clinical requirements in some cases, due to the long degradation period and stress-shielding effect. In this work, two different surface treatments, sandblasting and ultrasonication, are studied as an efficient way to modify the biodegradation behavior of pure iron. Sandblasting can accelerate the biodegradation rate of pure iron remarkably. The ultrasonication treatment functions as an external treatment owning excellent controllability, which allows modification of the biodegradation behavior based on clinical needs. These two surface treatments are expected to be suitable to be on different iron-based materials. applied Moreover, the cytocompatibility of surfaces treated by ultrasonication and sandblasting, respectively, have been evaluated.

METHODS: Iron foil (purity 99.5%) was used as the substrate. For the sandblasting treatment group, iron samples were sandblasted with two particles, F80 and F320 (different particle sizes). For the ultrasonication treatment group, pure iron samples were immersed in two different solutions under the ultrasonication treatment with different parameters. Electrochemical tests and immersion tests were conducted for both groups in (simulated body fluid) SBF and in Dulbecco's modified Eagle medium (DMEM). The surface morphology and composition were characterized by SEM, FTIR, EDX, and XPS. Finally, the cytocompatibility of samples after these two treatments were evaluated by using human osteoblast-like cells (MG-63).

**RESULTS:** Pure iron samples treated with sandblasting show different surface roughness. Average ( $R_a$ ) and maximal ( $R_{max}$ ) surface roughness of the F80 sample is higher than that of the F320 sample. Potentiodynamic polarization in SBF indicates that the passivation region of pure iron is diminished after the sandblasting treatment.

Electrochemical impedance spectroscopy (EIS) and weight loss in a long-term immersion test confirm that pure iron after sandblasting treatment

shows a higher biodegradation rate as compared to the untreated iron. It is noteworthy that the degradation rate of sandblasted samples remains significantly higher during long-term immersion tests, whereas for untreated Fe the dissolution rate significantly slows down with time.

The pure iron presents different biodegradation behavior under ultrasonication treatment in SBF and DMEM. Biodegradation rate of pure iron can be accelerated by ultrasonication in DMEM solution, while no acceleration effect is observed in SBF solution. Compact degradation product layers form on samples immersed in DMEM. The longterm EIS measurement illustrates that the corrosion mechanism changes from charge-controlled to oxygen diffusion-controlled after davs immersion in DMEM. The degradation product layers block the diffusion of oxygen and therefore decrease the biodegradation rate of the substrate. By using the ultrasonication treatment, degradation product lavers can be removed and biodegradation rate can be accelerated.

Proliferation and adhesion of MG-63 cells on samples treated by sandblasting and ultrasonication, respectively, show no significant difference compared to untreated Fe surfaces.

#### **DISCUSSION & CONCLUSIONS:**

Biodegradation rate of pure iron can be accelerated by both sandblasting and ultrasonication treatments. Biodegradation behavior is related to the sandblasting particle size, and the acoustic strength of ultrasonication, as well as the operating time. No adverse influence from both surface treatments on the cytocompatibility was found. This work demonstrates the significant potential of sandblasting and ultrasonication treatments for modifying the biodegradation behavior of ironbased materials.

# Microstructure and degradation of WE43 bone scaffolds fabricated by Selective Laser Melting

L Berger<sup>1</sup>, L Jauer<sup>2</sup>, F Bär<sup>1</sup>, E Faude<sup>1</sup>, R Schäublin<sup>1</sup>, J H Schleifenbaum<sup>2,3</sup>, J F Löffler<sup>1</sup>

<sup>1</sup> Laboratory of Metal Physics and Technology, Dept of Materials, ETH Zurich, Zurich, Switzerland

<sup>2</sup> Fraunhofer Institute for Laser Technology ILT, Aachen, Germany. <sup>3</sup> Digital Additive Production, RWTH Aachen University, Germany

INTRODUCTION: Selective Laser Melting (SLM) is a promising method to fabricate magnesium-based, biodegradable structures for bone support. Of special interest is the high-strength and highly corrosion resistant Mg-Y-RE-Zr alloy WE43. It is FDA-cleared and already applied for medical devices. Parts are typically fabricated by powder extrusion, but for more complex geometries SLM appears to be a promising manufacturing alternative. However, the influence of process parameters and the process-related high cooling rates on microstructure are not fully understood yet.

METHODS: Bulk material and open-porous structures (dimension: 10×10×10 mm<sup>3</sup>) were manufactured using a single-mode ytterbium fiber laser (IPG YLR-200) with 230 W maximum output power, a galvanometric scanner (SCANLAB hurrySCAN 20) and a f-theta focussing lens (SILL S4LFT 3254/126), generating a spot diameter of approximately 90 µm in the focal plane (Fig. 1). Gas-atomized WE43 powder of particle sizes 20μm was used (ELEKTRON®MAP+43, Magnesium Elektron Powders, Manchester, NJ, USA). The specimens were manufactured with a layer thickness of 30 µm and a hatch spacing of 40 um. The microstructure was investigated using optical light microscopy, scanning electron microscopy and a 200 kV transmission electron microscope with energy-dispersive X-ray spectroscopy mapping of ScopeM ETH. Additionally, corrosion in simulated body fluid was measured.

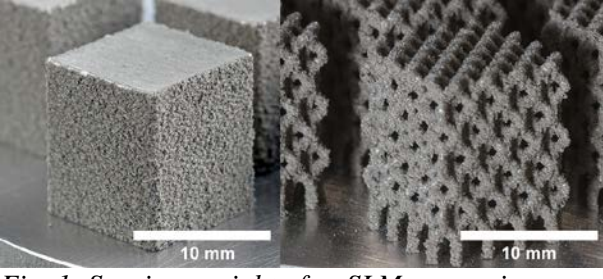


Fig. 1: Specimens right after SLM processing.

**RESULTS:** The samples exhibited minimal bulk porosity with grain sizes of approximately 1  $\mu$ m and finely dispersed secondary phases. Additionally, shells of  $Y_2O_3$  were observed. The corrosion tests on polished bulk samples revealed a degradation rate of 0.61 mg/cm²/day, which is comparable to reference samples of powder-extruded material (0.53 mg/cm²/day).

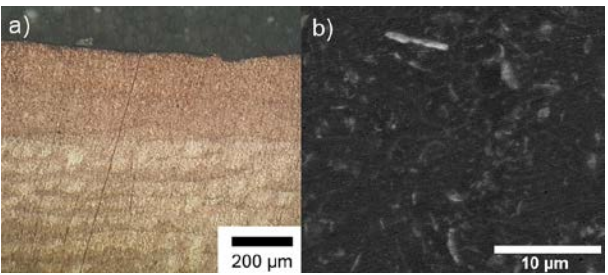


Fig. 2: a) Cross-section with clearly visible printing layers and a last layer (top) with a remelting zone of 250-300 µm. b) Finely dispersed Y- and RE-rich secondary phases.

**DISCUSSION & CONCLUSIONS:** Successful fabrication of WE43 scaffolds could demonstrated with comparable low degradation rates to conventionally production paths. The very small grain sizes of finely distributed secondary phases, caused by the high cooling rates during the SLM process, lead to grain-size hardening and precipitation-hardening and therefore also greatly improved mechanical properties. A remaining challenge is the particles sintered on the surface. They can mostly be removed by shot-peening, which, however, results in a very rough surface. methods Chemical or electrochemical suggested to improve surface quality.

### Synthesis and characterization of magnesium scaffolds by liquid phase sintering using different space holding materials

Shweta Singh, Naresh Bhatnagar

<u>Department of Mechanical Engineering, Indian Institute of Technology Delhi, New Delhi</u> India

**INTRODUCTION:** Magnesium based scaffolds are one of the most recent class of biomaterials as it can reduce the problem of other polymeric scaffold materials with inferior properties. Owing to magnesium's highly reactive nature, it is difficult to produce magnesium based porous products. Space holding method using liquid phase sintering is one of the promising method of producing magnesium porous products. However, very little work is available to understand the impact of various space holding particles (shape, size and volume fraction) on the properties of magnesium based scaffolds and its removal challenges. Present work attempts to fabricate and characterize magnesium (Mg)based interconnected porous specimen by combining space holder technique with liquid phase sintering. A comparative analysis is also done to identify the most suitable space holding material for Mg based interconnected porous parts.

**METHODS:** In this work, open cell Mg3Zn metal foams are fabricated using nine different spaceholding materials, ammonium bicarbonate (NH<sub>4</sub>)HCO<sub>3</sub>, carbamide (CO(NH<sub>2</sub>)<sub>2</sub>), ammonium bicarbonate + carbamide (5:1), magnesium carbonate (MgCO<sub>3</sub>), NaCl, polylactic acid (PLA), poly methyl methacrylate (PMMA), sugar and polyurethane (PU). Figure 1, shows the step-bystep schematic of the fabrication process with magnesium porous specimen fabricated in present method.



Figure 1: Steps in foam fabrication process using space holding particle and Porous Mg

3 wt. % of zinc (Zn) is added in magnesium powder to enhance the strength as well as corrosion resistance of Mg. This happens due to the lower melting temperature of Zn than Mg resulting into liquid-solid interaction.

**RESULTS:** Mechanical testing and microstructural characterization are performed by

compression testing and SEM/EDX analysis. Porosity, pore size,

pore morphology and pore interconnectivity are calculated using micro-computed tomography (μCT) scan. Cytotoxicity tests are in the process of being performed to confirm the biocompatibility of the Mg-foams and to verify its usability as a scaffold. The fabricated specimen is expected to be biocompatible beacause complete thermal degradation of ammonium bicarbonate and lower carbamide occurs at comparatively temperature. Results show that the combination of ammonium bicarbonate and carbamide in the ratio a 5:1 is probably the best choice of space holding material as it induces more than 70 % porosity and compressive strength up to 21 MPa. Figure 2, shows a µ-CT and SEM image of porous Mg structure fabricated by present technique.

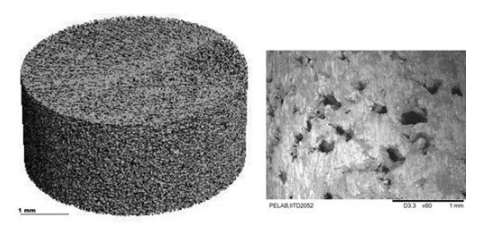


Figure 2: μ-CT and SEM image of Mg3Zn specimen (porosity ~73%)

DISCUSSION & CONCLUSIONS: A detailed comparative analysis of various space holding particles is done. Mg-based porous parts of high porosity have been fabricated successfully with optimum strength by utilizing the concept of liquid phase sintering. Porosity, pore size and strength are controlled by adjusting the space holder particles. Liquid phase sintering enhanced the overall strength. Mg-based porous parts fabricated in the present work are expected to be a promising candidate for a scaffold material because of possibility of new tissue growth through the interconnected pores and degradation of Mg in the body with time.

### Effect of various heat treatments on the microstructure and mechanical properties of WE43 Mg alloy

F D'Elia<sup>1</sup>, A Kopp<sup>1</sup>, C Ptock<sup>1</sup>, N Hort<sup>2</sup>

1 Meotec GmbH & Co. KG, Aachen, Germany. 2 Magnesium Innovation Centre, Helmholtz Zentrum Geesthacht, Geesthacht, Germany.

**INTRODUCTION:** Magnesium (Mg) WE43 has high potential for use as resorbable implants due to its high strength, good corrosion resistance and biocompatibility. In fact, the only two current CE-labelled market available Mg resorbable implants (i.e. MAGNEZIX compression screw and Magmaris scaffold) are both produced from WE43. During production of WE43-based implants, the processing parameters play a significant role in the overall performance of the material. Specifically, altering heat treatment parameters (e.g. temperature, time) can impact the final microstructure of the material and ultimately its overall mechanical properties. Thus, selection of the proper heat treatment method is crucial to producing Mg alloys suitable for biomedical applications.

**METHODS:** In this study, the effect of various T6 heat treatment methods on alloy microstructure and properties was investigated. mechanical Magnesium alloy WE43 ingots were produced via a modified direct chill casting method1 at the Magnesium Innovation Centre (MagIC) Helmholtz-Zentrum Geesthacht in Germany. The alloy was prepared from high purity (99.99%) Mg ingots with additions of 4 wt% pure (99.9%) Y and 3 wt% pure (99.9%) Nd. The cast ingots were then sent to Meotec GmbH & Co. KG in Aachen, Germany where they underwent various T6 treatments. Extensive microscopy (optical and scanning electron) was carried out on the samples prior to heat treatment (i.e. as-cast), after solutionising and quenching (i.e. T4-treated) and finally after ageing (i.e. T6-treated). Finally, both microhardness measurements and mechanical testing were carried out after each treatment stage.

**RESULTS:** Heat treatment was found to have a pronounced effect on alloy microstructure for WE43. In the as-cast state, secondary phases were seen dispersed along interdendritic regions (Figure 1a). Such secondary phases are typically Mg41Nd5, Mg12Nd and Mg22Y52. In the case of the T4-treated alloys (Figure 1b), most of the secondary phases were dissolved into the matrix (Figure 1b). Such

dissolution of the phases into the matrix facilitates the formability (e.g. extrusion, rolling) of the material and is hence a critical step for production purposes. The transformation of alloy microstructure by heat treatment was also found to have an impact on the hardness and mechanical properties of the WE43 alloy. In particular, hardness values were generally found to increase after each treatment stage. In contrast, mechanical testing demonstrated that in some cases alloy strength was enhanced and ductility reduced with heat treatment, while in other instances the opposite was obtained.

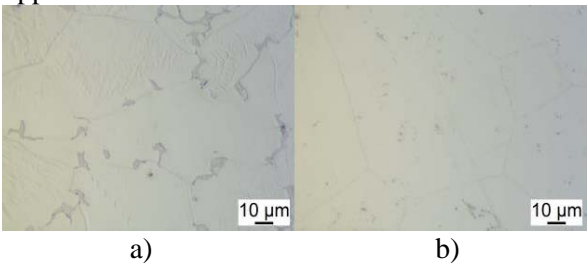


Fig. 1: WE43 alloy microstructure in a) the as-cast state and b) T4-treated state.

DISCUSSION & CONCLUSIONS: The results suggest that heat treatment significantly alters alloy microstructure and mechanical properties of WE43 Mg alloy. The properties of WE43 can therefore be systematically tailored to suit the requirements for specific applications. Certain treatment methods can be carried out to accommodate applications where high ductility is required, while other methods can tailor the alloy properties to suit applications where high strength is of utmost importance. Hence, this demonstrates the possibility of enhanced applications for WE43 in biomedical applications.

**ACKNOWLEDGEMENTS:** The authors are grateful to Mr. G. Meister from MagIC for carrying out the casting experiments and to Ms. L. Pham and Mr. I. Schestakow from Meotec for help with sample preparation.

# Choice of Mg-1.2Zn-0.5Ca-0.5Mn alloy and heat treatment strategy: a candidate alloy for bioresorbable skeletal fixation

M Elahinia<sup>1</sup>, H Ibrahim<sup>1</sup>, D Dean<sup>2</sup>, AD Klarner<sup>3</sup>, AA Luo<sup>3</sup>, I Valerio<sup>2</sup>, R Skoracki<sup>2</sup>, M Miller<sup>2</sup>

<sup>1</sup>Department of Mechanical, Industrial and Manufacturing Engineering, University of Toledo, Toledo, OH USA. <sup>2</sup>Department of Plastic Surgery, <sup>3</sup>Department of Materials Science and Engineering, The Ohio State University, Columbus, OH USA.

**INTRODUCTION:** During the last decade, Mg alloy biomaterials have been developed for use as skeletal fixation materials. These materials are biodegradable and have lower density and relatively higher strength compared to biodegradable polymers used in degradable skeletal fixation devices. However, there are concerns that Mg alloy fixation devices may: have insufficient strength, degrade too quickly, and may include toxic elements (e.g., Al, Cd and Pb).

There is also interest in patient-specific, biodegradable fixation hardware produced by powder-bed additive manufacturing (AM). Postfabrication processes (e.g., heat treatment and coating) are important tools that may improve patient-specific resorbable fixation performance. It is important to note that mechanical treatments are not suitable for parts produced in their final shape since they involve large plastic deformations.

To this end, we have produced Mg-1.2Zn-0.5Ca-0.5Mn alloy samples that can be heat-treated and MAO coated with biocompatible ceramics. The chemical composition of the alloy was carefully chosen to optimize the age hardening effect and corrosion.

METHODS: An Mg alloy with 0.5 wt.% content of both Ca and Mn and 1.2 wt.% Zn was selected because it was expected to result is the best age hardening response. A Zn/Ca atomic ratio from 1.4 to 2.4 was expected to result in the highest age hardening response and relatively higher corrosion resistance. The designed Mg-1.2Zn-0.5Ca-0.5Mn (Zn/Ca atomic ratio of 1.47) alloy was solution-treated at 510 °C for 3 hours then quenched in water. The samples were then artificially-aged in an oil bath for 3 hours at different temperatures (100, 150, 200 and 250 °C). The prepared samples were tested for their mechanical and corrosion properties.

**RESULTS:** An age hardening temperature of 200 °C was found to result in the optimum age hardening effect (Fig. 1). The yield and ultimate compressive strength of the alloy increased from 71.7 MPa and 304.1 MPa to 122.8 MPa and 352.8 MPa, respectively, after the heat treatment process (Fig. 2). Also, the *in vitro* corrosion rate of the

heat-treated alloy (0.75 mm/year) was almost half that of the untreated alloy (1.4 mm/year).

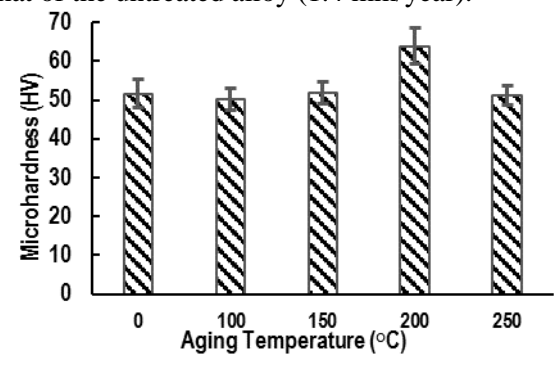


Fig. 1: Microhardness of the heat-treated alloy for 3 hours at different age hardening temperatures (N=15 readings at each temperature).

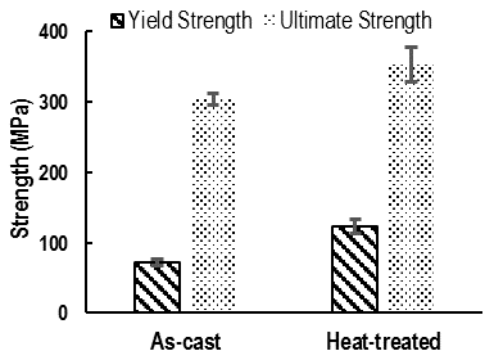


Fig. 2: Compressive strength of the as-cast and heat-treated alloy at 200  $^{\circ}$ C and 3 hours (N = 5 specimens for each case).

**DISCUSSION & CONCLUSIONS:** Aging Mg-1.2Zn-0.5Ca-0.5Mn (wt.%) alloy samples at 200 °C for 3 hours was found to result in the best age hardening effect. Simultaneously, the 3 hours heat treatment process reduced the corrosion rate of the Mg alloy studied by almost half.

**ACKNOWLEDGEMENTS:** This work has been partially supported by Third Frontier (State of Ohio)

TVSF grant #15-79

### Anti-thrombotic behaviour of ZX11 using anodization technique

E. Mirtaheri<sup>1</sup>, N. Munroe<sup>1</sup>

<sup>1</sup> <u>Mechanical and Materials Department</u>, Engineering Centre, Florida International University, Miami, FL, US

INTRODUCTION: The of implantation cardiovascular stents via angioplasty and its aftercare therapy are fraught with incidences of thrombosis (blood clots). Using biodegradable implants not only reduces the risk of late stent thrombosis, but also negates the need for secondary surgery and lowers the cost and patient morbidity. Magnesium and a number of its alloys draw on good attributes such as biodegradability that make them suitable for stent applications. However, a major concern with magnesium is the high degradation rate during the initial periods of implantation that compromise cell viability and proliferation. Application of a polymer coating has proven to be an effective method for controlling the degradation rate. This study focused on assessing the corrosion behavior of a surface treated ZX11 alloy in PBS as well as its platelet adhesion using porcine blood in a flow chamber.

**METHODS:** Solution heat treatment at 420°C for 12 hrs followed by air cooling. Surface treatments: Mechanical polishing (MP) using 600 SIC paper followed by anodization to produce a passivating oxide (MP+A). Dip-coating in polyglycolic-cocaprolactone (PGCL) (90/10) to provide an impermeable barrier (MP+A+P). Wettability measurement: Contact angle analysis was used to measure the surface energy and assess its effect on platelet adhesion. Platelet adhesion: Fluorescence microscopy and the software "ImageJ" were used to quantify platelet adhesion on each sample.

#### **RESULTS:**

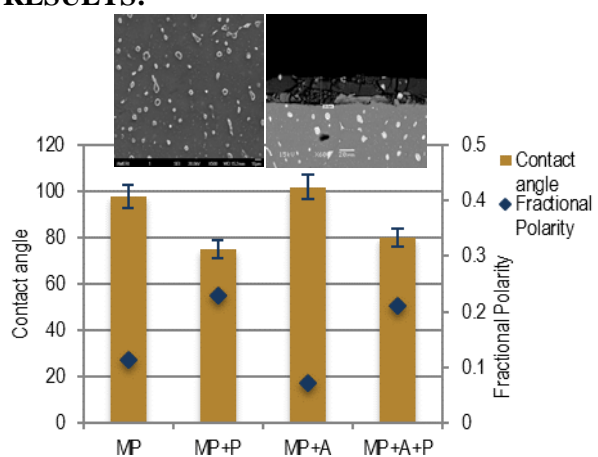


Fig. 1: Contact angle and fractional polarity measurement on surface treated ZX11 alloy.

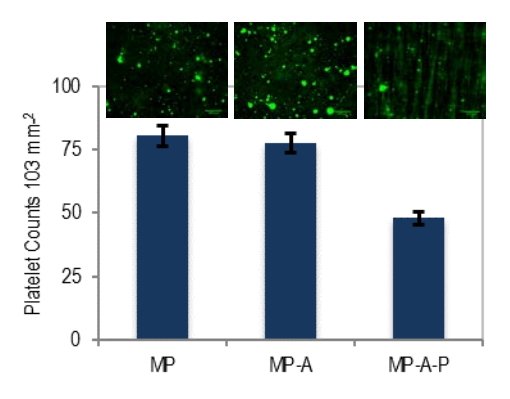


Fig. 2: Platelet counts for different sample surfaces.

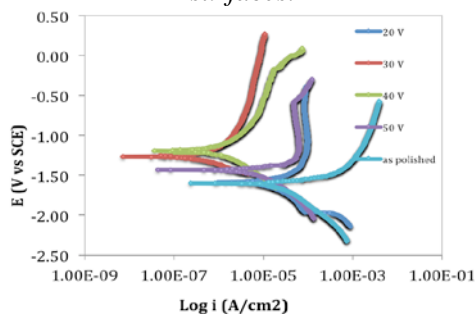


Fig. 3: Potentiodynamic polarization curves for different surface treatments.

**DISCUSSION & CONCLUSIONS:** Anodization increased hydrophobicity and decreased fractional polarity while polymer coating decreased hydrophobicity and increased fractional polarity. There was an optimum anodization voltage at which the lowest corrosion rate was observed. The least platelet adhesion and corrosion rate occurred on PGCL coated anodized ZX11, which implies reduced thrombogenicity and improved corrosion behaviour. There was an inverse relationship between platelet adhesion and fractional polarity, i.e. as the fractional polarity of a surface increased, the platelet adhesion decreased.

ACKNOWLEDGEMENTS: The author wants to acknowledge Dr. Sharan Ramaswamy, Danique Stewart and Ricardo Hausz for their assistance with platelet adhesion test.

### Fe-Mn-C alloys for biodegradable metallic implants: influence of Mn content

B. Occhionero<sup>1</sup>, C. Paternoster<sup>1</sup>, C. A. Biffi<sup>2</sup>, A. Tuissi<sup>2</sup>, D. Mantovani<sup>1</sup>

<sup>1</sup><u>Laboratory for Biomaterials and Bioengineering</u>, Dept. of Min., Met. and Mater. Eng. CHU de Quebec Research Centre, Laval University, Québec City, Canada - <sup>2</sup><u>National Research Council</u> – <u>Institute of Condensed Matter Chemistry and Technologies for Energy</u>, CNR ICMATE Lecco, Italy.

**INTRODUCTION:** In recent years, biodegradable metals (BMs) for developing temporary vascular and osteosynthesis devices are gathering an increasing worldwide interest. BM should offer appropriate mechanical properties, sufficient X-ray visibility, especially for small devices, and suitable cytocompatibility. Several BM systems were proposed, respectively based on Mg, Zn and Fe. Fe-based alloys have often a consistent amount of Mn. The effect of this element is evident from a mechanical, electrochemical and biological point of view. In this work, Fe-Mn-C alloys, with different Mn contents, were produced by casting; the properties of these alloys were studied, to understand the effects of the microstructural and surface condition states on the degradation behavior.

MATERIALS AND METHODS: Fe-12Mn-1.2C. Fe-16Mn-0.9C and Fe-20Mn-0.6C wt. % were melted in a vacuum arc furnace, from a Fe-Mn mother alloy and pure Fe and Mn metals. The materials were cold rolled with intermediate annealing steps to a final thickness of 0.6 mm. Five samples for each alloy were annealed for 1 h at 800 °C in Ar/5 vol. % H<sub>2</sub> atmosphere. A 14-day static immersion test (ASTM G31) was performed to evaluate the degradation properties of the materials immersed in modified Hanks' solution (MH). The characterization techniques used for the study of the alloy structure, corrosion behaviour and surface morphology were X-ray diffraction, scanning electron microscopy and energy dispersive X-ray spectrometry. Both the degraded sample surface and the degradation products were investigated.

**RESULTS:** Homogeneity of produced ingots was checked by EDS on cross sections. All the materials presented a dendritic structure, which became fully austenitic after the thermomechanical treatment. The main presence of austenitic phase was confirmed by XRD studies. After the static degradation tests, the formation of crystalline compounds was found on the surface: they could be attributed to the presence of carbonates and especially to MnCO<sub>3</sub><sup>2</sup>. XRD analyses of the degraded samples surfaces showed the presence of austenite for Fe-12Mn-1.2C and Fe-16Mn-

0.6C,MnCO<sub>3</sub> peaks and traces of austenite were found for degraded Fe-20Mn-0.6C. The degradation products obtained after the static immersion test showed the presence of phosphate and carbonate groups, confirmed by XPS results. The degradation rate was around 0,15 mm/year, and it was the same for all the samples; it increased slightly for alloys with higher Mn contents.

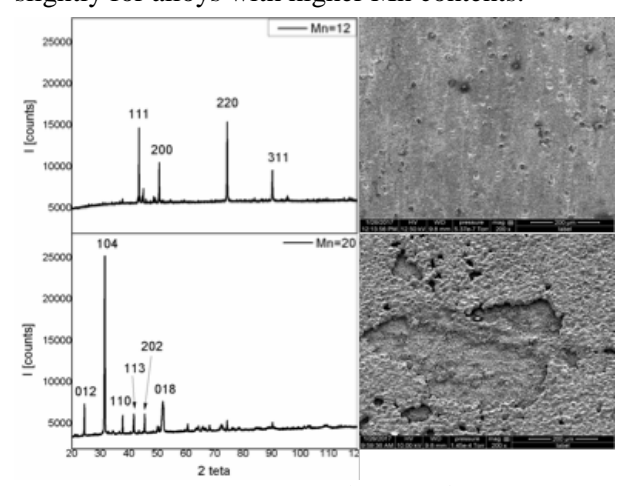


Figure 1: XRD patterns (left) and SEM images (right) after the static immersion test, respectively for Fe-12Mn-1.2C (up) and Fe-12Mn-1.2C (down).

**DISCUSSION & CONCLUSIONS:** The amount of Mn in the alloys affected not only the corrosion rate of the alloys, but also the degradation morphology and the formation of degradation products. The degradation rate slightly decreased because of the formation of a stable layer of MnCO<sub>3</sub> on the metal surface, highlighted by XRD; this layer was more evident for alloys with a higher Mn content.

ACKNOWLEDGEMENTS: The authors would like to thank V. Dodier, D. Marcotte, and N. Moisan (Laval University) and M. Pini and G. Carcano (CNR ICMATE Lecco). This work was partially funded by NSERC-Canada, FRQ-NT-Quebec and CFI-Canada and by Dr. D. Colombo, Lecco Italy. BO contribution was carried out in the framework of her MSc thesis work, under the supervision of Prof. M. Vedani (PoliMi, IT).

#### Development of Zn-Ag-Mn alloys for future bioabsorbable vascular stents

E. Mostaed<sup>1</sup>, M. Sikora-Jasinska<sup>1,2</sup>, A. L. Ramirez-Ledesma<sup>1</sup>, L. Levesque<sup>2</sup>, D. Mantovani<sup>2</sup>, M. Vedani<sup>1</sup>

Department of Mechanical Engineering, Politecnico di Milano, Milan, Italy. Lab. for Biomaterials & Bioengineering (CRC-I), Dept. Min-Met-Materials Engineering & Research Center CHU de Québec, Laval University, Québec City, Canada.

INTRODUCTION: stents bioabsorbable metal simultaneously exhibiting proper mechanical properties and desirable degradation rate is still an open challenge. Magnesium (Mg), iron (Fe), zinc (Zn) and their related alloys have been proposed as degradable materials for stenting applications. Over the last two decades, Mg- and Fe- based alloys have been widely investigated to use as degradable vascular stents. Mg degrades too rapidly and rarely homogenous, deteriorating the stent's mechanical integrity. In case of Fe, very low degradation rate along with the incomplete absorbtion of the corrosion products make it not yet suitable for the stenting application. Recently, Zn has been proposed as an alternative candidate due to its excellent biodegradability adaptability to tissue regeneration. However, the main concern of using Zn stent is its poor mechanical properties which are far below the benchmarks required for a cardiovascular stent material. Thus, by improving the Zn mechanical properties, many potential problems related to the Mg and Fe could be solved. In this study, several Zn-Ag based alloys are proposed as potential degradable materials.

**METHODS:** Various binary Zn-Ag and ternary Zn-Ag-Mn alloys were developed by meltingcasting process. Samples were subsequently extruded at 250°C with an extrusion ratio of 14:1 obtain cylindrical rods. Microstructural characterization was assesses using optical and scanning electron microscopy (SEM). Phase identification was carried out on the as cast. extruded and degraded samples by X-ray diffraction. Mechanical properties were assessed by tensile testing on the extruded samples at room and elevated temperatures. Corrosion behavior of the alloys was characterized by performing potentiodynamic polarization and static immersion tests in Hanks' modified solution. The solution temperature and pH were adjusted to  $37 \pm 1$  °C and 7.4, respectively.

**RESULTS:** Table 1 lists the mechanical characteristics and corrosion rates of the investigated materials. Microstructural observation

showed a significant grain refinement occurrence in extruded Mn-containing alloys due to the mechanism of particle simulated grain nucleation. Mechanical characterization revealed that the addition of 0.5 wt.% Mn merely resulted in markedly enhancement of yield and ultimate tensile strengths for both 2.5Ag and 5Ag containing alloys. Interestingly, despite Mn addition and increase in Ag content, the measured fracture elongations for all the investigated alloys remained >30%, which are far above the benchmark value for stent materials (>20%). Electrochemical test results indicated slightly faster corrosion rates of the Zn-Ag-Mn alloys than those measured for Mn free counterparts. Furthermore, SEM imaging after removal of the corrosion products revealed that micro-galvanic corrosion is more pronounced in the samples with higher Ag content due to the higher volume fraction of second phase particles.

Table 1. Mechanical and corrosion properties of the extruded samples.

Material	Yield strength (MPa)	Tensile strength (MPa)	Elongation (%)	Corrosion rate (µm.y <sup>-1</sup> )
Zn	58 ± 6	116 ± 6	60 ± 8	133 ± 10
Zn2.5Ag	147 ± 4	203 ± 5	35 ± 4	137 ± 21
Zn5Ag	205 ± 6	253 ± 8	36 ± 3	144 ± 7
Zn2.5Ag0.5Mn	236 ± 4	282 ± 2	32 ± 1	146 ± 9
Zn5Ag0.5Mn	253 ± 2	302 ± 5	31 ± 3	146 ± 13

**DISCUSSION & CONCLUSIONS:** In this study. combined effects of Ag and Mn additions, as Zn alloying elements, to for potential cardiovascular stents was extensively investigated. Based on the obtained results, both mechanical properties and degradation rates fulfil or even exceed the clinical benchmarks. Moreover, superplastic behavior at moderate temperatures in alloys with the finest microstructure suggests improved forming properties, very appealing for the manufacture of devices such as mini-tubes as stent precursors.

### Descaling and electropolishing of Fe-13Mn-1.2C for biomedical applications

Agung Purnama<sup>1,2</sup>, Carlo Paternoster<sup>1</sup>, Stephane Tourgeon<sup>1</sup>, Pascale Chevalier<sup>1</sup>, Diego Mantovani<sup>1</sup>

<sup>1</sup>Lab. Biomaterials and Bioengineering, CRC-I, Dept. Min-Met-Materials Eng, Laval University, Canada, <sup>2</sup>Center for Innovation Technology (CIT), CHU Bordeaux, France

INTRODUCTION: Fe-Mn-C allovs were reported as a potential candidate for cardiovascular stent applications due to their superior mechanical properties and degradability, especially in a chloride-rich environment. The combination of high strength and ductility makes this family of alloys suitable for the fabrication of low thickness devices. On the other hand, stent manufacturing processes involve several steps, the final ones being the surface finishing (descaling, electropolishing and passivation). These steps are needed to control the surface features, both from a chemical and topological point of view. In this the chemical composition and the morphology of Fe-13Mn-1.2C (Hadfield steel) surface was assessed, after the combination of a standard mechanical polishing and cleaning process (C), a descaling step (A or B), an electropolishing solution (1, 2 or 3) were studied.

MATERIALS AND METHODS: 1 cm<sup>2</sup> 1-mm thick samples (Polstar Inc., Toronto, ON, Canada) were mechanically polished using abrasive paper up to 1200 grid. The samples were studied by scanning electron microscopy and energy dispersive X-ray spectroscopy, atomic force microscopy (AFM), profilometry, X-rav photoelectron spectroscopy and contact angle. The used descaling and electropolishing solutions are presented in table 1.

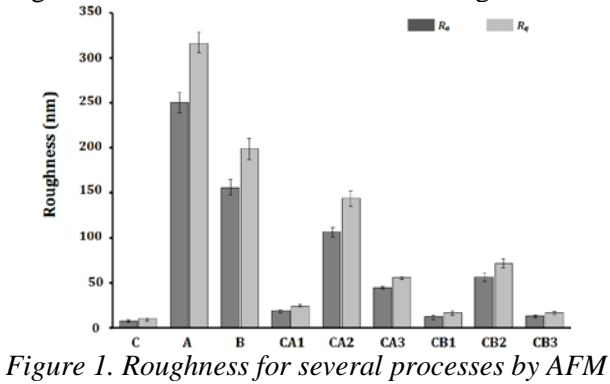
Table 1. Solution composition and working condition for the descaling and electropolishing processes

Descaling-1 (A)		Descaling-2 (B)
4.5 mL HNO <sub>3</sub> 15.4	4.5 mL HNO <sub>3</sub> 15.4M	
0.5 mL HF 48%		0.4 mL H <sub>2</sub> O <sub>2</sub> 30%
90 mL deionized water		99 mL deionized water
Utra sonic bath		Utra sonic bath
45°C		60°C
1 minute		1 minute
Electropolishing-1	Electropolishing-2	Electropolishing-3

Electropolishing-1	Electropolishing-2	Electropolishing-3
470 mL acetic acid glacial 30 mL perchloric acid 60% 10-20 V; 0.3A 25°C 3 x 5 minutes	300 mL H <sub>2</sub> SO <sub>4</sub> 0.1M 200 mL deionized water 1.5-6 V; 0.2A 25°C 2 x 5 minutes	350 mL ethanol 100% 50 mL glycerin 99% 100 mL perchloric acid 30% 6-15 V; 0.3A 60°C 4 × 5 minutes

**RESULTS AND DISCUSSIONS:** The descaling step (Figure 1) increased the surface roughness,

while the electropolishing process decreased it to a value close to that of the mechanically polished samples. "A" type descaling was responsible for a higher roughness compared to "B" type. Moreover, the electropolishing solution #1 showed a lower efficaciousness, compared to that of solutions #2 and #3 treatments, despite the previous descaling treatment. The CB1 condition provided the lowest surface roughness, compared to that of other available combinations. Descaling electropolishing processes influenced the contact angle with the same trend as surface roughness.



**CONCLUSIONS:** Descaling and electropolishing decreased the roughness closer to that of the as mechanically polished (C). The combination of "B" type descaling and electropolishing solution #1 provided the lowest surface roughness compared to other combinations available. Further analysis of XPS needs to be conducted in order to verify the chemical composition of the resulting surfaces.

**ACKNOWLEDGEMENTS:** This work was partially supported by NSERC-Canada, CIHR-Canada, FRONT-Quebec, and MRI-Quebec. The authors would like to acknowledge the NSERC Postdoctoral Fellowship awarded to Agung Purnama.

### Zn-Ag based alloy wires for future absorbable surgical sutures

E. Mostaed<sup>1</sup>, A. L. Ramirez<sup>1</sup>, M. Sikora-Jasinska<sup>1,2</sup>, C.A. Biffi<sup>3</sup>, A. Tuissi<sup>3</sup>, D. Mantovani<sup>2</sup>, M. Vedani <sup>1</sup>

<u>Department of Mechanical Engineering</u>, Politecnico di Milano, Milan, Italy. <sup>2</sup> <u>Lab. for</u> <u>Biomaterials & Bioengineering (CRC-I)</u>, Dept. Min-Met-Materials Engineering & Research Center CHU de Québec, Laval University, Québec City, Canada. <sup>3</sup> <u>National Research Council</u>— Institute of Condensed Matter Chemistry and Technologies for Energy, CNR ICMATE Lecco, Italy

INTRODUCTION: Bioabsorbadable sutures are in great demand for wound and incision closure applications. An ideal suture should be strong enough to sustain high stresses in heavily loaded tissues. Furthermore, it has to possess good ductility and elasticity to accommodate wound edema and recoil to the initial length with wound retraction. Presently, polymeric absorbable sutures have been licensed in medical Nevertheless, their strength and creep behaviour is not adequate for hard tissue applications. During the last decade, Mg has been widely investigated as a potential metal for medical applications. However, in the field of suture materials there are only few investigations on Mg. Indeed, alongside too fast and non-uniform degradation, its intrinsic poor ductility at room temperature makes the preparation of Mg wire more difficult through cold drawing process. Zn has been recently introduced as a potential metal due to its excellent biocompatibility, while its main constraint is insufficient mechanical properties. Hence, by improving the Zn mechanical properties through microstructure design and processing, many problems related to Mg could be solved. In this study, a novel Zn-Ag-Mn alloy wire is proposed as a potential degradable suture material.

**METHODS:** Zn-5.0Ag-0.5Mn (ZAM) alloy was developed by melting-casting process at 700°C. The alloy was then extruded at 350°C to obtain wires with a diameter of 2 mm. The wires were subsequently multi-pass cold drawn. Annealing was carried out at 270°C. The cold drawing and annealing treatment were performed down to a reduction of wire diameter of 0.15 mm. Microstructure of the wires was characterized using optical and scanning electron microscopy. Mechanical properties were assessed by tensile testing on cold drawn (CD) and annealed (AN) wires.

**RESULTS:** Fig. 1a shows that the AN wire exhibits remarkably refined grains alongside with the pronounced presence of secondary phases with

a wide size range of  $0.1\text{-}10\mu\text{m}$ . Fig. 1b clearly shows that the CD wire with a diameter of 0.15 mm can be easily tied into a closed knot.

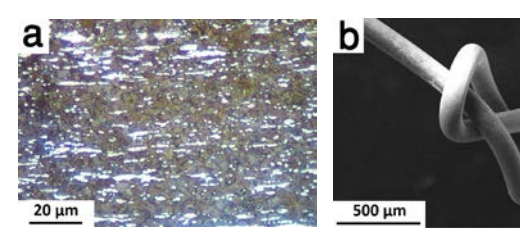


Fig. 1: (a) Microstructure of the AN wire and (b) view of a knotted CD wire with diameters of 0.15 mm.

Table 1 lists the mechanical properties of the investigated wires along with the other recently reported Zn and Mg wires. As seen, the wire before and after annealing exhibits markedly improved tensile strength and exceptionally high elongations. Such an outstanding combination of strength and ductility has not been reported in the literature thus far.

Table 1. Comparison of mechanical properties of the ZAM wires and reported Zn and Mg alloy sutures.

Material	Diameter (mm)	Tensile strength (MPa)	Elongation (%)
ZAM (CD)	0.26	$378 \pm 9$	$23 \pm 5$
ZAM (AN)	0.26	$323 \pm 1$	$42 \pm 2$
Zn0.2Li [1]	0.25	220	24
MgCa0.8 [2]	0.27	$235 \pm 9$	9 ± 4

**DISCUSSION & CONCLUSIONS:** In this study, Zn-5.0Ag-0.5Mn alloy is proposed as a promising candidate for degradable suture applications. Results revealed that in addition to its proper degradation rate, the extraordinary combination of strength and elongation make this alloy suitable for high surface per volume ratio applications.

**ACKNOWLEDGEMENTS:** The authors would like to thank G. Carcano (CNR ICMATE Lecco)

### Microstructural evolutions of homogenized and as-extruded MgSnZnMn alloy

LD Hou $^{\! 1}$ , Y Pan $^{\! 1}$ , Z Li  $^{\! 1}$ , H Zhao  $^{\! 2}$ , JH Su  $^{\! 1}$ , LK Hu  $^{\! 1}$ , YF Zheng  $^{\! 1,3}$ , L Li  $^{\! 1}$  \*

<sup>1</sup> <u>Center for Biomedical Materials and Engineering</u>, Harbin Engineering University, Harbin, China <sup>2</sup> <u>Hospital of Heilongjiang Province</u>, Harbin, China <sup>3</sup> <u>Department of Materials Science and Engineering</u>, College of Engineering, Peking University, Beijing, China

**INTRODUCTION:** Mg-3Sn-1Zn-0.5Mn alloys were newly developed with the aim of being suitable biodegradable metal for degradable implant applications. As-extruded Mg-3Sn-1Zn-0.5Mn alloy was prepared and the microstructure and interfacial structure of twin performance have been investigated comprehensively.

**METHODS:** A cylindrical billet of 40 mm in diameter and 250 mm in length was machined from the cast ingot. After homogenization at 723 K for 24 h, the homogenized ingots were put into a chamber with a diameter of 40 mm, and then were extruded to round bars with a diameter of 14 mm at an extrusion ratio of 8. Forward extrusion was adopted at a temperature of 643 k, with an extrusion rate of 1.5m/min. The microstructure characteristics was analysed by the optical microscopy (OM) and the transmission electron microscope (TEM) technique.

**RESULTS:** Fig. 1 shows optical micrographs of Mg-3Sn-1Zn-0.5Mn alloys. Fig. 2, Fig. 3 and Fig. 4 show TEM micrographs of Mg-3Sn-1Zn-0.5Mn alloys.

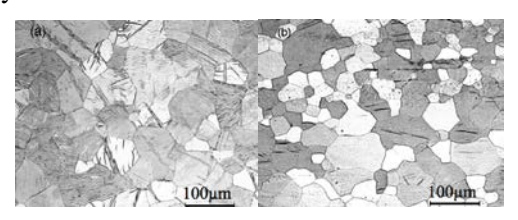


Fig. 1: OM microstructure of Mg-3Sn-1Zn-0.5Mn alloys under two conditions: (a) homogenized, (b) as-extruded

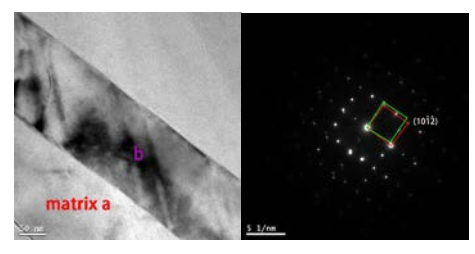


Fig. 2: TEM micrographs of homogenized Mg-3Sn-1Zn-0.5Mn alloys including bright field images and SAD patterns.

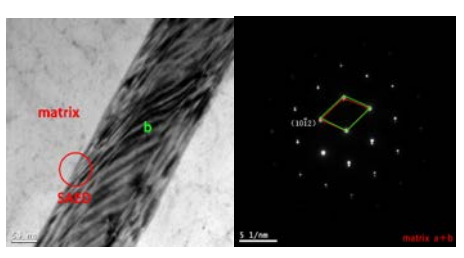


Fig. 3: TEM micrographs of as-extruded Mg-3Sn-1Zn-0.5Mn alloys including bright field images and SAD patterns.

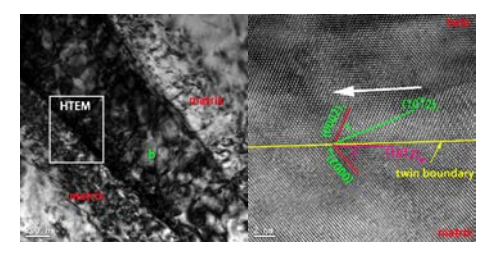


Fig. 4: TEM micrographs of as-extruded Mg-3Sn-1Zn-0.5Mn alloys including bright field images and HRTEM patterns.

**DISCUSSION & CONCLUSIONS:** In the homogenized status and as-extruded status, the orientations of twins in Mg-3Sn-1Zn-0.5Mn alloy

are all  $\{10\overline{1}2\}$  <  $10\overline{1}1$ >. In Fig. 2 SAD patterns, the discrepancy between the angle of diffraction spots is due to the existence of defects in the

 $\{10\overline{1}2\}$  twin boundary. The defect is due to the dislocation accumulation in the twin boundaries during plastic deformation process.

As-extruded Mg-3Sn-1Zn-0.5Mn alloys with fine equiaxed grain underwent complete dynamic recrystallization. The HRTEM image of the twin boundary between the internal twins indicates that

it is a planar, stress-free boundary, and  $\{10\overline{1}2\}$  twin boundary in as-extruded alloy is not in the

 $\{10\overline{1}2\}$  twinning plane with large angle deviation.

**ACKNOWLEDGEMENTS:** The Fundamental Research Funds for the Central Universities.

#### Microstructure stability of Mg-Y alloys with Zn or Ag

V Kodetova, B Smola, I Stulikova, H Kudrnova, M Vlach, T Kekule

Faculty of Mathematics and Physics, Charles University, Prague, Czech Republic

INTRODUCTION: Volume fraction, orientation and distribution of the long period ordered structure (LPSO) play a significant role in modulating the mechanical performance of Mg alloys with Y and Zn. LPSO phases with structural blocks of 5-8 close-packed atomic planes form various types with different numbers of atomic planes in the structural block and with different stacks of the blocks. The 18R metastable phase transforms during a thermal treatment into a stable 14H phase and both are the most frequently observed ones. Both Zn and Ag additions lead to a decrease of stacking fault (SF) energy and promote formation of basal planar defects, whereas Y stabilizes the long periodicity of LPSO phases.

**METHODS:** Mg-Y alloys with Zn and Mn - Mg4Y1Zn1Mn (WZM411), Mg3Y2Nd1Zn1Mn (WEZM3211) and Mg-Y alloys with Zn addition - Mg2Y1Zn (WZ21), Mg2Y1Nd1Zn (WEZ211) were squeeze cast in Ar + 1% SF $_6$  atmosphere. Materials alloyed by 1 Ag - Mg2Y1Nd1Ag (WEQ211) and Mg4Y2Nd1Ag (WEQ421) (all figures in wt.%) were gravity cast. Microstructure and its development by heat treatment were studied and compared to physical and mechanical properties.

**RESULTS:** Grain size of the cast alloys ranges from 50 to 100 μm. Melt cooling resulted in segregation of grain boundary eutectic (Fig. 1a) or eutectic particles. The only exceptions were the WZ21 and the WEQ421 alloys, but particles of LPSO decorate grain boundaries in the WZ21 cast alloy – Fig. 1b. It proved that Zn, Ag and Nd suppress solubility of Y in Mg. Nanoscale basal precipitate plates were observed in all as cast states. They tend to cluster in normal direction to basal plane and are thus structure units/precursors to the LPSO – see Fig. 2. The basal plates develop from SF by ordered embedding of Y and Zn or Ag.

The transient 18R LPSO transforms into the stable 14H structure during isochronal annealing up to ~ 350°C and higher and basal plate density decreases. It influences mechanical properties indistinctly and is connected with a slight heat flow. The LPSO structure develops even during long high temperature annealing at 500°C in the WZM411 and WEQ211 alloys and temperature 525°C is necessary to dissolve these particles.

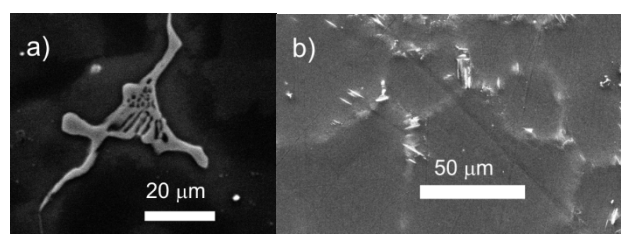


Fig.1: a) Grain boundary eutectic in cast WEQ211 alloy. b) Particles of the LPSO along grain boundaries of the cast WZ21 alloy

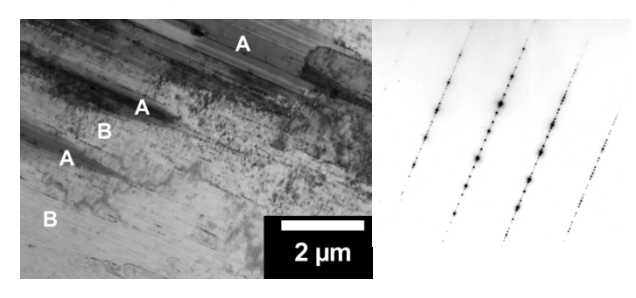


Fig.2: A-18R long period stacking structure,  $B-\alpha$ -Mg matrix with basal plates of LPSO structure units in the cast WZM411 and electron diffraction from 18R LPSO, [11-20]  $\alpha$ -Mg zone.

**DISCUSSION & CONCLUSIONS:** Solutes Zn and Ag are promising candidates in Mg alloys due to their antibacterial effects. The LPSO structure inherent to Mg alloys with small amount of Zn or Ag improves hardness only moderately. But these structures can deteriorate biocorrosion essentially as observed e.g. in the WEZM3211 alloy. Very long high temperature thermal treatment is necessary to dissolve these structures. Addition of Nd depresses formation of the 18R LPSO particles. Individual very thin basal plates with SFs image attributes ( $\gamma$ 'or  $\gamma$  phase of the Mg-Y-Zn sequence) exist in grain interiors of all alloys.

**ACKNOWLEDGEMENTS:** Financial supports by the Czech Science Foundation (GACR), project No. 16-12828S and by the Specific Academic Research Projects (No. 260 449) of the Charles University are gratefully acknowledged.

### Mg-1Ca bone screws designed by FEA method and pullout strength testing

X.C. Zhou<sup>1</sup>, Y.F. Zheng<sup>1,\*</sup>, Liqun Ruan<sup>2</sup>

<sup>1</sup><u>Department of Materials Science and Engineering,</u> College of Engineering, Peking, University, No.5 Yi-He-Yuan Road, Hai-Dian District, Beijing 100871, China, <sup>2</sup><u>Faculty of Engineering,</u> Kumamoto University, 2-39-1 Kurokami, Kumamoto 860-8555, Japan

INTRODUCTION: Bone screws and plates are used to treat bone fractures. In many cases, they need to be removed after the bones are healed. In order to avoid second surgery, bone screws made of biodegradable metals are studied to replace traditional bio-inert ones. Traditional bio-inert bone screws tend to have thin threads because it's easier to be screwed into the bone while the fixation is stable after the implantation. Magnesium and its alloys have similar elasticity moduli with human bones which leads to less stress shielding. Their degradation products are non-toxic and magnesium ions will facilitate bone healing. All these advantages make magnesiumbased alloys promising materials for bone screws. Mg-1Ca alloy was chose in this work.

METHODS: The threads disappeared quickly [Nina et al., 2011] and the screw would lose its holding power before the bone was healed. For better fixation, magnesium-based bone screws should have thicker threads than traditional bioinert ones. Based on the parameters of bio-inert and biopolymer bone screws, the thread width was increased and an initial Mg-1Ca bone screw geometry model was built using Pro/Engineer. Then the model was imported into Hypermesh to generate the mesh. At last the mesh was imported into Abaqus for pullout strength analysis. Experiments were carried out using Mg-1Ca alloy screws and 20# rigid polyurethane foam provided by SAWBONES according to ASTM standards.

**RESULTS:** During the pullout process, bone elements near the peripheries of the screw's threads gradually reach their maximum strength (Fig 1(a)). When the contact force between the bone and screw reaches its maximum, the screw will be pulled out from the bone. The maximum contact force equals pullout strength. For the screw, large stress concentrates in the core (Fig 1(b)). But pullout strength was provided mostly by the threads, the maximum stress locates between the core and the proximal surface of the

threads. For orthopedics, thin threads provide large pullout

strength. But for degradable Mg alloys, the threads must be thickened to provide mediumterm fixation. Fig 2 shows the simulated and experimental results of pullout strength. Not all the experimental results match the simulated one. There are two important reasons: the synthetic bone isn't homogeneous and the screw was screwed into the bone by handwork.

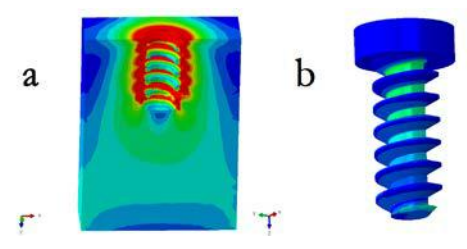


Fig. 1: a, Mises stress contour plot of bone; b, Mises stress contour plot of screw.

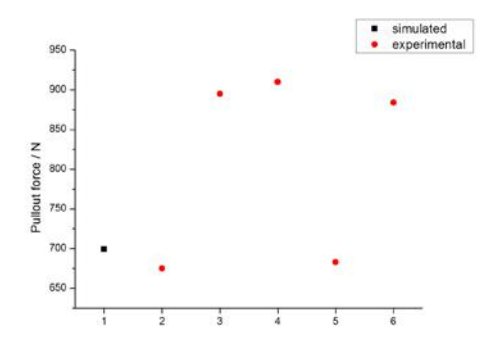


Fig. 2: Simulated (black) and experimental (red) results of pullout strength.

**DISCUSSION & CONCLUSIONS:** Many screw's parameters affect the pullout strength such as pitch and thread width. Pullout strength is not the only criterion for the mechanical property of bone screw. Due to the existence of degradation, the design of Mg-based alloy screws would be quite different from traditional bio-inert metal ones to achieve medium-term fixation.

### Microscopic study of corrosion process of fine Mg structures

H. Hornberger<sup>1</sup>, C. Mayer<sup>1</sup>, F. Witte<sup>2</sup>

<sup>1</sup> <u>Lab biomaterials, faculty mechanical engineering</u>, OTH Regensburg, Germany. <sup>2</sup>, <u>JW Institute</u> and Centre for musculoskeletal Surgery, Centre for regenerative Therapies, Charité Berlin, Germany

**INTRODUCTION:** As known the challenge concerning Mg materials is the control of the degradation and corrosion process. The common corrosion testing procedures for biometals are based on the inert and corrosion resistant metals like titanium and or stainless steel. However, in case of Mg-materials, the corrosion rate has a different meaning, not an inverse measure of the corrosion resistance but a measure for manageable degradability. The aim of the study is to determine the advanced corrosion process of fine and fragile Mg structures, as the corrosion rate may vary strongly depending on the method applied [1]. Furthermore, the corrosion rates of scaffolds and inhomogeneous structures cannot be studied using electrochemical methods used for Mg bulk sample surfaces [2].

**METHODS:** For the study Mg scaffolds and Mg foils were immersed in corrosive NaCl solution. In various time intervals the samples were removed and carefully dried. The samples before and after immersion tests were studied by a  $\mu$ -computed topography (CT) Phoenix v|tome|x. The portion of porosity was analysed using the software VG Studio max Volume Graphics.

**RESULTS:** The structure of scaffolds and foils before and after the corrosion process takes place are monitored by  $\mu$ -CT, Fig. 1. The determination of the corrosion rate is complicated if components and sample structures become smaller, parts of the

structures disappear and new topographic structures arise due to inhomogeneous corrosion.

The increasing degradation rate correlates with increasing surface area per volume.

**DISCUSSION & CONCLUSIONS:** In this study Mg scaffolds and foils are studied by  $\mu$ -CT in order to show the interaction of electrolyte with fine fragile Mg structures.

**ACKNOWLEDGEMENTS:** We would like to acknowledge the help from frank Witte.

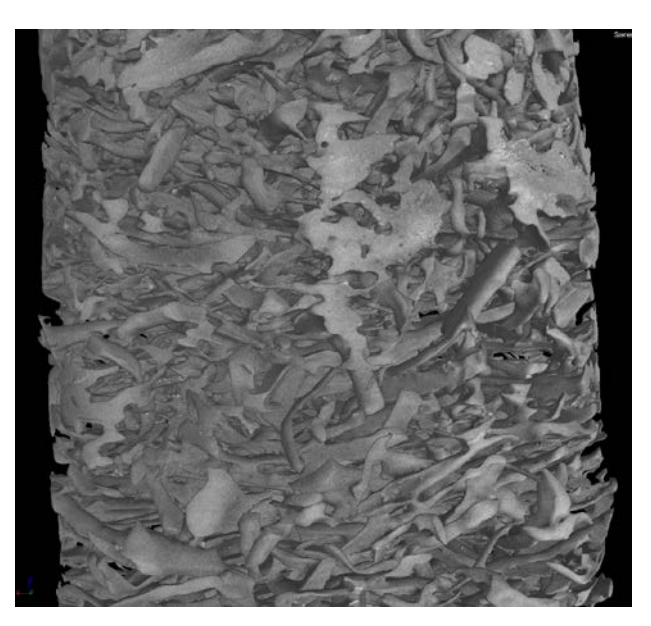


Fig. 1: μ-Computer-topography of Mg scaffold

# Fully biodegradable pla/mg composites obtained by colloidal techniques as feedstock for a variety of implant shapes

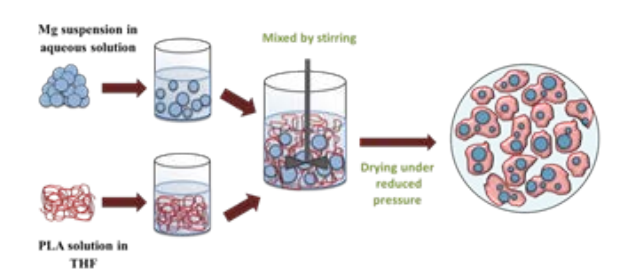
A. Ferrandez, 1,2 B.Ferrari, M. Lieblich, M. Multigner, JL Gonzalez-Carrasco 1,4

<sup>1</sup>CENIM-CSIC, Spain, <sup>2</sup>ICV-CSIC, Spain, <sup>3</sup> Rey Juan Carlos Univ, Spain, 4CIBER-BBN, Spain

INTRODUCTION: PLA/Mg composites have been suggested as a suitable bioabsorbable biomaterial where PLA and Mg cover for the other's limitations. With regards to the neat polymer. Mg particles improve mechanical properties, regulate cell behaviour inflammatory response, enhances the osteogenic commitment, and decrease bacteria viability, without altering physiological pH during in vitro degradation. Mg anticipates the degradation of PLA, thus processing conventional thermoplastic routes must restricted when considering composites with a high volume fraction of reinforcement.

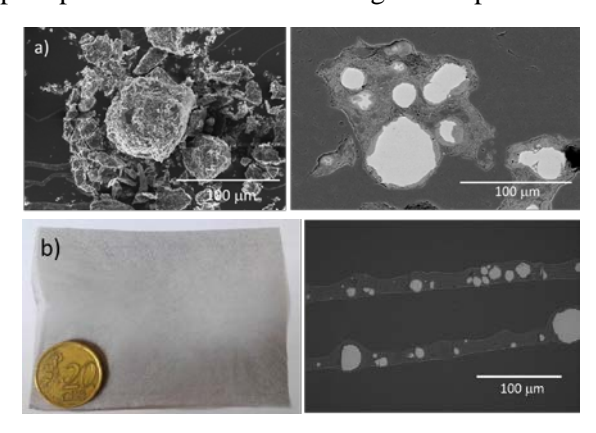
The aim of this work is to exploit the colloidal techniques to obtain homogenous blends of PLA and Mg microparticles at ambient temperature, avoiding the drawbacks associated to the thermal degradation of the polymer. Due the high reactivity of Mg, a careful control of initial suspension "structure" and its evolution during fabrication is required. Consolidation of colloidal suspensions into dense, homogeneous green bodies as granules, films, wires and 3D struck is the main objective of this work.

**METHODS**: The approach involves four basic steps: (1) suspension preparation, (2) consolidation into the desired component shape, (3) removal of the solvent, and (4) densification to produce the final microstructure and shape required for optimal performance.



**RESULTS:** The Mg surface colloidal behavior was controlled by adding PEI to the suspension at pH 11-12. Tetrahydrofuran (THF) was used as solvent of PLA. Strong agitation of PLA solutions

and Mg suspensions was used to prevent precipitation of PLA. Processing of composites



with a wide range of Mg content was engineered to obtain granules in the microscale (adding small amount of water) or films by tape casting.

Fig.1 SEM micrographs of a) granules of PLA/35Mg, and b) films pf PLA/50Mg



Granules of PLA/Mg composite were extruded to obtain wires of 2 mm in diameter that can be used, for instance, to fabricate scaffolds of controlled porosity.

Fig. 2 SEM micrographs of wires and scaffolds

**CONCLUSIONS:** Colloidal processing techniques provide good dispersion of Mg micro particles and higher control of the microstructure since all of them remain fully surrounded by polymer, avoiding the drawbacks associated to the thermal degradation of the polymer when using thermoplastic routes.

**ACKNOWLEDGEMENTS:** MAT2015-63974-C4-1 from MINECO and MULTIMAT Challenge: S2013/MIT-2862 (CM) are acknowledged.

# Additive manufacturing of pure Zn by selective laser melting: improving process stability for porosity reduction

L Monguzzi<sup>1</sup>, AG Demir<sup>1</sup>, B Previtali<sup>1</sup>

<sup>1</sup>Department of Mechanical Engineering, Politecnico di Milano, Milan, Italy.

INTRODUCTION: The union of additive manufacturing techniques with biodegradable metals appears as a natural evolution of the technology for next generation of customized implants. Laser based additive manufacturing methods, which provide high precision and geometrical freedom, rely mainly on the fusion of powder feedstock. Selective laser melting (SLM) is one of these processes, where the laser scans a powder bed, fusing the build part layer by layer. Pure Fe and Fe-based alloys are processed stably, since the process is well-established for similar materials used for other industrial applications. Mg and its alloys constitute further difficulties due to their high reactivity. A certain peculiarity of Zn and its alloys is their very low melting and vaporization points. This renders the process highly unstable and high fractions of porosity have been observed within the process. This underlines the fact that novel solutions in terms of process equipment have to be developed in order to achieve high density components in pure Zn and Zn-alloys. This work describes the developed solutions to achieve pure Zn parts with >99% density using SLM.





Fig. 1: High speed camera images showing the powder bed a) at the start of the process and b) during the scanning.

**METHODS:** Pure Zn powder was use throughout the study with 15 μm average size (Metalpolveri, Brescia, Italy). An open SLM platform, namely

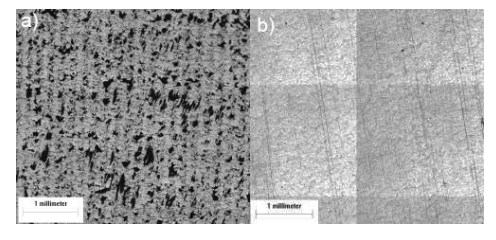


Fig. 3: Cross section of SLM produced pure Zn with  $F=22 \text{ J/mm}^3 F=67 \text{ J/mm}^3$ .

Powderful, was used for the experiments, which could be modified for processing under different atmospheres<sup>2</sup>. A multimode active fiber laser (IPG Photonics YLR-1000, Cambridge, MA, USA) was the energy source coupled to a scanner head producing (El.En. Scan Fiber, Florence, Italy) producing a 212 µm spot size on the material surface. The powder bed was built in house Videos were acquired with a high speed camera (Fastcam synchronous with Mini AX200) external illumination (Cavilux HV) to assess the process instabilities.

**RESULTS:** Due to the very low vaporization point, pure Zn vapour and powder accumulates into the process chamber. This results in the scattering of the laser beam before reaching the powder bed. Hence, complete fusion is not possible. At a single layer level, the high-speed images showed that the high pressure gradient generated around the scanning laser beam pushes the powder away from the process zone. Resultantly, the laser beam melts only the substrate or the previous layer (see Fig.1). Stable processing conditions could be achieved by processing in open atmosphere and using a side gas jet along with a fume extractor. By the correct adjustment of fluence (see Fig.2), fully dense specimens size could be achieved (see Fig.3).

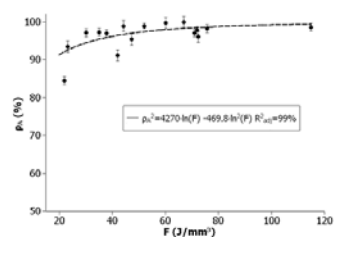


Fig. 2: Apparent density as a function of fluence.

**DISCUSSION & CONCLUSIONS:** Most of the current industrial SLM system lack flexibility in the management of atmospheric conditions. Further development of processing strategies is essential for realization of thin structures, essentially required for lattice structures and stents.

**ACKNOWLEDGEMENTS:** El.En, Taglio, and BLM are gratefully acknowledged for the technical support provided during the project.

### Optimisation of the corrosion rate of iron-based alloys for bioresorbable stent applications by surface acidification

S Reuter<sup>1</sup>, C Georges<sup>2</sup>, P J Jacques<sup>1</sup>

**INTRODUCTION:** Biodegradable materials progressively become of interest for stent applications. Indeed, a stent has fulfilled its task after 6-12 months and is therefore not needed anymore. Bioresorbable stents could be a way to prevent late complications such as late thrombosis A: Stents need to be mechanically strong, making steel a good candidate. However, its corrosion rate is too low. Furthermore, during the corrosion of the stent in the blood environment, different layers form on top of the metal, hindering the oxygen diffusion towards the metal. A way to increase the corrosion rate thus needs to be found. The pH of the environment greatly influences the presence of these layers; an acidic pH favours their dissolution, which could help in activating the corrosion. However, the blood environment needs to keep a pH close to physiological pH (7.4) and thus only the near stent surface can undergo an acidification without affecting the blood system too much. The present work investigates the influence of hydrogen in Febased alloys on the corrosion rate.

**METHODS:** Hydrogen charging was conducted either electrochemically or thermally on Fe-based alloys. The influence of the hydrogen concentration as well as the presence or not of hydrogen traps on the corrosion mechanism in SBF (simulated body fluid) is assessed by means of immersion tests. These tests allow to mimic closely what happens *in vivo*. Potentiodynamic polarisation tests were also conducted to highlight the influence of the chemical composition on the corrosion rate. Tensile tests were also carried out.

**RESULTS:** The content of hydrogen influences the corrosion rate in a way highlighted by immersion tests and characterization of the surface layers.

#### DISCUSSION & CONCLUSIONS:

Bioresorbable stents made of steel could become a solution to avoid late complications due to the presence of a foreign body in the blood environment. In order to accelerate the corrosion

of steel, surface acidification could be implemented, leading to a dissolution of the corrosion layers that hinder the oxygen transport and thus decreasing the corrosion rate.

**ACKNOWLEDGEMENTS:** The FRIA and ARC are thanked for funding this research.

<sup>&</sup>lt;sup>1</sup> <u>Université catholique de Louvain, Institute of Mechanics,</u> Materials and Civil Engineering, IMAP, Louvain-la-Neuve, Belgium <sup>2</sup> <u>Centre for Research in Metallurgy – CRM Group</u>, Liège, Belgium

## Transmission electron microscopy study of the early-stage biocorrosion events in magnesium-based lean alloys

M. Cihova<sup>1</sup>, K. von Petersdorff-Campen<sup>1</sup>, R. Schäublin<sup>1,2</sup>, P. Schmutz<sup>3</sup>, J. F. Löffler<sup>1</sup>

<sup>1</sup> <u>Laboratory of Metal Physics and Technology</u>, Department of Materials, ETH Zurich, 8093 Zurich, CH; <sup>2</sup> <u>Scientific Center for Optical and Electron Microscopy</u>, ETH Zurich, 8093 Zurich, CH; <sup>3</sup> <u>Laboratory of Joining Technologies and Corrosion</u>, EMPA, 8600 Dübendorf, CH.

**INTRODUCTION:** While the impact of the microstructure on the corrosion of magnesium alloys is generally well acknowledged, the underlying mechanisms are still not well understood. In particular, its role for the initiation of localized corrosion is debated. Its investigation is especially challenging for lean alloys due to their very low intermetallic phase fraction of <1 % and submicrometric intermetallic particles (IMPs). One candidate of such Mg-lean alloys is the rareearth element (REE)-free MgZn1.0Ca0.3 (in wt.%), named ZX10, which is promising due to its attractive mechanical and corrosion properties. For the characterization of microstructure-corrosion relations of this material high spatial resolution is required, which can be achieved by (scanning) transmission electron microscopy ((S)TEM). Such analysis allows obtaining chemical and structural information on the microstructure, including the structure and composition of the secondary phases, as well as on the formed corrosion products.

**METHODS:** Heat-treated (HT) ZX10 was chosen as a model system. HT parameters were defined to obtain specimens with only one of the possible IMPs, i.e. either the binary Mg<sub>2</sub>Ca or the ternary IM1 phase with composition Ca<sub>3</sub>Mg<sub>x</sub>Zn<sub>15-x</sub>  $(4.6 \le x \le 12$ , in at.%), while keeping the overall composition constant. Detailed microstructural characterization was performed in TEM (FEI Talos®, ScopeM) and high-resolution STEM (FEI Themis<sup>®</sup>, CIME EPFL Lausanne), both equipped with an energy-dispersive X-ray spectrometer (EDX). The initial corrosion events upon immersion in simulated body fluid were studied using both ex situ and quasi-in situ corrosion methods. While the former was performed in cross-sectional TEM (xTEM) of bulk specimens, standard TEM 3 mm discs were used for the latter. In both cases, electron transparency was obtained by ion milling.

**RESULTS:** STEM/EDX analysis confirmed the temperature-dependent microstructure of ZX10 as predicted from thermodynamic calculations. After the *ex situ* immersion, a multilayer corrosion film, as suggested in literature is observed in xTEM

(Fig. 1). Moreover, the individual layers differ not only in their chemical composition but also in their structural properties: a highly porous Mg-and O-rich layer at the ZX10 interface covered by an outer dense Ca-P-rich layer is observed. Time-resolved investigation suggests a steady increase of the porous-layer thickness, whereas the Ca-P-rich layer thickness remains constant and appears to depend mainly on the immersion conditions.

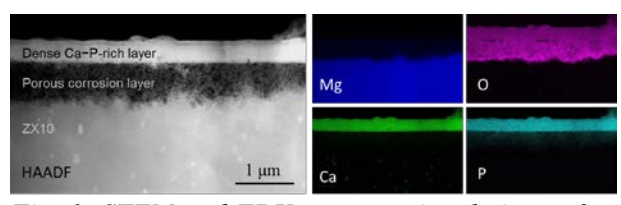


Fig. 1: STEM and EDX cross sectional views of a ZX10 surface corroded by simulated body fluid.

The *quasi-in situ* corrosion study reveals that grain boundaries are preferentially attacked whereas the ternary IMPs are protected from anodic oxidation. The latter suggests the cathodic activity of the IM1 phase, where the hydrogen-reduction reaction is facilitated. Despite the small volume fraction of grain boundaries and IMPs, both microstructural features appear to initiate localized corrosion and thus govern the early-stage corrosion in ZX10.

**DISCUSSION & CONCLUSIONS:** (S)TEM equipped with an EDX detector proves to be a powerful tool to study the initial corrosion events as a function of the underlying microstructure even if the instability of the corrosion products in the electron beam makes their structural characterization challenging. Despite their low volume fraction, the grain boundaries and IMPs determine the initial corrosion events in the Mglean alloy ZX10.

**ACKNOWLEDGEMENTS:** The authors acknowledge support by the Swiss National Science Foundation (SNF Grant No. 200021-157058) and by the Scientific Centre for Optical & Electron Microscopy (ScopeM) at ETH Zürich.

### Comparison of electrochemical behavior of Fe and Fe-Mn alloy for biomedical application

P Kunert<sup>1</sup>, R Toulova<sup>2</sup>, D Mantovani<sup>2</sup>, K Hueskers<sup>3</sup>, <u>WD Mueller<sup>1</sup></u>

1 <u>Charité Universitaetsmedizin</u> Berlin, D, <sup>2</sup> <u>Laval University</u> Quebec, CAN, <sup>3</sup> <u>Institute Medical</u>

<u>Diagnostic</u> Berlin, D

**INTRODUCTION:** Fe pure and Fe-alloys are of interest for biomedical application because of their metallic properties and the biological acceptance of their metal ions create during degradation. Because of the fact that electrochemical measurements have the opportunity to mimic in vivo near conditions, it is of interest to assess their electrochemical behavior. The Mini Cell System (MCS) has demonstrated its advantages therefore, especially in case of development of new alloys and or testing of modifications in vitro. The aim of this work was to assess and to compare the electrochemical behavior of Fe pure with a Fe-Mn alloy. Pure Fe and a Fe-Mn-C alloy were investigated.

**METHODS:** Specimens were applied delivered, only soft surface treatment were performed clean to the surface. The electrochemical measurements were made using the MCS connected to a potentiostate in three different electrolytes, Ringer solution pH 1, Ringer solution pH 7.4 and cell culture medium (BMEM) pH 7.4. The protocol was changed in contrast to measurements. The open measurements were made up to 7500s, followed by first cyclic voltammograms with  $\pm$  500 mV around EOCP additionally second voltammograms in a range between -0.75 and +1.0 V vs. SCE. Roughness measurements and analysis of the material loss after cyclic loading were performed with a 3D surface analyzing system (IF-Alicona). At least a surface analysis by SEM/EDX were made. The solution was analyzed by ICP MS. **RESULTS:** Fig 1 presents a collection of  $E_{OCP}$  vs. t curves where at pH 1 hydrogen evolution can be observed, visible in the curves at breaks during the measurements. As the I vs. E curves show, to see in Fig.2., typical differences are seen depend on the kind of electrolyte and the pH. Interesting are the cyclic voltammograms which clear show characteristic differences as well in the CV 1 as in the CV 2 conditions. At last the oxidation is cell culture solution a little depressed obviously because of the phosphate content of BMEM. In comparison between Fe pure and Fe-Mn alloy the last is even more electrochemically active in BMEM as Fe pure. The surface analysis shows clear under strong oxidation conditions a not

uniform degradation, spots and little islands in the spot are observable.

**DISCUSSION & CONCLUSIONS:** In both cases the chloride ion concentration is strong interacting with the material and try to solve the oxidized parts at the surface. In case of BMEM the phosphate content blocked the surface by building related phosphate compounds which are less soluble as the chlorides.

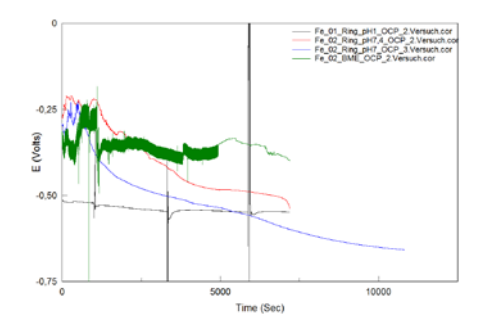


Fig. 1:  $E_{OCP}$  vs. t curve for Fe-pure in ringer solution at pH 1(black) and pH 7.4 (red and blue) and in BMEM at pH 7.4(green).

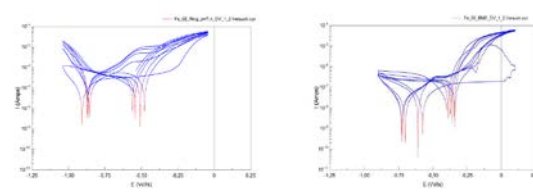


Fig. 2: cyclic I vs E curves for Fe-pure in ringer solution at pH 7.4(left) and in BMEM at pH 7.4 (right).

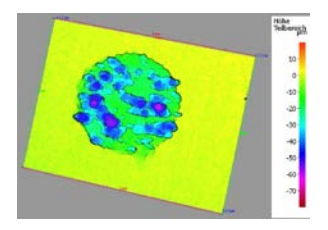


Fig. 3: If 3D image of degradation after electrochemical treatment in BMEM at pH 7.4, pitting is clear to see.

The degradation rate of Fe-Mn alloy is higher as the Fe-pure. The degradation under mild conditions is more or less homogeneously. In BMEM the degradation is slowly as in pure chloride containing electrolytes.

### Formation of corrosion layers on Mg in cell culture medium under different conditions

V Wagener<sup>1</sup>, S Virtanen<sup>1</sup>, C

<sup>1</sup> <u>Chair for Surface Science and Corrosion</u>, Department of Materials Science, University of Erlangen-Nuremberg

**INTRODUCTION:** The formation of calcium-phosphate structures on Mg in cell culture medium (CCM) is a well-known phenomenon. At the same time, a dark grey layer is formed under the Ca-P precipitations that is supposed to consist also of Ca-P. The aim of this study is to investigate the influence of different immersion parameters on the layer morphology and thickness and on corrosion resistance of the formed layer.

**METHODS:** Cp Mg samples were immersed for 1, 3 and 5 days CCM at room temperature (RT) under atmospheric conditions and in the incubator at 37°C with 5% CO<sub>2</sub>. To investigate the influence of the presence of proteins, fetal calf serum (FCS) was added to CCM in the incubator. Formed layers were analysed by cross-sectional SEM images, EDX and electrochemical measurements (impedance spectroscopy and potentiodynamic polarization).

**RESULTS:** SEM images of cross-sections after 3d immersion in CCM under the different conditions are shown in Fig. 1 a), b) and c). While an outer dense layer is formed at RT, completely porous structures are observed in the incubator with and without FCS. Layer thicknesses stay in the same range for the immersion at RT, while in the incubator layer thicknesses increase strongly over time (Fig. 1f). The addition of FCS reduces the dimensions of the layer. Electrochemical measurements (Fig. 1d and e) show a strong increase in corrosion resistance for the layers formed at RT. For layers formed in the incubator, corrosion behaviour is similar to cp Mg.

**DISCUSSION & CONCLUSIONS:** Enhanced corrosion resistance for immersion in CCM at RT is mainly due to the formation of a compact outer layer, while layers formed in the incubator are completely porous and do not improve the corrosion behaviour. The porous structures are supposed to be caused by hydrogen evolution due to Mg dissolution. As the CCM is not strongly buffered under atmospheric conditions, significant pH increase is taking place, leading to a self-limitation of Mg corrosion. The self-limitation is also the reason for stable layer thicknesses at RT. As the formation of Ca-P is triggered by the release of Mg ions, layer thicknesses increase

strongly in the incubator where corrosion is not self-limited due to good buffering by higher CO<sub>2</sub> concentration.

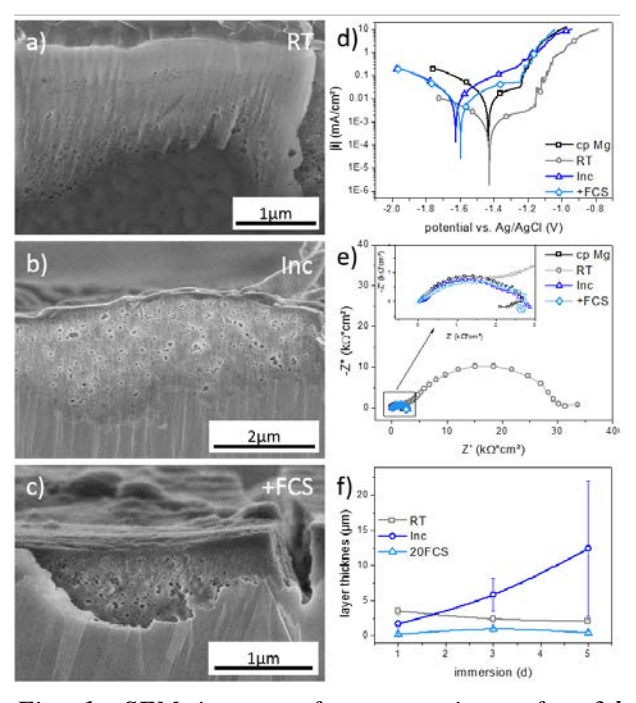


Fig. 1: SEM images of cross-sections after 3d immersion in CCM at RT (a) in the incubator (b) and in the incubator with the addition of FCS (c). Corresponding results of potentiodynamic polarization (d) and EIS (e). Development of layer thicknesses are shown in (f).

Layer dimensions are reduced significantly for the addition of FCS, as the formation of Ca-P is affected due to protein attachment (proved by XPS).

**ACKNOWLEDGEMENTS:** The authors thank DFG for funding.

### Influence of process condition on in vitro corrosion of fine resoloy wire

AJ Griebel<sup>1</sup>, JE Schaffer<sup>1</sup>, R Menze<sup>2</sup>, M Stekker<sup>2</sup>, B Bittner<sup>2</sup>

<sup>1</sup> Fort Wayne Metals, Fort Wayne, IN, USA. <sup>2</sup> MeKo Laser Material Processing, Sarstedt, Germany

**INTRODUCTION:** When absorbable metal devices become ubiquitous in the clinic, Mg alloy wire will play a key role in enabling functional forms such as staples, sutures, and peripheral stents.

Recent works have demonstrated the feasibility of producing such wires out of magnesium alloys, as well as assessed properties like tensile strength and fatigue<sup>1-3</sup>. One promising alloy is Resoloy®, a Mg-Dy-based alloy developed by MeKo for absorbable stents. While significant *in vitro* corrosion testing of laser-cut Resoloy stents has been conducted, there is a lack of corrosion data for Resoloy wire. Here, the influence of wire process conditions on *in vitro* corrosion is studied.

**METHODS:** Conventional cold wire-drawing practices were employed to produce 0.25 mm Resoloy wire with various thermomechanical process (TMP) conditions. Wires were drawn with 50% cold work followed by thermal treatment at 250, 350, 400, 450, or 500°C, providing a range of microstructures and tensile properties.

To assess impact of TMP condition on corrosion, two modes of corrosion testing were used. First, 4.0 mm lengths of wire were immersed each in 250 ml PBS (pH = 7.4) at  $37^{\circ}$ C for up to 45 hours (N = 4). Second, wire coils were placed into silicone tubing with flowing  $37^{\circ}$ C PBS for 45 hours, with images recorded every minute.

**RESULTS:** Tensile properties for each condition can be seen in Table 1.

*Table 1. Tensile properties of 6 TMP conditions.* 

Condition	UTS (MPa)	YS (MPa)	Elongation (%)
50% CW	495	474	2.0
250°C	568	550	2.3
350°C	524	498	5.2
400°C	429	412	11.6
450°C	348	317	18.3
500°C	330	258	17.6

Static corrosion testing reveals an increased corrosion rate for the 450°C and 500°C conditions (Fig. 1), per measurement of dissolved Mg<sup>2+</sup> per initial surface area over time. Dynamic corrosion testing of 250 and 500°C conditions gave increased rates compared to static (0.046 vs 0.020 mg/mm<sup>2</sup> for 250°C, 0.043 vs 0.035 mg/mm<sup>2</sup> for 500°C).

After 45 hours, the wires had blackened but were intact (Fig. 2). Notably, while the mean rate of corrosion was increased in dynamic corrosion as compared to static, the difference between the 250°C and 500°C conditions was reduced in dynamic corrosion.

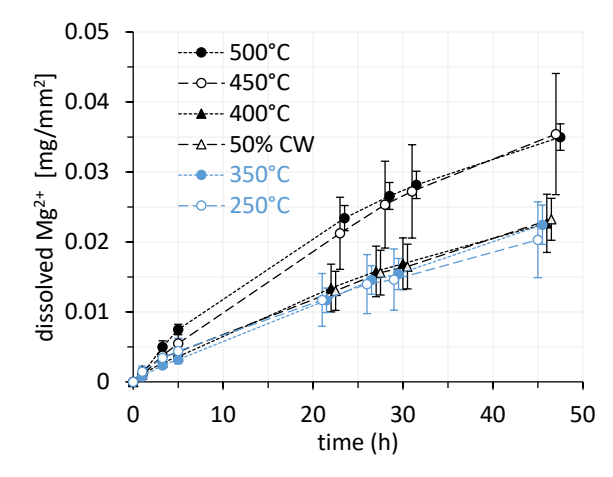


Fig. 1: Static corrosion of the 6 TMP conditions.

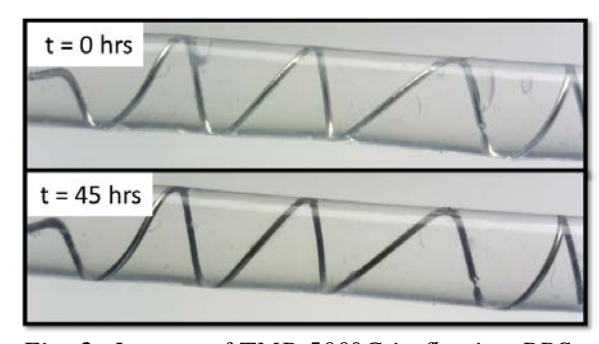


Fig. 2: Images of TMP 500°C in flowing PBS at 0 and 45 hours of corrosion.

**DISCUSSION & CONCLUSIONS:** Corrosion testing is ongoing to further explore the impact of TMP condition as well as static vs dynamic media. Interestingly, the 450 and 500°C conditions corrode more quickly in static but not dynamic flow conditions. Future work should include *in vivo* testing and could use similar techniques to assess the impact of coatings.

**ACKNOWLEDGEMENTS:** Resoloy® has been developed and registered by MeKo and Helmholtz-Zentrum Geesthacht

### Facing phenomenological problems of protective coating layers on bioresorbable materials

P Hiester<sup>1</sup>, A Kopp<sup>1</sup>, N Zumdick<sup>2</sup>, D Zander<sup>2</sup>

<sup>1</sup> <u>Meotec GmbH & Co. KG</u>, Aachen, Germany <sup>2</sup> <u>Lehrstuhl für Korrosion und Korrosionsschutz,</u> GI Aachen, RWTH Aachen University, Germany

INTRODUCTION: Coating layers provide the opportunity to adjust the rate of degradation of bioresorbable implants selectively and thus ensure the function of the implant. In most coating processes of components with complex geometries cavities characteristic problems inhomogeneous coating layer arise. The layer thickness decreases away from the component surface or the layer is not even applied on the entire surface. A successful protective coating requires a closed and homogeneous layer. This is accompanied by rounding off edges and corners which can reduce the effect of the implants intended function like blades or rivets. The plasma electrolytic oxidation (PEO) is a conversion process that transforms the surface of a light metal into its associated oxid-cereamic. As this is not a deposition process the coating can be applied on the outer surface as well as in cavities by using adjusted parameters.

**METHODS:** Magnesium scaffolds with channels widths of 0.4 mm - 0.8 mm were manufactured by EDM (electrical discharge machining). On these test specimen phosphate- and silicate-based electrolytes in combination with specific current forms were tested with the aim of applying a homogenous ceramic oxide layer on the outer surface as well as in the channels of the scaffold. In a next step, the sharpness of the edge of coated uncoated rivets, were tested. Rivets, manufactured by EDM (Fig 2.), were coated by PEO with various layer thickness. In a test setup with a tensile testing machine, coated and uncoated rivets were pushed a specific distance into artificial bones while measuring the required force. After the treatment, the specimens were investigated via SEM and cross section preparation.

**RESULTS:** The combination of a phosphorus electrolyte and low-frequency pulsed DC-current provided the best coating results (Fig.1). The cross sections indicate a porous, homogenous and closed coating with an average layer thickness of 15  $\mu$ m on the outer surface and 10  $\mu$ m layer thickness on the inner surface.

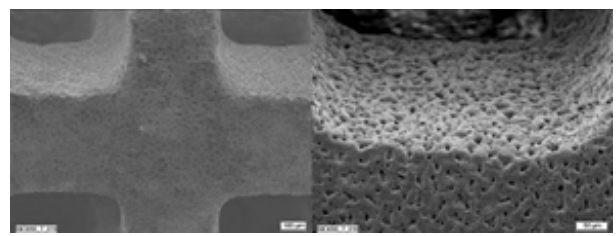


Fig. 1: Porous layer produced by PEO on a thinwalled scaffold with a channel width of 0.6 mm

The microscopic investigations of the magnesium rivets showed a closed and dense coating layer. The geometry although were altered as the edges and spikes were rounded by the layer (Fig.2.). The pressure testing revealed an increased average force of 30% for pushing the coated rivet into the bone the same distance. The force rises with increasing layer thickness.

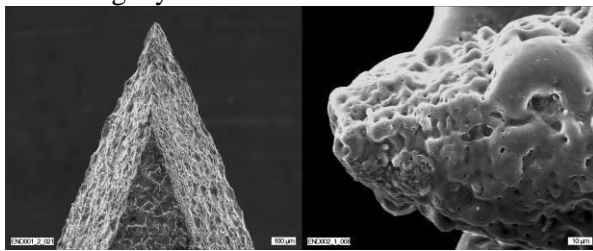


Fig. 2: left, magnesium rivet manufactured by EDM, right, rounded edge of rivet coated by PEO

#### DISCUSSION & CONCLUSIONS:

Phenomenological problems of protective layers on fast degrading components can be minimized by using the PEO-process. It is shown a method for the application of a homogenous and closed oxid-ceramic coating on complex geometries and narrow cavities that reduces the rate of degradation. Problematically appears the loss of sharpness caused by PEO, although it can be reduced by thinner layer thickness. Compromises between sufficient surface protection and an adequate function must be determined individually for each application.

### Effects of different coatings on a hollow magnesium-strontium scaffold for bone regeneration in critical-size long-bone defects

WD Wang<sup>1</sup>, LL Tan<sup>1</sup>, K Nune<sup>2</sup>, D Misra<sup>2</sup>, K Yang<sup>1</sup>

<sup>1</sup>Institute of metal research, CAS, Shenyang, P.R. China. <sup>2</sup> University of Texas at EI Paso, USA.

defects **INTRODUCTION:** Massive bone constitute a major challenge in orthopedic practice. Autografts are considered as gold standard, despite significant problems arising from limited amount of donor bone, donor-site morbidity and concaved due to the rapid absorption. Currently, a myriad of scaffolding materials are under investigation, among these the potential clinical applications of M alloys have attracted increasing interest, owing to the superior mechanical properties similar to the cortical bone than ceramic, polymer and most loadbearing metal-based orthopedic implants like titanium or stainless steel. However, the majority of the studied Mg alloys for orthopedic applications turn to the form of a solid monolith (bar or rod). The present work reports a hollow, cylindrical Mg-Sr scaffold cage with morselized bone filled inside, which is advantageous over its lightweight design while alleviating depression caused by the fast degradation of morselized bone as well as reducing the H<sub>2</sub> evolution amount

METHODS: Due to our previous work, the Mg-1.5wt.%Sr alloy was used after hot-extrusion and pickling the oxide scale during processing. Generally, various surface modification are designed with different clinical demands. In this study, three coating methods are selected including MAO, showing a relatively thick, dense and hard oxide coating which has excellent adhesion to the substrate and offers protection against wear and corrosion, and also Ca-P chemical deposition coating, as is considered to be bioactive and can improve the osseointegration of implants. Moreover a bio-functional strontium phosphate conversion coating with addition of nutrient trace element is applied. According to the rabbit criticalsize ulna defect model, cylindrical cages were fabricated into 15mm length, 4mm max diameter and 0.5mm wall thickness, with 1 mm-diameter apertures distributed uniformly.

**RESULTS:** The three coatings on Mg-Sr alloys showed different surface morphology features as described. As for the corrosion studies in vitro evaluated by immersion test in Hank's solution and electrochemical performance, Ca-P chemical

deposition coating showed the most effective corrosion resistance compared to the other two methods. Both strontium phosphate conversion and Ca-P chemical deposition coating indicated better biocompatibility and osteogenic properties than MAO coating, according to cell proliferation, adhension, cytoskeleton staining assay et al. As can be seen from the X-ray radiograph, MAO and SrP conversion coating showed larger amount of cortical bone regeneration, owing to more release of osteoinductive metal ions. While Ca-P chemical deposition coating demonstrate much less gas evolution (Fig. 1).

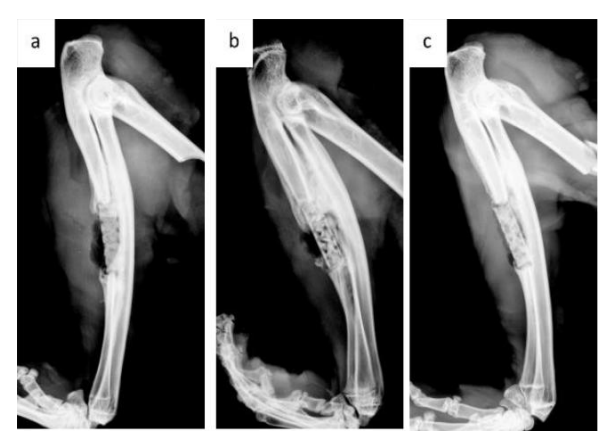


Fig. 1: Representative radiographs after 4 weeks' implanation of (a) MAO coating, (b) strontium phosphate conversion coating (c) Ca-P chemical deposition coating.

**DISCUSSION & CONCLUSIONS:** Different coatings on Mg-Sr alloy showed different degrees of degradation and bioacticity in vitro, while in vivo studies implied better osteoinductive properties for hollow Mg scaffold cages with more release of nutrient elements like Mg<sup>2</sup>,Ca<sup>2+</sup>, Sr<sup>2+</sup>. However, further research are needed to understand the mechanism of bone regeneration from such scaffolds.

### Degradation behaviour evaluation of Mg-3Sn-0.5Mn alloy wire for gastrointestinal anastomosis staples

Z Li 1\*, XD Song 1, YN Tan 1, AD Li 2, HY Wang 2, SS Bao 1, ZH Tian 1, YF Zheng 1,3, L Li 1

<sup>1</sup> <u>Center for Biomedical Materials and Engineering</u>, Harbin Engineering University, Harbin, China <sup>2</sup> <u>The First Affiliated Hospital of Harbin Medical University</u>, Harbin, China <sup>3</sup> <u>Department of Materials Science and Engineering</u>, College of Engineering, Peking University, Beijing, China

**INTRODUCTION:** Mg-3Sn-0.5Mn alloy wire was developed for degradable gastrointestinal anastomosis staples. Mg-3Sn-0.5Mn alloy wire with 0.38mm diameter was prepared and a series of *in vitro* degradation evaluations of wire were presented.

METHODS: Mg-3Sn-0.5Mn alloy wires were prepared by extrusion and drawing. *In vitro* degradation behavior was evaluated by immersion test method and by potentiodynamic polarization test. The measurement of degradable property was carried out in the SBF, artificial intestinal juice and intestinal juice of adult male rats (weight 280-320g). Preparation of 1000ml artificial intestinal juice is as follows: 6.8g KH<sub>2</sub>PO<sub>4</sub> completely dissolved in deionized water. The pH was adjusted by adding 0.4% NaOH solution until the pH was 6.8. 10g pancreatin dissolved in deionized water. Mixed the two kinds of solutions and added deionized water. PBS buffer solution was used to dilute the intestinal juice of rats.

#### **RESULTS:**

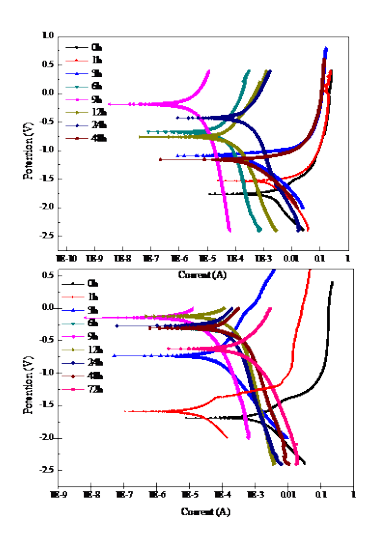


Fig. 1: The potentiodynamic polarization curves of Mg-3Sn-0.5Mn wire in SBF.

Fig. 2: The potentiodynamic polarization curves of Mg-3Sn-0.5Mn wire in artificial intestinal juice.

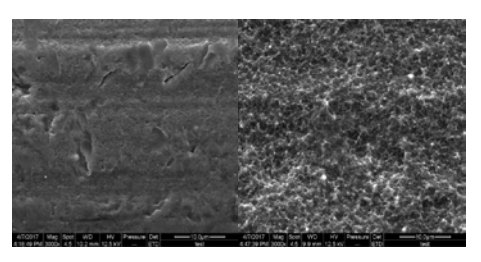


Fig. 3: SEM micrographs of Mg-3Sn-0.5Mn wire immersed in intestinal juice of rats for 30min (left picture) and for 12h (right picture).

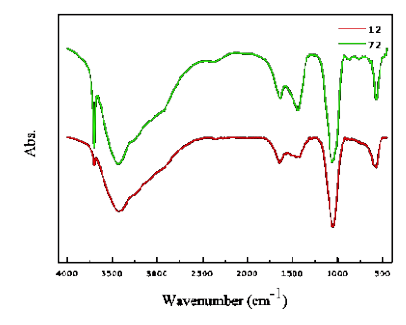


Fig. 4: FT-IR patterns of Mg-3Sn-0.5Mn wire immersed in intestinal juice of rats for 12 hours or 72 hours.

**DISCUSSION & CONCLUSIONS:** Compare with the corrosion products in SBF, it takes more time to form a stable Mg (OH) <sup>2</sup> film on wire surface in artificial intestinal fluid. The Mg (OH) <sup>2</sup> film obtained in artificial intestinal fluid is good at corrosion resistance.

Compared with immersion in SBF and artificial intestinal fluid, micro cracks did not appear on the corrosion surface after 12h immersed in intestinal juice of rats, and the corrosion rate decreased.

**ACKNOWLEDGEMENTS:** The work was supported by the Fundamental Research Funds for the Central Universities.

### Long-term degradation behaviour of pure Fe and Fe-Mg<sub>2</sub>Si composites for biodegradable implant applications

M Sikora-Jasinska<sup>1,2</sup>, P Chevallier<sup>2</sup>, E Mostaed<sup>1</sup>, S Turgeon<sup>2</sup>, C Paternoster<sup>2</sup>, M Vedani<sup>1</sup>, D Mantovani<sup>2</sup>

<sup>1</sup><u>Department of Mechanical Engineering</u>, Politecnico di Milano, Milan, Italy
<sup>2</sup><u>Lab. for Biomaterials & Bioengineering (CRC-I)</u>, Dept. Min-Met-Materials Engineering & CHU de Quebec Research Center, Laval University, Québec City, Canada

INTRODUCTION Iron based materials have shown high potential for biodegradable metallic (BM) implant applications. However, concerns regarding their slow corrosion rate are not yet completely allayed. Moreover, their corrosion behavior, which is a critical aspect of BMs science, is not fully understood. A better understanding of the surface passivation of Fe-based materials could lead to the design of smarter and surface responsive BMs with controlled degradation rates at distinct stages of implantation. Additionally, the corrosion products generated by gradually dissolving BMs may disturb the local physiological equilibrium at the implantation site. Their formation should be evaluated in the short- and long-term tests. For a better understanding of the corrosion mechanism, a series of immersion tests in different exposure intervals was performed. Furthermore, the influence of Mg<sub>2</sub>Si addition on corrosion behavior was evaluated.

MATERIALS & METHODS Powder metallurgy Fe and Fe-1%Mg2Si samples were used for static immersion tests in modified Hanks' solution. Samples were immersed in a controlled environment for 1, 10, 20, 50 and 100 days, respectively. Scanning electron microscopy (SEM), energy dispersive X-ray spectrometry (EDS), X-ray diffraction (XRD), and attenuated total reflectance Fourier transform infrared spectroscopy (ATR-FTIR) used were characterization techniques. Corrosion rates were calculated with weight loss method at different corrosion stages.

**RESULTS & DISCUSSION** Fig. 1 shows the cross section of Fe and Fe-1%Mg<sub>2</sub>Si after 10 and 100 days of immersion. The thickness and composition of the passive films formed on the samples' surfaces varies with the material composition and immersion time.

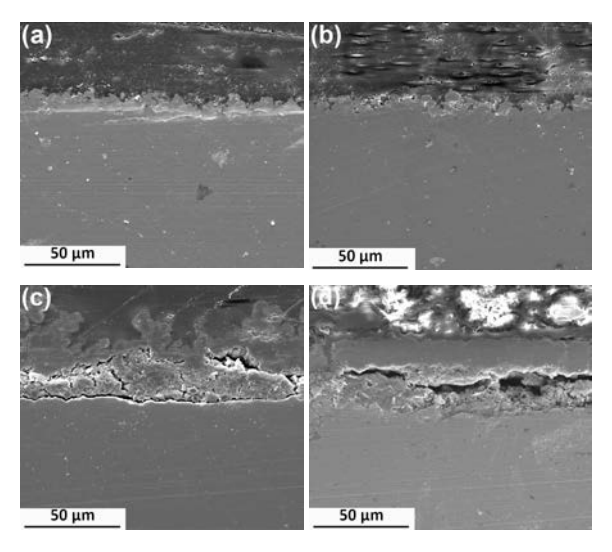


Fig 1 Cross section of the experimental specimens after immersion times of 10 days a) Fe, b) Fe-Mg<sub>2</sub>Si and after 100 days c) Fe, d) Fe-Mg<sub>2</sub>Si.

biscussion & conclusions Fe-Mg<sub>2</sub>Si showed a higher corrosion rate compared to that of pure iron at all stages of the corrosion experiment. The addition of Mg<sub>2</sub>Si plays a key role in the degradation/ passivation process as well as in the degradation mechanism. Fe degradation rate at distinct stages of the immersion strongly depends on the composition and stability of the formed oxide, hydroxide, carbonate and phosphate films. Additionally, in this work details about the corrosion behavior on long term exposure times to physiological environment are highlighted, adding knowledge on corrosion mechanism of degradable implant materials.

**ACKNOWLEDGEMENTS:** The authors would like to thank the MRI-Italy for partially funding this research.

# The effect of extrusion conditions on the corrosion and mechanical properties of biodegradable binary Mg alloys for orthopaedic applications

R.N. Wilkes<sup>1</sup>, M. P. Staiger<sup>1</sup>, G. J. Dias<sup>2</sup>

<sup>1</sup><u>Department of Mechanical Engineering</u>, University of Canterbury, Private Bag 4800, 8140 Christchurch, New Zealand, <sup>2</sup><u>Department of Anatomy School of Medical Sciences & Centre for Bioengineering and Nanomedicine</u>, University of Otago, PO Box 913, Dunedin, New Zealand.

**INTRODUCTION:** The unique properties of Mg and its alloys have prompted significant research into their potential as biodegradable implants for orthopaedic applications. The biocompatibility, tailorable corrosion rate and mechanical properties exhibited by these materials have been studied extensively in recent years. However, there is still a need for a more detailed understanding of how thermomechanical processing affects mechanical and corrosion properties. crystallographic texture that evolves during the thermomechanical processing of Mg alloys is known to influence the corrosion and mechanical properties of Mg. However, the effect of texture on the corrosion behaviour of Mg alloys is not widely reported, although it could be a potentially useful method for controlling the biodegradation of Mg alloys in vivo.

**METHODS:** In the present work, the effect of variable extrusion conditions (temperature and rate) on the microstructure, corrosion behaviour and mechanical properties of a binary Mg alloy are examined. A Potentiostat (Bio-Logic VSP) was used to examine the electrochemical characteristics of the Mg alloy immersed in Earle's balanced salt solution (EBSS) buffered by a 5% CO<sub>2</sub> atmosphere. Both potentiodynamic polarisation (PDP) and electrical impedance spectroscopy (EIS) tests were carried out alongside immersion tests to better understand the degradation characteristics of the material. The microstructure and texture of the extruded alloys was analyzed via electron backscatter diffraction (EBSD).

### **RESULTS AND DISCUSSION:** Electrochemical tests showed that texture plays

a role in determining the corrosion resistance of the alloy. Surfaces made up of primarily basal (0001) texture displayed superior corrosion resistance compared to those with prismatic

(1010) and (1210) planes. Samples that were extruded at temperatures higher than 300°C experienced larger grain sizes, lower strength, improved ductility and more random basal texture. In general, the extrusion conditions that produced a sample with the best combination of corrosion and mechanical properties were temperatures between 280°C and 320°C and a minimal extrusion rate that allowed for smooth extrusion, as well as a controlled exit temperature.

**CONCLUSIONS:** This systematic study provides useful data for the development of biodegradable Mg-Zn alloys for orthopedic applications, as the extruded alloys showed improved strength and corrosion resistance. Furthermore, this study highlights the importance of considering extrusion texture when designing biodegradable Mg based implants due to the anisotropic properties of the material following thermomechanical processing.

**ACKNOWLEDGEMENTS:** The authors acknowledge the New Zealand Health Research Council (HRC) for providing the funding for this research.

# Mechanical and corrosion properties and biocompatibility of ultrafine-grained magnesium alloy WE43 after severe plastic deformation

NS Martynenko<sup>1</sup>, EA Lukyanova<sup>1,2</sup>, NYu Anisimova<sup>3</sup>, MV Kiselevskiy<sup>3</sup>, NYu Yurchenko<sup>4</sup>, GA Salishchev<sup>4</sup>, GI Raab<sup>5</sup>, N Birbilis<sup>6</sup>, SV Dobatkin<sup>1,2</sup>, YZ Estrin<sup>1,6</sup>

<sup>1</sup> <u>Laboratory of Hybrid Nanostructured Materials</u>, National University of Science and Technology "MISIS", Moscow Russia. <sup>2</sup> <u>A.A. Baikov Institute of Metallurgy and Materials Science of the Russian Academy of Sciences</u>, Moscow, Russia. <sup>3</sup> <u>N.N. Blokhin Russian Cancer Research Center</u>, Moscow, Russia <sup>4</sup> <u>Belgorod National Research University</u>, Belgorod, Russia <sup>5</sup> <u>Ufa State Aviation Technical University</u>, Ufa, Russia <sup>6</sup> <u>Department of Materials Science and Engineering</u>, Monash

University, Melbourne, VIC 3800, Australia

INTRODUCTION: Magnesium allovs are promising considered as materials osteosynthesis implants, which can be completely metabolized by the body without any pathological effect on the surrounding tissue or detrimental systemic changes. However, low mechanical properties of the alloys hinder their broad use. The techniques of severe plastic deformation (SPD) make it possible to impart an ultrafine-grained structure to the alloys. In the present work, the effect of various SPD techniques on the microstructure. mechanical and corrosion properties, and biocompatibility in vitro of the WE43 magnesium alloy of the Mg-Y-Nd-Zr system was studied.

METHODS: The alloy was deformed by equal channel angular pressing (ECAP), and multiaxial deformation (MAD). Electrochemical corrosion was studied in a Na0.9%Cl solution. Biocompatibility tests were performed *in vitro* upon incubation of both undeformed and SPD-treated alloy samples in erythrocyte suspension (hemolysis assay), mononuclear lymphocytes (cytotoxicity assessments), and a culture of multipotent mesenchymal stromal cells (MSCs) (cell proliferation assay).

**RESULTS:** Microstructure examination of the alloy, which in the initial undeformed state had a grain size of ~100  $\mu$ m, showed that, in both cases, SPD leads to the formation of ultrafine-grained structure (with the average grain size of 0.5-1  $\mu$ m) containing precipitates (~0.3  $\mu$ m in size) of intermetallic phases enriched with rare earth metals. SPD provides a significant increase in the strength of the alloy. After ECAP, the alloy that in the initial homogenized state had the ultimate tensile strength UTS = 220 MPa, yield strength YS = 150 MPa, and tensile elongation EL = 10.5% exhibited the following values of these quantities:

UTS = 300 MPa, YS = 260 MPa, EL = 12.4%. The measurements after MAD returned the values of

UTS = 300 MPa, YS = 210 MPa, and EL = 17.2%. Thus, along with the strength characteristics, ECAP and MAD also raised ductility. The electrochemical corrosion of the alloy was shown not to be affected by SPD processing.

Deformation of the alloy resulted in slowing down of induced hemolysis, especially after MAD, relative to that of the undeformed alloy. The reduction in the cytotoxic effect was promoted by ECAP and MAD. The least pronounced cytopathogenic effect on MSCs was exhibited by ECAP and MAD processed specimens, whereas cell proliferation on the undeformed alloy samples was inhibited. The greatest alkalization of the culture medium was observed for these conditions. An evaluation of the biodegradation rate of the alloy in the fetal bovine serum (FBS) showed that the samples of the alloy treated by ECAP or MAD underwent the smallest weight loss.

**DISCUSSION&CONCLUSIONS:** SPD leads to an increase in the strength of the WE43 alloy by 40%. Grain refinement has a beneficial effect on the biocompatibility of the alloy: the induced hemolysis decreases, as does the cytotoxicity; the cell proliferation ability increases, while the degradation rate slows down.

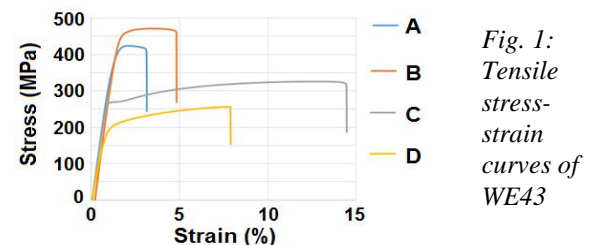
ACKNOWLEDGEMENTS: Part of this work relating to studies of biocompatibility was funded by the Ministry of Education and Science of the Russian Federation (grant #14.A12.31.0001) and the Increased Competitiveness Program of NUST «MISiS» (grant#K2-2016-062). Funding support of investigations of microstructure, mechanical performance, and corrosion properties was provided by the Russian Science Foundation (project #17-13-01488).

### Stress corrosion of cold drawn and aged WE43 wires in different setups

P Maier<sup>1</sup>, AJ Griebel<sup>2</sup>, WD Mueller<sup>3</sup>, JE Schaffer<sup>2</sup>

<sup>1</sup>University of Applied Sciences Stralsund, Stralsund, Germany. <sup>2</sup>Fort Wayne Metals Research Products Corp., Fort Wayne, IN, USA. <sup>3</sup>Charite Berlin, Universitätsmedizin, Germany

INTRODUCTION: Cold-drawn Mg wires offer mechanical advantages compared to warm worked metal without compromising corrosion properties. WE43 wire in the 4 conditions: A (as-drawn), B (aged at 250°C), C (annealed at 400°C) and D (annealed at 500°C) (see tensile properties in Fig. 1) retain substantial strength after corrosion in Ringer solution at body-temperature over 20 days [2]. Condition B shows the highest strength before and after corrosion. C recrystallizes the material, and D recrystallizes and causes grain growth. Stress corrosion, an open point in the previous study, is the focus of this study.



METHODS: Wire parts of a diameter of 1mm and a length of 30mm were bent to a deflection of 10mm. Released from the testing machine, springback was measured. Samples were put back in the setup seen in Fig.2, back to the deflection of 10mm. Anodized Al-screws and POM-plates were used in the <u>first run</u> (4 days corrosion) and <u>second run</u> (20 days corrosion). The <u>third run</u> used POM screws in place of Al (20 days corrosion). All setups were placed in 500ml Ringer solution at a temperature of 37°C.

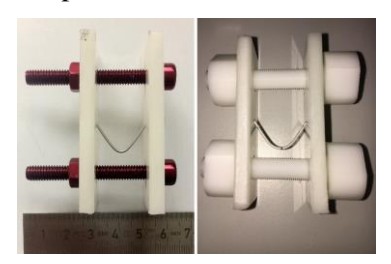


Fig. 2: Stress corrosion setup, left: with Alscrews, right: with POMscrews

**RESULTS:** The highest springback was found in wire B. Deep pitting corrosion was observed in the <u>first run</u> for wires B (Fig. 3) and D, while A and C were free of pitting under the same condition.



Fig. 3: Corrosion pit in wire condition B in setup with Alscrews after 4 days, first run

As a result of pitting corrosion, wires B and D broke into pieces. A failure in such a short time was not expected, so the experiments were repeated (second run). Since after 4 days no fracture occurred, the exposure time was extended to 20 days. Only 1 wire D failed. To eliminate the influence of the Al-screws, POM-screws were used in the third run. No wire condition failed, and no significant pitting corrosion was seen (Fig. 4). Summarizing, wires A and C showed the highest remaining cross-sectional area, B corroded more quickly but uniformly, and D showed pitting. During 20 days the POM screws did not creep.

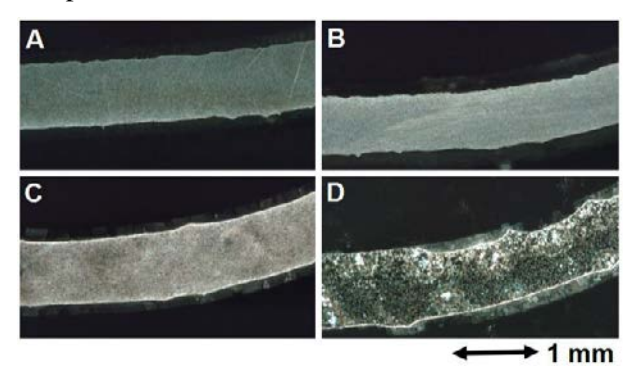


Fig. 4: Micrographs of wires A, B, C and D after 20 days corrosion under bending stress in the POM setup

**DISCUSSION & CONCLUSIONS:** Even though there was no direct contact, the WE43 wires served as the anode in a galvanic cell with the Al-screws during the <u>first run</u>. The following equation describes the electric field strength (capacitor) building up:

$$E = \frac{V}{d}$$
 E: electric field strength V: potential difference d: distance /here ~5 mm/

For condition B, the field strength seems to be high enough to cause strong pitting corrosion. During the first run, the Al-screws lost the cathodic effect due to passivation by the Ringer solution. This reduced the galvanic coupling in the second run, and the wires, apart from 1 wire D, did not fail. When the Al was removed, all WE43 wires survived 20 days corrosion time. Only wire D showed non-uniform corrosion. Summarizing this study, it is not recommended to use Al-parts in corrosion setups, even with no direct contact. Finally, cold drawing does not increase corrosion.

### Iron-based biodegradable alloys: importance of the testing parameters for corrosion evaluation via immersion tests

A Thomas<sup>1</sup>, E Scarcello<sup>2</sup>, D Lison<sup>2</sup>, PJ Jacques<sup>1</sup>

<sup>1</sup><u>Materials and process engineering (IMAP)</u>, Institute of Mechanics Materials and Civil Engineering, Université catholique de Louvain, Louvain-la-Neuve, Belgium. <sup>2</sup><u>Louvain Centre for Toxicology and Applied Pharmacology (LTAP)</u>, Institut de recherche expérimentale et clinique, Université catholique de Louvain, Woluwe-Saint-Lambert, Belgium.

INTRODUCTION: Cardiovascular diseases such as arteriosclerosis are widespread nowadays. Implanting a stent in the injured blood vessel is a common solution. Currently, permanent stents are used and could lead to long-term complications, such as restenosis. To avoid these issues, biodegradable stents are developed. They have to offer the required mechanical support to the blood vessel during the healing period (about one year), be biocompatible, and corrode at a suitable rate, i.e. in 1-2 years. This work deals with the evaluation of the corrosion properties of iron-based alloys by immersion tests. It highlights the importance to follow a well-established protocol to obtain reliable and reproducible results.

METHODS: The protocol has been defined for pure iron. Sheets were produced by melting pure iron pieces (Alfa Aesar, 99.99%) in an arc furnace. After a heat treatment of 10 minutes at 1000°C, the cast ingots were hot rolled to a thickness lower than 2mm. Since edges of square samples are favourable to corrosion, the chosen sample shape was a disk. Disks of 11mm in diameter were machined by electrical discharge machining. Both sides of the samples were polished and then cleaned in an ultrasonic bath of ethanol.

The samples were immersed in a pseudo-physiological solution (simulated body fluid, SBF), with a composition mimicking the ionic composition of blood plasma. The pH was in the range 7.3-7.5. Samples were placed in an oven at 37°C. The test duration was 7 days. The ratio of the volume of solution to the sample surface was kept constant and close to 20ml/cm<sup>2</sup>. Samples were fixed in the flask, to avoid shocks and prolonged contact of a face with the flask. This prevents any disturbance on the stability of layers deposited/formed during the corrosion process.

The corrosion rate was estimated by released ion concentration, measured by ICP and by mass loss after removal of the corrosion products. The surface after corrosion was characterized by SEM+EDS. The influence of different

parameterson corrosion was investigated. (a) The effect of the solution stirring was observed by comparing the immersion in static and stirred conditions. (b) Samples have been polished down to different levels: down to #1200 SiC paper, down to 1 $\mu$ m and down to 1 $\mu$ m followed by 1minute OPS. (c) The buffer has been modified: samples have been immersed in SBF alone (pH at 7.3-7.5 by adding HCl), SBF+50mM HEPES, and SBF+50mM TRIS.

**RESULTS:** We show that the considered parameters influence the corrosion rate. Corrosion is faster in a stirred solution than in static conditions. The polishing performed on the sample changes its roughness. It seems that samples polished down to 1200 grit are corroded more slowly than the ones polished down to 1μm or OPS. The buffering system has an important impact on corrosion. Indeed, adding 50mM of TRIS to SBF greatly increases the corrosion rate. No noticeable difference is observed between SBF alone and SBF+50mM HEPES in terms of corrosion rate.

**DISCUSSION & CONCLUSIONS:** Based on these results, the following protocol has been validated. Since blood circulates in the body, the solution is stirred, preventing the accumulation of corrosion products close to the sample surface. The stent surface being smooth, polishing is carried out down to 1μm. A solution buffered with 50mM HEPES is used to maintain a constant pH. A further improvement would be to test the physiological buffer, namely the HCO<sub>3</sub>-/CO<sub>2</sub> system.

By imposing specific parameters, we ensure the reliability and reproducibility of the experiments, enabling a comparison of the corrosion behaviour of different materials.

**ACKNOWLEDGEMENTS:** The authors thank the FRIA and the ARC for the funding of this research.

### Does solution change frequency affect the degradation rate for static corrosion immersion test? A study on pure iron immersed in Hanks' solution.

Beatrice Occhionero<sup>1</sup>, Sergio Loffredo<sup>1</sup>, William Bouchard, Carlo Paternoster<sup>1</sup>, Diego Mantovani<sup>1</sup> <u>Laboratory of Biomaterials and Bioengineering</u>, CRC-I, Department of Mining, Metallurgical and Materials Engineering & CHU de Quebec Research Centre, Laval University, Quebec City, Canada

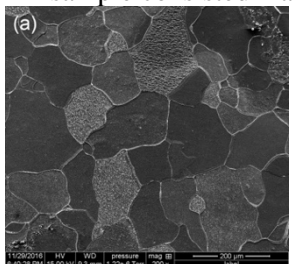
**INTRODUCTION:** The static degradation immersion test is one of the most widespread method to evaluate corrosion behavior of metals; it is used also to assess the degradation behavior for materials aimed at biomedical applications. The test is described and regulated by ASTM NACE G-31. In the present work, pure Fe samples were immersed in Hanks' solution for a period of 14 days. The effect of different solution change frequency was studied, to evaluate the degradation pattern and the formation of degradation products.

MATERIALS & METHODS: 20 x 10 x 1 mm<sup>3</sup> iron samples were mechanically polished until a mirror surface finishing was reached. Samples were weighted before and after the test with a 5 digit precision digital balance (Analytical Plus, Ohaus, USA). The test was performed in sterilized 100 mL Pyrex bottles (Corning Incorporated, NY 14831, Germany). The degradation test was carried out in an incubator ( $T_{incubator} = 37,0 \pm 1$  °C,  $p_{rel}$ .  $CO_2 = 5\%$ , 85% humidity) for 14 days. Three kinds of static degradation tests were carried out: the first one was without any solution change (FN samples), the second one with a solution change at days 4 and 9 (FY samples), and the third one with a solution change every 2 days (FT samples). Degradation products were collected for every solution change and at the end of the test. Degraded surfaces and degradation products were analyzed from the morphological point of view through optical and scanning electron microscopy. Chemical analyses have been performed by energy dispersive x-ray, x-ray photoelectron and Fourier infrared transform spectrometry (FTIR) and atomic absorption spectroscopy. The corrosion rate was evaluated according to ASTM G-31<sup>1</sup>.

**RESULTS:** Degraded surfaces of FN, FY, FT samples did not show any specific features: the grain orientation was responsible for the different morphologies (Fig. 1a) found after the degradation products removal. Surface degradation was homogeneous, as there were no relevant signs of pitting. Grain boundaries were put in evidence by the degradation process. Degradation products

were coarser and richer in phosphates for the FT condition (Fig. 1b).

**DISCUSSION & CONCLUSIONS:** Grains with different orientations present also different corrosion rates. Degradation products of FN and FY sample consisted mainly in iron oxides,



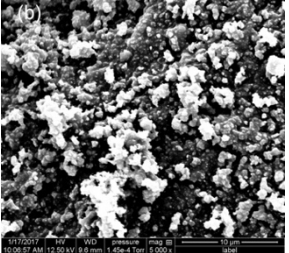


Fig. 1a: surface of a degraded iron sample after a 14 day static immersion test (mag. 200x). Fig. 1b: degradation products collected at the end of static immersion degradation test (mag. 5000x).

Table 1: corrosion rates of pure iron samples.

	Average corrosion rates		
	FN	FY	FT
CR (mm/y)	0,093	0,084	0,138
St. Dev.	0,003	0,002	0,005
Plus	0,004	0,002	0,005
Minus	0,003	0,002	0,005

hydroxides and phosphates<sup>3</sup>, while FTIR analysis on FT degradation products showed mainly the presence of carbonates. Even if iron carbonates are not stable in these conditions<sup>2</sup>, their presence could be detected during their formation, in particular at day 6 and 10. FT sample corrosion rate was the highest one (table 1). This could be attributed to the continuous supply of ions responsible for triggering the process of Fe corrosion, leading to the formation of Fe hydro-oxides, which is strongly affected by the environment (pH, temperature, presence of Cl<sup>-</sup>, SO<sub>4</sub><sup>2-</sup>, etc.).

**ACKNOWLEDGMENT:** The authors would like to thank V.Dodier, D.Marcotte, N.Moisan at Laval University. This work was partially funded by NSERC-Canada, FRQ-NT-Quebec, CFI-Canada

### Research on selection of in vitro testing solutions for biodegradable magnesium: a standardization view

S.X.Zhang <sup>1</sup>, J.Y. Liu<sup>1</sup>, X. Wang <sup>1</sup>, H.D. Xu <sup>1</sup>, H.L.Wu <sup>2</sup>, J.H.Ni <sup>2</sup>, X.N. Zhang <sup>1,2</sup>

<u>Suzhou Origin Medical Technology</u> Co.,Ltd, <u>School of Materials Science and Engineering</u>,

<u>Shanghai Jiao Tong University</u>

**INTRODUCTION:** The biodegradable Mg has now been developed as implantable devices. However, the standardization of in vitro degradation testing is still undetermined. It is quite important to establish standard in vitro testing methods<sup>1</sup>. In the present study, the stabilities of several common used solutions are compared.

**METHODS:** Four kinds of solutions were used, including physiological saline (0.9% NaCl), Hank's solution, m-SBF, and Dulbecco's PBS (PBS). The stabilities of these solutions were detected by monitoring the pH changes at 37°C in water bath and at 4°C in refrigerator (commonly storage circumstance of m-SBF) without any samples. Then high-purity Mg discs with a diameter of 8 mm and a thickness of 1 mm were immersed in these four solutions, separately, in the 37°C water bath. The weight loss ratios ((original weight weight immersion)/original weight) were recorded after 2 weeks immersion. In order to investigate the influence of buffered ingredient in m-SBF, a HEPES solution with a concentration of 17.892 g/L was also used.

#### **RESULTS:**

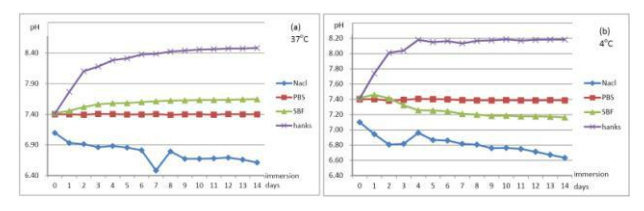


Fig. 1: pH changes of four solutions under  $37^{\circ}C$  (a) and  $4^{\circ}C$  (b)

Fig.1 shows the pH change of each solution without any samples (blank solution). It can be seen from Fig.1a that in the condition of 37°C, the pH of Hank's rises rapidly during 2 weeks and above 8.4. On the contrary, the pH of physiological saline drops to nearly 6.7 after 2 weeks. The PBS and m-SBF, however, are relatively stable. But the pH of m-SBF still rises to about 7.6, while the pH of PBS keeps nearly constant of 7.4. When under 4°C storage condition, Hank's and 0.9% NaCl both exhibit

high activity. m-SBF drops to about 7.2. PBS is still the most stable one, as shown in Fig.1b.

Fig.2 illustrates the weight loss ratios. The m-SBF has the highest weight loss and the Hank's is the lowest. In the HEPES solution, unfortunately, 96.4% of Mg sample is dissolved just after one day, suggesting the potential influence of HEPES, which is the main buffer source in m-SBF.

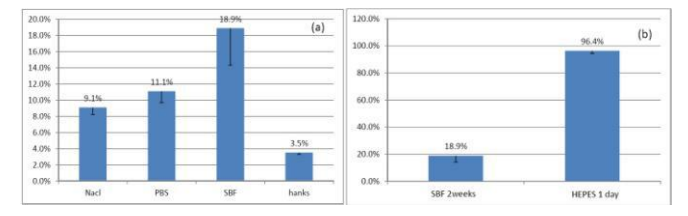


Fig.2 Weight loss ratios of high purity Mg. (a) in four simulated body fluids;(b) comparison of m-SBF and HEPES solution

DISCUSSION & **CONCLUSION:** Many researches have reported in vitro experiments, including comparison of in vitro degradation in different solution and exquisite testing bench to simulate the human body buffer system<sup>2</sup>. However, in the view of standardization, the aim of in vitro testing is not just mimicking the human body, but should check the properties of magnesium metals stably and can be repeatable<sup>1</sup>. Just as found in the present study, the stability of solution and the resulting weight loss of Mg are totally different. It seems the PBS is more stable and could be a suitable candidate of in vitro testing tool. The m-SBF is not stable due to its CO<sub>2</sub>-H<sub>2</sub>CO<sub>3</sub> buffer couple, which may be affected by the atmosphere. In addition, HEPES may also strongly affect the degradation behaviour of Mg.

**ACKNOWLEDGEMENTS:** This work was supported by the Natural Science Foundation of China (No. 51571142 and No. 51271117).

## Quantitative characterization of degradation processes *in situ* by means of a bioreactor coupled flow chamber using time-lapse SRµCT

B Zeller-Plumhoff<sup>1</sup>, F Feyerabend<sup>1</sup>, T Dose<sup>2</sup>, F Wilde<sup>2</sup>, A Hipp<sup>2</sup>, F Beckmann<sup>2</sup>, JU Hammel<sup>2</sup>, R Willumeit-Römer<sup>1</sup>

<sup>1</sup><u>Institute of Biometallic Materials</u>, <sup>2</sup><u>Institute of Materials Physics</u>, Helmholtz-Zentrum Geesthacht, Germany

**INTRODUCTION:** Magnesium (Mg) and its alloys are used increasingly in implant materials research as their good biocompatibility and biodegradability suggest a high potential for clinical application. The processes occurring during degradation are however highly complex and spatially variable, thus necessitating a time-resolved, three-dimensional analysis. To this end we have employed high-resolution synchrotron radiation-based micro computed tomography (SR $\mu$ CT) to image the process of Mg2Ag degradation during immersion in cell culture medium. A customized corrosion cell was designed to simulate the native environment during implant degradation.

METHODS: Time-lapse SRμCT was applied to study the degradation of a Mg2Ag pin in a cell medium in a custom-built flow cell *in situ* over five days. Imaging was performed at the HZG operated beamline P05 at the PETRA III storage ring, Deutsches Elektronen-Synchrotron (DESY), using a photon energy of 20 keV in absorption contrast mode with a voxel size of 2.5 μm. The tomography data was segmented semi-automatically using the ImageJ plugin WEKA. Fig.1 shows a tomographic slice and the corresponding segmentation of the Mg2Ag pin.

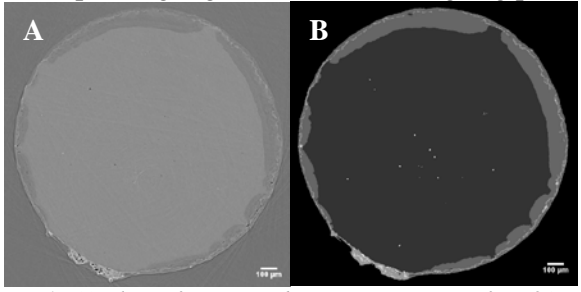


Fig.1: A) Slice of tomographic reconstruction of Mg2Ag pin after 5 days of degradation. B) corresponding segmentation using WEKA plugin. It is possible to differentiate the bulk material, a general degradation layer and a bright layer within. Regions of hydrogen evolution (\*) are visible.

To characterize the degradation the images were radially resliced and a number of parameters was determined using Matlab® R2016a (The MathWorks Inc., USA): Degradation rate, mean Mg radius over time, mean radial position and tortuosity of a phosphate layer, mean volume of

differentiable components, number and volume of cracks in degradation layer (1).

**RESULTS:** The 3D nature of the tomographic images allowed the identification of a general degradation layer, as well as a bright (phosphate) layer within, as well as regions of hydrogen development (gas bubbles) and the shrinkage of the bulk magnesium surface over time. The volume change of all components was non-linear. After 5 days the non-uniform degradation has resulted in the formation of regions of strong radial degradation and regions that appear unaffected by the corrosion (see Fig. 2).

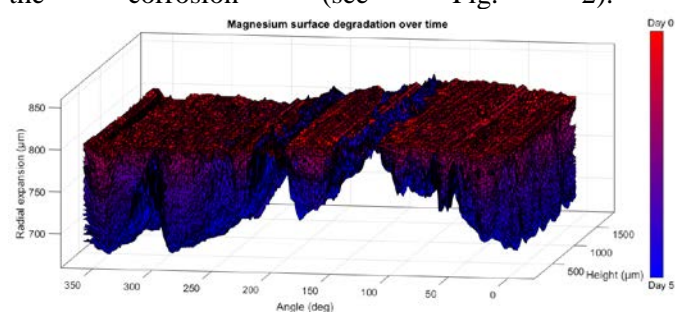


Fig.2: Degradation of bulk magnesium surface over time. Initially, the surface appears homogeneous (red), whilst after 5 days (blue) there are regions of strong degradation and regions that appear unaffected. The unaffected regions coincided with hydrogen evolution and material deposition.

**DISCUSSION & CONCLUSIONS:** In contrast to conventional methods used in the study of material degradation SRµCT has the advantage of enabling a 3D, non-destructive analysis of the degradation, thus leaving the sample intact for further analysis, e.g. by µXRF. However, whilst the absorption contrast allows a general distinction between different regions (e.g. bulk, degradation layer), no chemical analysis is possible. This may be circumvented by application of other synchrotron radiation techniques, ptychography. Tomography data further enables the development of image-based mathematical models to better understand the degradation processes and transport phenomena at hand. Finally, SRµCT helps to bridge the gap between in vitro and in vivo implant degradation studies by facilitating a higher-resolution analysis to identify the impact of varying resolutions on the comparison of degradation rates.

### In vitro corrosion behaviour and biocompatibility study of Mg-1Ca alloy with silk fibroin film for orthopaedic applications

Pan Xiong<sup>1</sup>, Yufeng Zheng<sup>2\*</sup>, Yan Cheng<sup>1\*</sup>

<sup>1</sup> <u>Center for Biomedical Materials and Tissue Engineering</u>, Academy for Advanced Interdisciplinary Studies, Peking University, Beijing 100871, China <sup>2</sup> <u>Department of Materials</u> Science and Engineering, College of Engineering, Peking University, Beijing 100871, China

INTRODUCTION: The high corrosion rate of magnesium alloys is the main limitation for their clinical applications in bone repair regeneration (Zhao et al., 2017). Therefore, the research on the improvement of Mg alloys corrosion resistance through surface coating has become a hot topic (Hornberger et al., 2012). Silk fibroin has got broad applications in bone tissue engineering because of its excellent mechanical and biocompatible properties (Koh et al., 2015). In the present work, the fluoride-treated Mg-1Ca alloy was further spin-coated by silk fibroin and the corrosion behaviour and the biocompatibility had been studied in vitro.

METHODS: The extruded Mg-1Ca alloy (wt.%) bar with a diameter of 12 mm was cut into 2mm thick slices, ground by up to 2000 grit SiC paper, and ultrasonically cleaned in acetone and ethanol, deionized water, respectively. The specimens were pre-treated by fluoride treatment, and followed by the coating of silk fibroin with spin-coating method. The immersion tests and electrochemical analysis in Hank's solution were conducted to evaluate the corrosion behaviours *in vitro* of the samples. Additionally, Mouse osteoblast-like cells (MC3T3-E1) were used for the *in vitro* biocompatibility measurements.

#### **RESULTS:**

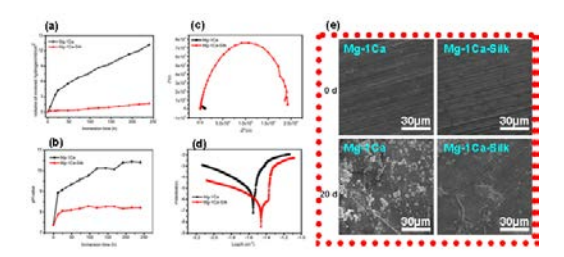


Fig. 1: Images of (a) the variation of Hydrogen evolution volume and (b) pH value immersed in Hank's solution for 10 days. (c) Nyquist plots and (d) potentiodynamic polarization curves obtained by the electrochemistry experiment. (e) the surface morphologies immersed in Hank's solution for 20 days.

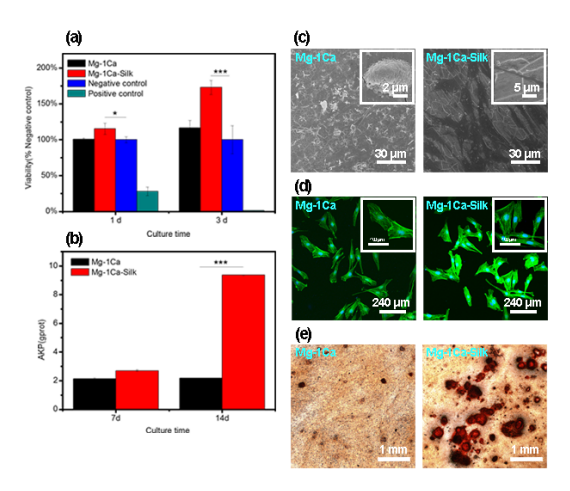


Fig. 2: (a) Viability of cells cultured in the extracts of each samples at 1 and 3 days by the CCK-8 assay kit; (b) the ALP activity of cells cultured in the extracts for 7 and 14 days; (c) Cell morphologies after cultured for 24h on bare and silk-coated Mg-1Ca alloy; (d) Actin-nucleus costaining of cells cultured for 6h in the extracts; (e) calcium (CAL) deposition of cells cultured for 28 days in the extracts.

**DISCUSSION & CONCLUSIONS:** Our study suggested that the silk fibroin could be utilized as effective film to decrease the corrosion rate of the Mg-1Ca alloy and improve the surface biocompatibility, which could be a promising candidate for biomedical applications.

ACKNOWLEDGEMENTS: This work was supported by the National Key Research and Development Program of China (2016YFC1102402), National Natural Science Foundation of China (Grant No. 51431002 and 31170909).

### Influence of Mg<sub>2</sub>Si addition on the mechanical properties and corrosion behaviour of powder metallurgy Fe-30Mn alloys.

M Sikora-Jasinska<sup>1,2</sup>, E Mostaed<sup>1</sup>, C Paternoster<sup>2</sup>, M Vedani<sup>1</sup>, D Mantovani<sup>2</sup>

<sup>1</sup>Department of Mechanical Engineering, Politecnico di Milano, Milan, Italy

<sup>2</sup>Lab. for Biomaterials & Bioengineering (CRC-I), Dept. Min-Met-Materials Engineering & CHU

de Quebec Research Center, Laval University, Québec City, Canada

INTRODUCTION Biodegradable metals used for cardiovascular applications are expected to completely degrade upon fulfilling their mission, that is supporting the damaged tissue during healing process without generating any toxic effects. Iron has shown promising potential for cardiovascular devices especially in the case of stent applications. However, its corrosion rate is too slow. One approach to solve the mentioned drawback is introducing second phases in the Fe matrix. Thus, in this study the effects of Mn and of Mg<sub>2</sub>Si as alloying element and reinforcement, respectively, on microstructure, mechanical properties and corrosion behavior of Fe-30Mn/Mg<sub>2</sub>Si composites have been evaluated. Corresponding mechanism of corrosion was also explored.

MATERIALS & METHODS Powder metallurgy was selected as a fabrication process of the material samples. Micro-hardness and tensile tests were performed to characterize the mechanical properties. Modified Hanks' solution was used for corrosion tests. Samples were immersed for two weeks in a controlled environment. Scanning electron microscopy (SEM), Energy dispersive X-ray spectrometry (EDS), X-ray diffraction (XRD) and attenuated total reflectance Fourier transform infrared spectroscopy (ATR-FTIR) were used to investigate the microstructure and the corrosion morphology and products. Corrosion rates were calculated by weight loss method accordingly to ASTM G31 standard.

**RESULTS & DISCUSSION** Hot rolling of the powders sealed in steel was applied and it resulted in consolidated samples with a fine microstructure. The addition of reinforcement improved the mechanical performance of the Fe-30Mn matrix and accelerated the corrosion rate. Surface morphology after static immersion test differed depending on the material composition, as shown in Fig. 1.

Fe-30Mn alloy was covered by a dense and uniform layer of degradation products, while the corrosion layer on the composite surface was not homogenous, showing uncovered areas with cracks between the aggregates.

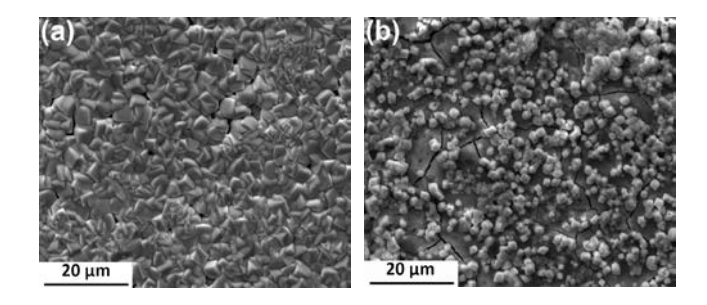


Fig 1: Surface morphology after corrosion test (a) Fe-30Mn alloy (b) Fe-30Mn/Mg<sub>2</sub>Si composite after 14 days of immersion in modified Hanks' solution

CONCLUSIONS Fe-30Mn/Mg<sub>2</sub>Si composites showed improved mechanical properties in terms of tensile strength and a higher corrosion rate compared to that of Fe-30Mn alloy. The addition of Mg<sub>2</sub>Si induced a significant contribution to the degradation/passivation process as well as on the corrosion mechanism of the investigated materials, especially in the initial stages of corrosion. In brief, Fe-30Mn based composites are promising candidates as biodegradable implant materials with proper mechanical properties and enhanced degradation rate.

**ACKNOWLEDGEMENTS:** The authors would like to thank NSERC Canada, and MRI-Italy and Quebec/Italy sub-commission of the Quebec Ministry of Intl Relations for partially funding this research.

### Electrochemical corrosion behaviour of electroformed Fe-Co alloys in the modified Hanks' solution

M Lotfollahi<sup>1</sup>, C Paternoster<sup>1</sup>, M Sikora-Jasinska<sup>1</sup>, D Mantovani<sup>1</sup>

<sup>1</sup> <u>Lab. for Biomaterials & Bioengineering (CRC-I)</u>, Dept. Min-Met-Materials Engineering, Laval University, Québec City, Canada

INTRODUCTION: Cardiovascular disease is one of the main causes of death throughout the world. Stenting is a recognised efficient clinical treatment. Since 2010, biodegradable metals (BMs) expected to disappear around 12 months after the implantation have been reported. Iron-based BMs are well known for their high mechanical properties and biological performances, however, low corrosion rate both in vitro and in vivo were also reported. Among various approaches to address this issue, electroforming technique has shown its potential in increasing degradation rate of iron by producing finer microstructure with high volume of grain boundaries that are susceptible to increase the corrosion rate. In this study, two different composition of Fe-Co alloy were electroforming produced by and their electrochemical corrosion behavior was investigated by potentiodynamic polarization.

**METHODS:** The samples were produced by electroforming from a chloride bath containing the chloride salts of both iron and cobalt metals. Electroforming were performed at current density of 2A/dm², and temperature and pH of bath was adjusted to 85°C and 1, respectively. Surface morphology of Fe-Co alloys was investigated by scanning electron microscopy. Potentiodynamic polarization (ASTM G59) tests were performed in the modified Hanks' solution (simulating the ionic composition of blood plasma). The temperature and pH of solution were adjusted to 37°C and 7.4, respectively. A platinum electrode and a calomel saturated electrode were used as counter electrode and reference electrode, respectively.

**RESULTS:** Surface morphology of Fe-Co alloys are shown in Fig.1. As can be seen, surfaces of both Fe-Co alloys consisted of acicular grains with average size of about 20µm. In addition, the surface of Fe-5%Co, circular slices with average of μm throughout size 1 the surface. Potentiodynamic polarization curves electroformed iron and Fe-5%Co and Fe-10%Co alloys are presented in Fig. 2. Values for E<sub>corr</sub> and i<sub>corr</sub> for electroformed iron and Fe-5%Co and Fe-10%Co alloys are (-0.433V, 23.9μA), (-0.339V,  $32.2\mu A$ ) and (-0.340V, 75.8  $\mu A$ ), respectively.

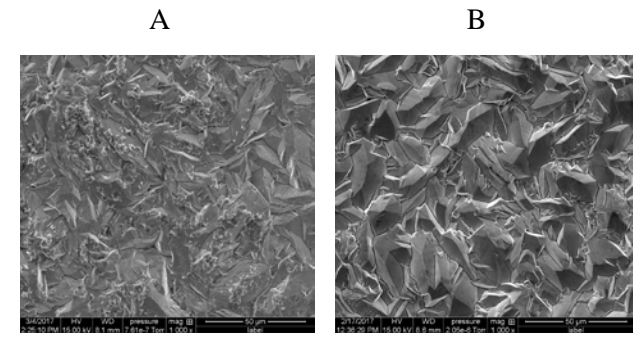


Fig. 1: SEM images of electroformed Fe-Co alloys with: A) 5%Co; B) 10%Co.

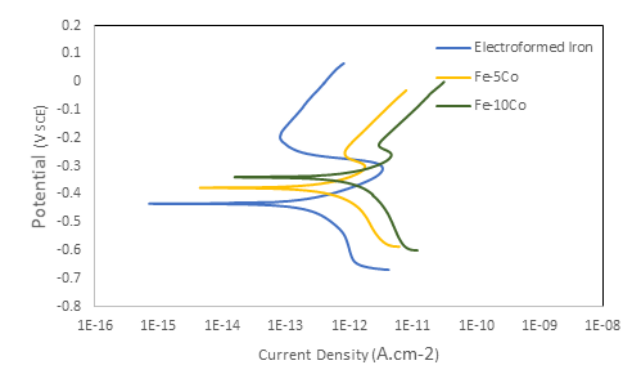


Fig. 2: Potentiodynamic polarization curve for electroformed iron, Fe-5%Co, Fe-10%Co.

**DISCUSSION & CONCLUSIONS:** The  $E_{corr}$  for alloys with higher amount of cobalt has shifted to more noble values. This finding is consistent with the standard reduction potential values for Co ( $E^\circ$ =-0.28V) and Fe ( $E^\circ$ =-0.44V). However, values of i<sub>corr</sub> for alloys with higher amount of cobalt increased. Higher corrosion rate for rolled Fe-3%Co in comparison to rolled iron was already reported by Lie B. *et al* (2014). In conclusion, alloying electroformed iron with cobalt increases degradation rate, and this trend continues for higher amount of cobalt.

**ACKNOWLEDGEMENTS:** NSERC-Canada.

## Microscopy linked electrochemistry – one step towards a better understanding of the degradation of biometals, demonstrated on Mg<sub>4</sub>Ag alloy

T. Zimmermann<sup>1</sup>, N. Hort<sup>2</sup>, F. Feyerabend<sup>2</sup>, R. Willumeit<sup>3</sup>, WD Müller<sup>1</sup>

<sup>1</sup> Charité Universitaetsmedizin Berlin, D., <sup>2</sup> Helmholtz Zentrum Geesthacht, Geesthacht, D., <sup>3</sup> Christian Albrechts University of Kiel, D.

**INTRODUCTION:** One critical problem for the application of Mg and Mg alloys as biometals is the reliable assessment of their degradation behavior. Several models have been proposed before. Obviously the sum reaction for Mg with water is very simple. Electrochemical methods are suitable to assess the degradation of biometals due to close in vivo conditions during experiments. Thereby the H<sub>2</sub> evolution is a limiting factor for reliable electrochemical analysis. The measurement and interpretation of the open circuit potential (Eocp) is a possibility but limited in case of Mg and Mg alloys, because a mixed potential is established due to the galvanic coupling of anodic - metal oxidation and cathodic - hydrogen evolution reactions. Accordingly, the position of EOCP depends on the variation of metal ion concentration, the rate of oxidation of Mg and of reduction of H<sup>+</sup> and the area in which these reactions takes place as well as other, unknown influences. In addition, polarization measurements are of interest for determining which electrochemical processes are

The question how and where the  $H_2$  evolution takes place and how it influences the degradation processes remains to be answered. The aim of this work was to develop a set up for a direct observation of the corroding surface with high resolution during electrochemical measurements and to associate electrochemical reactions with visible activities on the surface.

METHODS: A high resolution optical microscope, Keyence VHC 5000, was combined with a newly developed electrochemical cell which was linked to the Mini Cell System (MCS) in contact with a mini potentiostat. Mg<sub>4</sub>Ag alloys were used after polishing and etching to determine the grain size. Optical observation was done to assess the surface changes during open circuit measurements and determine the location of H<sub>2</sub> evolution after contact with cell culture solution. During the OCP measurements the hydrogen was removed by short refreshing of the electrolyte every 600s. Microscopic pictures were taken during EoCP vs t measurements to assess the changes of the surface conditions and structure. OCP measurement was followed by cyclic polarization, n=5, with  $\pm$ 500 mV around OCP with a scan rate of 10mV/s. Hereby where the measurement was filmed under the microscope. The Ag distribution in the alloy was analyzed by SEM/EDX measurements at the same place as the electrochemical measurements.

**RESULTS:** During the OCP measurements the  $E_{OCP}$  shifted in anodic direction, even after changing the electrolyte after 10 min. The  $E_{OCP}$  values at the end of each of the 10 min sequences are summarized in Table 1. During the OCP measurements the surface changed from metallic to an oxide covered one. In Figure 2 the 5 cycles are shown, where during the first and the last cycle no breakdown can be observed. The pictures clearly demonstrate that at the cathodic vertex potential a distributed, continuous  $H_2$  evolution takes place at oxide-free spots which are white in appearance. In passing the corrosion potential ( $E_{corr}$ , or  $E_{I=0}$ ) the gas evolution ceases. At the anodic vertex potential two different situations are observable: a) absence of surface breakdown, associated with absence of gas evolution and b) surface breakdown, where at a single location a strong gas evolution can be seen. This

position or spot shifts in position from cycle to cycle. The grain size was relatively large and so the measurements could be made nearly on a single crystal of about 700  $\mu m$  in diameter. The Ag distribution in the alloy is not completely homogenous, in fact it is accumulated in a dendritic fashion within the grains.

DISCUSSION & CONCLUSIONS: The anodic shift of Eocp is related to the creation of hydrogen which is accumulated in and at the surface of Mg₄Ag. The first cycle shows nearly reversible behavior, where it can be assumed that Mg + 2e<sup>+</sup> + 2H<sup>+</sup> ←→ MgH₂ takes place at the oxide-free "white" spots. During the cycles 2, 3 and 4 at three different places intensive H₂ evolution can be observed after breakdown of the oxide layer. The oxide layer was deposited during the OCP measurements, where new Mg(OH)₂ was formed because of the high evolution rate of hydrogen. The current density at the cathodic vertex potential does not change much from cycle to cycle, because the newly exposed Mg surface is covered with a protective layer. The "white" spots do not change in appearance or location at all.

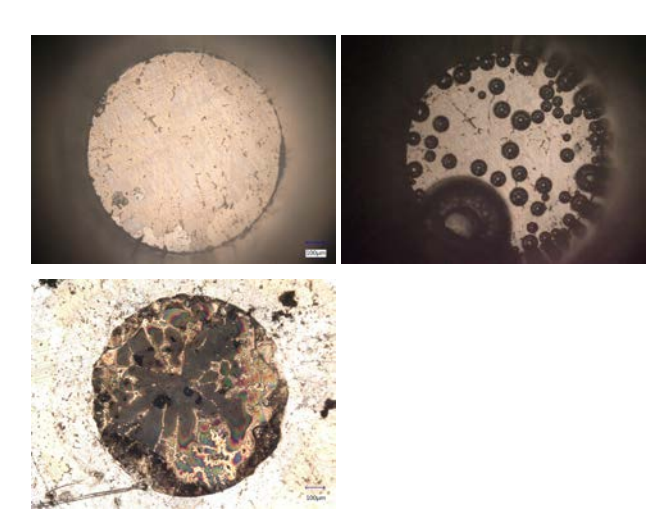


Fig. 1: Images of Mg4Ag surface before and directly after contact with cell culture solution (top row), Mg4Ag surface after OCP and cyclic loading in cell culture solution. Surface covering by oxides are seen and hydrogen evolution spots are marked.

In conclusion, this set up allows to observe the changes during the electrochemical measurement. It could be shown that at the beginning the Mg surface is covered with an oxide layer, the white spots are formed randomly as well as in part influenced by the Ag distribution. The Ag accumulations are not necessarily hydrogen evolution spots.

### Biodegradable stent obtained electrochemically and the corrosion behaviour of pure iron

S.Martirosyan, A.Hovhannisyan

Scientific Centre of Radiation Medicine and Burns, Yerevan, Armenia

**INTRODUCTION:** Pure iron stents have been developed electrochemically in a single step on the Al substrate, which, before the deposition of iron, has been chemically covered with zinc. The method permits to obtain  $20-100~\mu m$  thick uniform coatings. Stent diameter could vary in between 1.0-6.0~mm. Method permits to develop stents with various type of loop design directly coated on the substrate.

**METHODS:** The obtained stents and their corresponding tubes have been corrosion-tested by electrochemical tool methods. As is known, the stent material should sustain its integrity for 6-12 months and totally have to be degraded after 12-24 months. Three different iron samples were studied for the biodegradation experiments: "stent" (S-Fe), electrochemically obtained sample (99-Fe) and casted iron material (C-Fe). Also, the three samples, 99-Fe, S-Fe and C-Fe have been corrosion-tested in 0.9% NaCl solution at 37°C with the help of Tafel plots provided in Fig.1, carried out on CHI 660 D Electrochemical Workstation (USA) potentiostat.

**RESULTS:** The obtained results were processed and summarized in the table below:

Sample	logJ (A cm <sup>-2</sup> )	Corrsion rate (mm year <sup>-1</sup> )	Corr. potential., V
S-Fe	-3.3	5.8	-1.18
C-Fe	-3.7	2.3	-0.96
99-Fe	-3.6	2.9	-1.14

*Table. Equilibrium potentials for the three samples were in between –0.52 and –0.58 V.* 

Tafel plots show that electrochemically S-Fe sample is the most active, in other words tends to dissolve easily (5.8 mm per year), then comes our 99-Fe sample (2.9 mm per year), followed by C-Fe (2.3 mm per year).

Yet, interestingly, 99-Fe sample is not prone to passivation as it follows from the anodic passivation curves taken within large potential gap and presented in Figure 3. Scan rate was kept at 10 mV per sec. Again, the used electrolyte is 0.9% NaCl solution at 37°C.

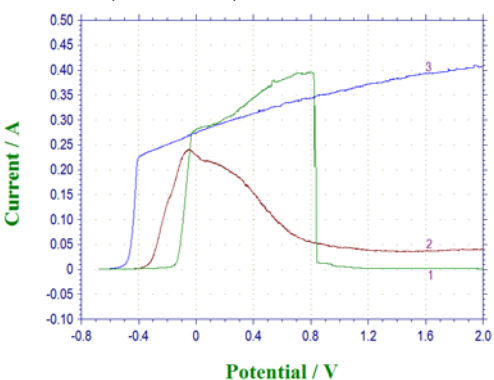


Fig. 1: Tafel plots of the samples: 1. S-Fe; 2. C-Fe; 3. 99-Fe

**DISCUSSION & CONCLUSIONS:** Thus, as it follows from Figure 1, 99-Fe sample, possibly, would hardly get passivated in blood environment. This is an essential point, because in this way, the would-be stent – made of 99-Fe material – should dissolve completely without producing solid-state corrosion remnants in the blood. On the other hand, as the corrosion rate of 99-Fe sample is lower than for the conventional S-Fe sample, hence, 99-Fe sample, possibly, would sustain its integrity for 6-12 months period as is the case with the S-Fe sample.

**ACKNOWLEDGEMENTS:** The study was supported by International Science and Technology Center (ISTC-2115).

### Fluorapatite as an osteoregenerative coating on bioresorbable scaffolds

Malcolm Caligari Conti\*<sup>1</sup>, Gianella Xerri<sup>1</sup>, Diego Mantovani<sup>2</sup>, Pierre Schembri Wismayer<sup>3</sup>, Emmanuel Sinagra<sup>4</sup>, Daniel Vella<sup>1</sup>, Joseph Buhagiar<sup>1</sup>.

<sup>4</sup> Department of Chemistry, Faculty of Science, University of Malta, Msida MSD 2080, Malta **INTRODUCTION:** The effects which sol ageing, coating heat treatment temperature and substrate have on the crystallinity and morphology of a fluorapatite coating are of major scientific importance when considering its application as an osteoregenerative surface. Iron-based, nonpassive, bioresorbable alloys, have been identified as good candidate materials for use in in vivo scaffolding applications. These provide adequate support during healing without leading to problems associated with permanent implant materials. These iron-based alloys do however have compromised cytocompatibility compared to other passive alloys. Therefore, the application of fluorapatite to the surface of the biodegradable metal may help to alleviate some of the less than properties excellent as regards to the cytocompatibility of the parent material. It is for this reason that the properties of the fluorapatite coating generated under different synthesis conditions must be explored.

**METHODS:** Fluorapatite was synthesised using the sol-gel route at three pH values and the sol was aged for a number of days. The coating that was determined to be of optimal morphology was then applied to an austenitic stainless steel (control) and a pure iron bioresorbable metal substrate. Each fluorapatite coating was analysed by means of X-ray diffraction, Fourier Transform Infrared Spectroscopy and by Scanning Electron Microscopy.

**RESULTS:** It was found that neutralisation the sol to pH  $\sim$  7, increased sol ageing time and high heat treatment temperatures improved the crystallinity of the produced fluorapatite. On stainless steel the optimum coating conditions were found to be that of a sol-gel coating applied at pH 0. This generated a very porous type morphology as shown in Figure 1.



Figure 1:Stainless steel coupon coated with Flourapatite at pH 0

This morphology however could not be reproduced on the pure iron, the bioresorbable substrate as shown in Figure 2.

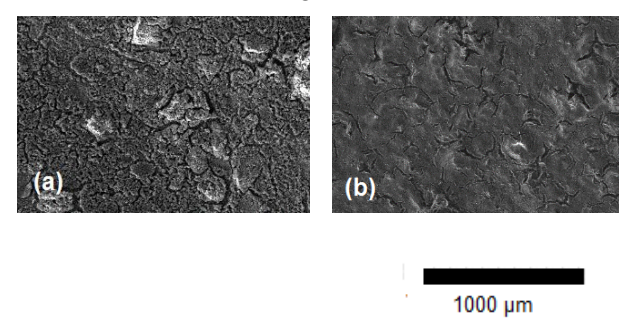


Figure 2: Iron coupon coated with Flourapatite at (a) pH 0 and (b) pH 7

**DISCUSSION & CONCLUSIONS:** At pH 0 on the iron substrate; a surface with a large number of irregularities and cracks was observed. This would be reflective of a coating, which lends itself well to the osteoregenerative aim of the final product.

ACKNOWLEDGEMENTS: Malcolm Caligari Conti is funded by the REACH HIGH Scholars Programme. The research work disclosed in this publication is partially funded by the REACH HIGH Scholars Programme — Post-Doctoral Grants. The grant is part-financed by the European Union, Operational Programme II — Cohesion Policy 2014- 2020 Investing in human capital to create more opportunities and promote the wellbeing of society -European Social Fund'.

<sup>&</sup>lt;sup>1</sup> Department of Metallurgy and Materials Engineering, Faculty of Engineering, University of Malta, Msida, MSD 2080, Malta

<sup>&</sup>lt;sup>2</sup> Laboratory for Biomaterials and Bioengineering, CRC-I, Department of Mining, Metallurgical and Materials Engineering & CHU de Quebec Research Centre, Laval University, Quebec City, Canada <sup>3</sup> Department of Anatomy, Faculty of Medicine and Surgery, University of Malta, Msida, MSD2080, Malta

# Chondrogenic differentiation of ATDC5-cells under the influence of Magnesium and Magnesium alloy degradation

AH Martinez Sanchez<sup>1</sup>, F Feyerabend<sup>1</sup>, D Laipple<sup>1</sup>, RWillumeit-Römer<sup>1</sup>, A Weinberg<sup>2</sup>, BJC Luthringer<sup>1</sup>

<sup>1</sup> Helmholtz-Zentrum Geesthacht, Institute of Material Research, Geesthacht, Germany. <sup>2</sup> Department of Orthopedics and Orthopedic Surgery, Medical University of Graz, Austria

**INTRODUCTION:** Treatment of children fractures remain a challenge as they should not provoke any growth disturbance. Resorbable biomaterial is one of solution to address this challenge. Thus magnesium (Mg) and its alloys are in a focus as biodegradable implant materials and as a potential alternative to permanent implants for application in children. Nevertheless effects of those materials on growth plate cartilage and chondrogenesis have been poorly evaluated.

**METHODS:** Linear growth of the long bones occurs through endochondral ossification i.e., proliferation and differentiation of the epiphyseal growth plates and its primary cell type, the chondrocyte. The ATDC5 cell line, derived from mouse teratocarcinoma, exhibits a sequential process analog to chondrocyte differentiation. It is thus an accepted model for chondrogenesis / endochondral ossification. Influence of pure Mg (PMg), Mg with 10 wt% of gadolinium (Mg-10Gd) and Mg with 2 wt% of silver (Mg-2Ag) on in vitro differentiation of ATDC5 cells was evaluated via indirect (alloys degradation products) and direct assays (cells directly cultured on samples).

**RESULTS:** Mg-10Gd showed a chondrogenic potential and the three extracts showed an inhibitory effect on ATDC5 mineralization (measured via gene expression). Cells cultured in Mg-10Gd and Mg-2Ag extracts exhibit the same proliferation and morphology than cells cultured in growth conditions. Mg-10Gd also induced an increase in production of extracellular matrix (ECM) and a bigger cell size, similar to the effects found with differentiation conditions. An increased metabolic activity was observed in cells cultured under the influence of Mg-10Gd extracts, indicated by an acidic pH during most of the culture period. After 7 days of direct assay, ATDC5 growth, distribution and ECM synthesis were higher on Mg-10Gd samples, followed by Mg-2Ag and PMg (Fig.1), which was influenced by the homogeneity and composition of the degradation layer.

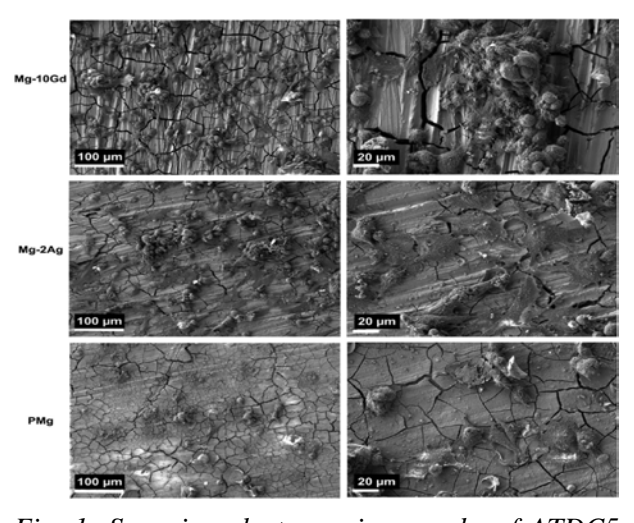


Fig. 1: Scanning electron micrographs of ATDC5 cells on Mg-10Gd, Mg-2Ag and PMg samples after 7 days of culture. Mg-10Gd: distribution of ATDC5, mostly as aggregates with rounded cell shape on the whole surface. Mg-2Ag: similar coverage as Mg-10Gd one but with lower cell aggregation and more spread morphology. PMg: lower cell number / aggregate spreading.

**DISCUSSION & CONCLUSIONS:** This study not only confirmed the tolerance of ATDC5 cells to Mg-based materials but also a chondrogenic effect of Mg-10Gd. Further studies in vitro and in vivo are necessary to evaluate cell reactions to those materials, as well as the effects on bone growth and the biocompatibility of the alloying system in the body.

ACKNOWLEDGEMENTS: This study has received funding from the Helmholtz Virtual Institute VH-VI-523 (In vivo studies of biodegradable magnesium based implant materials).

### DCPD/silver-based NPs coating on magnesium alloy scaffold for enhanced anticorrosion, osteogenesis and antimicrobial properties

Lei Zhang<sup>1</sup>, Jia Pei \*1, Gaozhi Jia<sup>1</sup>, Yi Hou<sup>1</sup>, Haodong Wang<sup>1</sup>, Guangyin Yuan \*1

<sup>1</sup> National Engineering Research Center of Light Alloys Net Forming and State Key Laboratory of Metal Matrix Composite, Shanghai Jiao Tong University, Shanghai 200240, China

INTRODUCTION: Magnesium and its alloys have been proposed as a class of revolutionary implant material in the orthopedic field due to their unique biodegradability and appropriate mechanical properties. However, the excessive degradation of magnesium-based scaffolds would largely undermine the implant lifetime and osseointegration properties. In addition, implantassociated infections remains another challenge as planktonic bacteria may simultaneously adhere onto medical implants and eventually evolve into biofilms, which always leads to the failure of the implants<sup>1</sup>. Here we report a novel multifunctional coating of DCPD/silver-based NPs on Mg-Nd-Zn-Zr (JDBM) alloy scaffolds, whose anti-corrosion properties and biological performance were investigated in vitro.

METHODS: The JDBM scaffold (Ø10×2 mm) was pre-treated to form a conversion MgF<sub>2</sub> film. Subsequently the pre-treated sample was coated with DCPD/silver-based NPs with in-situ chemical deposition method under optimized conditions, and characterized with SEM-EDX. The corrosion behaviour was studied by immersing the coated JDBM alloy scaffold in cell culture medium (DMEM). Osteoblast cells (MC3T3-E1) were used to evaluate the cytotoxicity of the coated JDBM alloy scaffold by direct cell adhesion assay. The antibacterial properties of the generated scaffold were characterized with two bacterial strains, E. coli and S. aureus, by spread plate method.

RESULTS: It can be observed from Fig. 1(a, b) that the coating consisted of silver phosphate NPs with an average size of ~800 nm on top of an underlying DCPD layer, which was integral and uniform with fine crystal grains. Direct cell adhesion assays of MC3T3-E1 osteoblastic cells after culturing for 1 day (Fig. 1(c)) showed a large number of well-spread osteoblast cells attached on the scaffold surface. For bacterial assay, after 12 h incubation of two bacterial strains with the samples, more than 99.9% of the bacteria were found to be dead in the DCPD/Ag-based NPs coating group, while there were significantly more live bacteria adhered on DCPD coating group and control group (Fig. 1(d)).

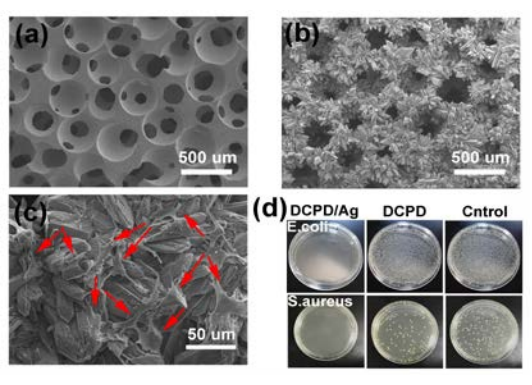


Fig. 1: Characterization of JDBM alloy scaffold before (a) and after coated with DCPD/silver-based NPs (b), morphology of osteoblast MC3T3-E1 cell adhered on the coating after 24 h of culture (c) and the antibacterial results (d).

**CONCLUSIONS:** DISCUSSION & Silver nanoparticles exhibit excellent antibacterial property with a broad spectrum for sterilization<sup>2</sup>. Even in small amounts, silver NPs present great antimicrobial property. Meanwhile, it was reported that a concentration range of 0.1-20 g mL<sup>-1</sup> of silver NPs induced no cytotoxic reactions to boneforming cells<sup>3</sup>. In this study, DCPD/silver-based NPs coating was for the first time generated on Mg alloy scaffolds through facile fabrication. On one hand, the composite coating fostered osteoblast adhesion and proliferation, excellent cytocompatibility. On the other hand, the as-obtained composite coating antibacterial properties against both gram-positive and gram-negative bacterial strains. Hence, the DCPD/Ag-based NPs coated JDBM scaffolds present great potential for tissue engineering application.

## Development and application of an osteoblast/osteoclast co-culture as a model to investigate in vitro effects of magnesium degradation products

S Behr, R Willumeit-Römer, B Luthringer

Helmholtz-Zentrum Geesthacht, Institute of Materials Research, Geesthacht, Germany

**INTRODUCTION:** The biodegradable implant materials provide the advantage of avoiding a second surgery. These materials should be resorbed by the body when their stabilising function is fulfilled. Magnesium (Mg) is of special interest as potential implant material because of its similar mechanical and physical properties compared to bone. However its fast degradation rate might be disadvantageous and can be tailored by adjusting the alloy composition, for example. Recently, in vivo studies highlighted the positive effect of Mg-silver based alloys on bone formation . The bone formation is a part of bone remodelling. In this process the bone forming cells or osteoblasts (OB) and the bone resorbing cells called osteoclasts (OC) are primarily involved. To unveil the mechanisms involved in the in vivo bone remodelling, we developed an OB/OC co-culture model and investigate the variations in the major inter- and intracellular signalling pathways.

METHODS: The co-culture consists of two human primary cell types: (I) peripheral blood mononuclear cell (PBMC; for OC) and (II) mesenchymal stem cells obtained from human umbilical cord perivascular cells (HUCPV; for OB). During indirect assays the co-cultures were exposed to Magnesium degradation products (MgDP) which were obtained according to EN ISO standards I. 10993-5:2009 and I. 10993-12:2012 (0.2 g material/mL  $\alpha$ -MEM with 10% FBS as extraction medium). Several alloys were selected. The Mg, Calcium (Ca), Silver (Ag), Gadolinium (Gd), and Phosphorous (P) contents were measured via inductively coupled plasma mass spectrometry (Table 1). The concentration of the MgDP in the cell culture media was equalized to 10 mmol/L Mg to observe the effect of Ag and Gd beyond Mg. Pure α-MEM with 10% FBS without MgDP was 28 The cell growth, differentiation and functional parameter were investigated for up to 28 days by biochemical assays, spectrophotometric and microscopical methods, targeting cell-specific markers. Among them, the activities of tartrate-resistant acid phosphatase (TRAP) and alkaline phosphatase (ALP) were measured to monitor OC and OB relation. The cell viability and metabolic activity were determined using water soluble tetrazolium (WST) test and lactate dehydrogenase (LDH) release. Moreover the co-culture was performed directly on different Mg - alloy targets to observe the change in cell response.

Table 1: Used materials and extracted ion concentrations (nD not determined):

Material	Ag (nmol/mL) at	Gd (nmol/mL)
	10 mmol Mg	at 10 mmol
		Mg
Mg	nD	nD
Mg-2Ag	0.96	nD
Mg-4Ag	3.35	nD
Mg-6Ag	3.42	nD
Mg-8Ag	5.84	nD
Mg-5Gd	nD	0.73
Mg-10Gd	nD	3.13

**RESULTS:** The cell number decreases in presence of MgDP for all types. Only in the presence of Gd, a significant increase of OB cell number can be observed. The enzymatic activity of ALP, an indicator for OB early mineralisation activity was increased after exposition to MgDP except Mg2-Ag and Mg-8Ag, at day 14. Another indicator for an elevated bone formation induced by Gd is the two-fold higher gene expression of initial Receptor activator of nuclear factor kappa-B ligand (RANKL) at day three of exposition. The OC activity and metabolism were also impacted by MgDP as indicated by several intracellular signals.

DISCUSSION & CONCLUSIONS: The results indicate that all MgDP disturbs the OC formation/differentiation and favours the OB differentiation. Silver seems to inhibit both OC and OB while Gd seems to express a synergistic effect with Mg on OB formation. Preliminary results indicate a similar behaviour in the direct on-target experimental set-up. Further work will be focused on the direct cultivation and the elucidation of underlying mechanisms via gene and protein expression studies.

### Reactive oxygen species: the hidden face of biodegradable Fe-based materials?

E Scarcello<sup>1</sup>, M Tomatis<sup>2</sup>, F Turci<sup>2</sup>, A Thomas<sup>3</sup>, P Jacques<sup>3</sup>, D Lison<sup>1</sup>

<sup>1</sup> <u>Louvain centre for Toxicology and Applied Pharmacology (LTAP)</u>, Brussels, Belgium. <sup>2</sup> <u>University of Turin</u>, Interdepartmental Centre Scansetti, Turin, Italy. <sup>3</sup> <u>Université catholique de Louvain</u>, Institute of Mechanics, Materials and Civil Engineering, IMAP, Louvain-la-Neuve, Belgium

INTRODUCTION: Based on their good mechanical properties and assumed biocompatibility, bioresorbable Fe-based materials have been proposed during the last decade as candidate alloys for manufacturing coronary stents. Previous investigations on the biocompatibility of metallic materials often overlooked the complexity of the biodegradation phenomenon and mostly focused on soluble ionic metallic forms released from the biocorrosion process for biological testing. In this work we investigate the possible implication of Reactive Oxygen Species (ROS) accompanying biocorrosion, and their potential role as a source of toxicity in a diseased tissue already submitted to oxidative stress.

**METHODS:** To document the implication of ROS in the biocorrosion process, acellular and cellular tests were conducted. First, we checked the ability of Fe-based materials to generate ROS by electron paramagnetic resonance (EPR) spectroscopy employing DMPO as spin-trapping agent. We evaluated the generation of carbon centred radicals (target molecule formate ion) and the surfacedriven Fenton reactivity (target molecule H<sub>2</sub>O<sub>2</sub>) by the different samples. On the other hand, we evaluated the in vitro cell viability on Human Umbilical Vein Endothelial Cells (HUVECs) using a WST-1 assay. Cells were exposed directly to iron powder (44890, Sigma-Aldrich®), or indirectly a porous membrane (Transwell<sup>®</sup>, CLS3381, Sigma-Aldrich®) to released iron ions. To confirm ROS implication, we also documented the mRNA expression of the oxidative stress response gene heme oxygenase-1 (HMOX-1) in HUVECs directly exposed to the same particles.

**RESULTS:** The EPR spectra (Fig. 1, 2) indicated, at each time point considered (10, 30 and 60 min), that all studied samples generated HO•, via a Fenton mechanism, and they were equally able to cleave the C–H bond of formate anion to generate a carboxyl radical (•CO<sub>2</sub><sup>-</sup>). Concerning the cellular tests, only the direct contact with the iron powder affected the viability of HUVECs (24 h), indicating that released ions alone are not responsible for the cytotoxic activity. The expression of *HMOX-1* is increased dose-dependently 4 h after exposure, confirming our hypothesis of oxidative stress.

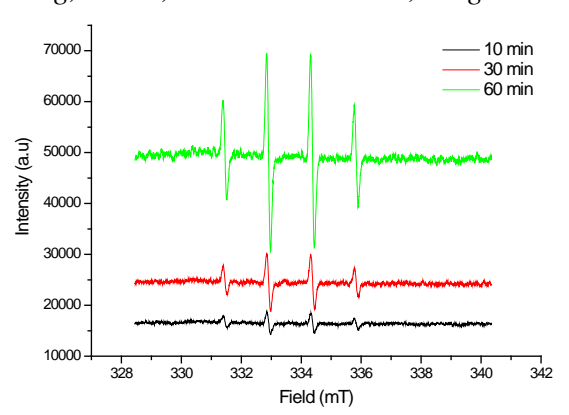


Fig. 1: EPR spectrum of DMPO/OH• obtained from iron powder (25 mg/ml).

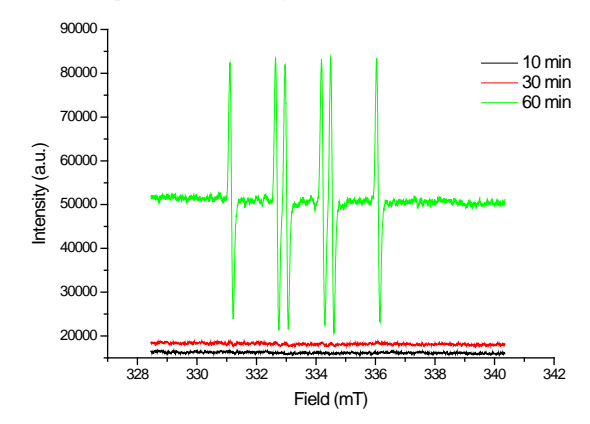


Fig. 2: EPR spectrum of DMPO/ ${}^{\bullet}CO_2^-$  obtained from iron powder (25 mg/ml).

biscussion & conclusions: ROS are known to be involved in the toxicity mechanism of several particles. We confirmed the ability of biodegradable Fe-based materials to produce ROS. The preliminary results support our hypothesis that ROS are involved in Fe-based materials toxicity through oxidative stress. Indeed, only a direct contact of the material with the endothelial cells showed a cytotoxic response, and increased the expression level of *HMOX-1*. Additional investigations are required to complete our work.

**ACKNOWLEDGEMENTS:** This project is part of an interdisciplinary research programme conducted under an ARC grant.

## Hyaluronic acid functionalised multifunctional silane coating on AZ31 Mg alloy for orthopaedic applications

Sankalp Agarwal<sup>1,2</sup>, Brendan Duffy<sup>1</sup>, James Curtin<sup>2</sup>, <u>Swarna Jaiswal<sup>1</sup></u>

<u>Centre for Research in Engineering and Surface Technology</u>, FOCAS Institute, DIT, Ireland
<u>School of Food Science and Environmental Health</u>, Cathal Brugha Street, DIT, Ireland

INTRODUCTION: Biodegradable magnesium (Mg) based alloys have been widely explored as potential biomaterials for orthopaedic implants due to their excellent biocompatibility and mechanical properties, which are similar to the natural bone<sup>1</sup>. However, rapid degradation in the physiological potential cytotoxicity, conditions. susceptibility to microbial infection deterred their clinical applications. The present study reports a hyaluronic acid (Hya) functionalised organosilane coating which not only enhances the corrosion resistance of AZ31 alloy but also improves the osteoinductive activity while acting as the bacterial anti-adhesive surface.

METHODS: The AZ31 Mg alloy were polished, ultrasonically cleaned and passivated in 5 N NaOH for 2 hr at 60 °C. The 2:1 molar ratio of MTES: TEOS (MT 2:1) and APTES (A, 400 mM) sols were prepared. The passivated AZ31-OH substrate was dip coated sequentially in MTES-TEOS (AZ31-MT) and APTES (AZ31-MT-A) sol-gels and cured at 120 °C for 1 h at each step. Furthermore, the amine terminated AZ31-MT-A surface was immersed in 0.1% w/v hyaluronic (Hya) for 4 hr and covalently coupled to achieve AZ31-MT-A-Hya surface. The electrochemical corrosion, biocompatibility and *S.aureus* (ATCC 1803) bacterial cell adhesion studies were conducted with the modified surfaces.

**RESULTS:** Fig 1 shows the impedance spectra of various coated substrates in buffered DMEM. The AZ31-MT and AZ31-M-A substrates showed a progressive increase in impedance ( $|Z|_{0.01\text{Hz}}$ ), whereas Hya functionalised AZ31-MT-A surface showed a decrease in impedance, but it is still two fold higher than the AZ31 alone.

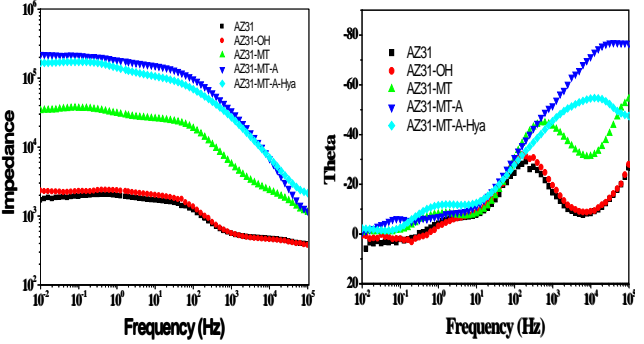


Fig 1: EIS spectra of different substrates

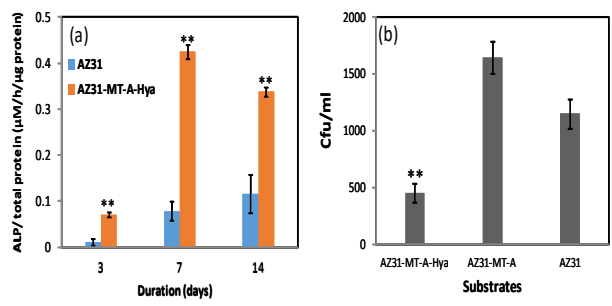


Fig 2: (a) ALP activity of MC3T3E1 osteoblast cells and (b) adhered viable S. aureus on different substrates. (Statistics: one-way ANOVA, \*\* P < 0.01)

Fig 2(a) shows the ALP activity of MC3T3E1 osteoblast cells cultured on the Hya functionalised surface. The AZ31-MT-A-Hya surface showed significant higher (p < 0.01) ALP activity as compared to the AZ31 alone. Fig 2(b) shows the quantification of adhered viable bacteria cell count on different substrates after exposure to the suspension of *S.aureus* in PBS for 4 hr at 37 °C. The Hya modified surfaces showed a significant reduction (p < 0.01) in bacteria cell count as compared to the AZ31 and corrosion resistant AZ31-MT-A substrate, indicating the bacterial anti-adhesive property of Hya. This also indicates the susceptibility of corrosion-resistant Mg surface to the bacterial colonisation.

DISCUSSION & CONCLUSIONS: The EIS analysis showed that the siloxane network of silane coating enhanced the corrosion resistance of Mg alloy<sup>1</sup>. However, Hya modified surface cause increase in corrosion, which may be due to the silane coating being saturated with the electrolyte (MES buffer, pH 5.5) used during covalent coupling reaction. Furthermore, Hya possesses stronger ability to differentiate the osteoblast cells and its hydrophilic nature attributed to the higher ALP activity of osteoblast cells and reduced adhesion of S.aureus on the surface respectively<sup>2,3</sup>. Hence, such multifunctional coatings on Mg alloy are highly desired for orthopaedic applications.

**ACKNOWLEDGEMENTS:** Authors acknowledge DIT for the financial support.

#### A new approach for measuring magnesium degradation rates

E.P.S. Nidadavolu<sup>1</sup>, F. Feyerabend<sup>1</sup>, T. Ebel<sup>1</sup>, R. Willumeit-Römer<sup>1</sup>, M. Dahms<sup>2</sup>

<sup>1</sup> Institute of Materials Research, Helmholtz-Zentrum Geesthacht, 21502 Geesthacht, Germany <sup>2</sup> Materials Technology, Hochschule Flensburg, Kanzleistraße 91–93, Flensburg 24943, Germany

**INTRODUCTION:** Determination of degradation rates for magnesium alloys by ASTM G31-12a standard has its own limitations. The primary limitation is the unrealistic approach extrapolating the single time point measurements (3 or 7 days) to the order of a year. This additionally poses the question of homogeneity in the degradation as it is a time dependent process. In order to determine the alloys degradation rate and morphology of degradation layer, long term tests in relation to the alloys intended stay in the body have to be performed. In the present study, long term immersion (LTI) tests were performed on powder metallurgy (PM) processed Mg-0.3Ca alloy, and on cast and extruded Mg-2Ag alloys.

**METHODS:** Immersion test has been employed as the standard method in determining the 'Mean degradation depth MDD, h ( $\mu$ m)' of the investigated alloys. DMEM Glutamax with 10% fetal bovine serum (FBS) was used as cell culture medium. 1% penicillin streptomycin was added as anti- bacterial agent. Cleaning and sterilization of PM processed samples was performed in an ultrasonic bath using cyclohexane and ethanol as reagents respectively. For cast and extruded Mg alloys gamma sterilization was performed. Incubation was carried out in 37 °C, 20%  $O_2$ , 5%  $CO_2$ , 95% rH cell culture environment. Removal of degradation layer was carried out using chromic acid (180g/L in distilled water) treatment.

**RESULTS:** The MDD, h ( $\mu m$ ) values of the investigated alloys were calculated using the following equation:

$$h = \Delta m/A\rho \tag{1}$$

The ASTM stipulated formula for measuring the corrosion rate (CR, mm/y) of the alloy is:

$$CR = \Delta m \ 8.76*10^4 / At\rho$$
 (2)

where,  $\Delta m$  (g) represents the mass change of the sample before and after immersion test when an alloy with the density of  $\rho$  (g/cm<sup>3</sup>) has its surface area A (cm<sup>2</sup>) exposed to the medium for a time of t (h).

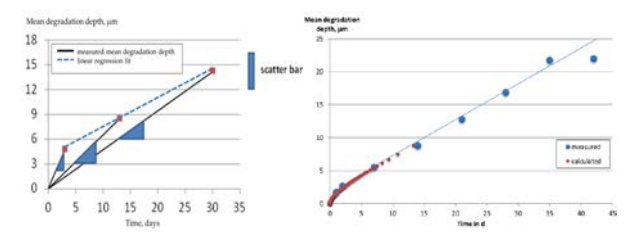


Fig. 1: MDD,h (µm) vs time (d) plots for Mg-2Ag(left) and Mg-0.3Ca (right). The blue lines in both figures indicate the linear regression fit for the measured data.

**DISCUSSION & CONCLUSIONS:** The usual behaviour reported in the literature (by ASTM approach) about the decrease in corrosion rate with increasing immersion time can be seen in Figure 1 (left). It is indicated as a decrease in the slope values of the black lines at their respective immersion times. The fact that degradation is rather linear is shown by the linear regression fit (blue line). This fact, however, is concealed when evaluated using Eq.2 for degradation rate interpretation. In the plot with more discrete time points (right), linear degradation behaviour is observed for Mg-0.3Ca alloy after 5 days of immersion. The degradation rate is now a constant value which is obtained from the slope value of the linear regression line; 0.51µm/d (blue line). This method is more realistic in assessing the degradation rate and behaviour of the alloy compared to single time point measurements. If the alloy is homogenous, number of samples per time point can also be reduced.

**ACKNOWLEDGEMENTS:** The authors would like to thank all the colleagues for the input of data and contributing to scientific discussions. The research leading to these results has received funding from the Helmholtz Virtual Institute "*In vivo* studies of biodegradable magnesium based implant materials (MetBioMat)" under grant agreement n° VH-VI-523.

### Investigation of corrosion initiation on as-cast Mg-Ca-Zn using XANES

<u>D Zander</u><sup>1</sup>, NA Zumdick<sup>1</sup>, B Hesse<sup>2</sup>, P Zaslansky<sup>3</sup>, C Fleck<sup>4</sup>

<sup>1</sup> Chair of Corrosion and Corrosion Protection, RWTH Aachen University, Germany. <sup>2</sup> ESRF - The European Synchrotron, France. <sup>3</sup> Department for Restorative and Preventive Dentistry, Charité - University Medicine Berlin, Germany. <sup>4</sup> Institute for Material Sciences and Technologies, Technical University Berlin, Germany.

**INTRODUCTION:** Corrosion investigations of biodegradable Mg alloys, especially of Mg-Ca-Zn, usually focus on the corrosion behaviour and mechanisms during mid- and long-term exposure to corrosive mediums, such as SBFs.

In this study, the corrosion initiation on low alloyed Mg-Ca-Zn were investigated with regard to the initial surface changes of the surface. Microstructural features that possibly cause localized corrosion were identified. Special focus lies on the identification and evolution of corrosion products with respect to individual and combined components present in the electrolyte.

**METHODS:** Flat ZX11 die cast samples prepared with 4000 SiC paper were immersed in various alterations of Hank's balanced salt solution. Immersion times ranged from 30 minutes to 24 hours. The corroded samples were investigated via scanning electron microscopy (SEM) and energy dispersive spectroscopy (EDX). Additionally, at ESRF (Grenoble, France), synchrotron x-ray fluorescence ( $\mu$ -XRF) and synchrotron x-ray adsorption near-edge spectroscopy (XANES) were conducted.

**RESULTS:** The SEM investigations after 150 minutes of corrosion time revealed randomly distributed local corrosion attacks with a volcanolike appearance, as representatively shown in Figure 1.

A central Fe-containing particle with high mass contrast was observed inside these volcano-like structures. In the surrounding area, high Mg and O contents with an atomic Mg/O ratio of ~ 0.5 were detected via EDX. Around this area, a circular seam of Ca, O and P was detected.

The XRF maps showed similar circular-vulcano like enrichments of Ca and P. Via XANES and the use of the finger-print method (comparison of measured and known spectra) amorphous calcium phosphate was detected as a corrosion product.

Magnesium phosphates spectra were measured in the vicinity of the corrosion attacks that were formed on Mg-Ca-Zn immersed in a solution without calcium. In a solution without chlorides, severe localized corrosion was observed and similar corrosions products to those being formed in full Hanks solution were observed.

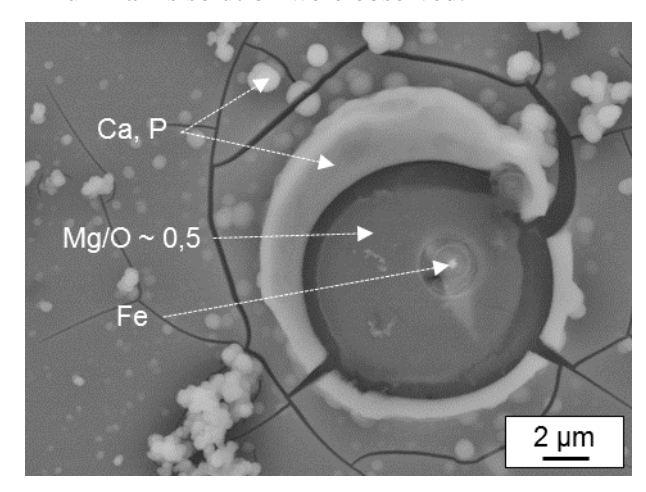


Fig. 1: Scanning electron micrograph of ZX11 after a 150-minute immersion in Hanks' balanced salt solution.

DISCUSSION & CONCLUSIONS: Impurities, such as iron containing particles, were identified as corrosion initiation sites. Even in a solution without chlorides, which are known to cause localized corrosion, localized corrosion was observed. With calcium in the solution, amorphous calcium and magnesium hydroxide formed as initial corrosion products. The formation of calcium phosphate as a direct corrosion product of magnesium may play an important role for the in vivo formation of bones and osseointegration.

## Effect of magnesium-degradation products and hypoxia on the angiogenesis of human umbilical cord vein-derived endothelial cells

Lei Xu, Regine Willumeit-Römer, Bérengère Luthringer

Helmholtz-Zentrum Geesthacht Centre for Materials and Coastal Research, Institute of Materials
Research, Institute of Metallic Biomaterials
Max-Planck-Straße 1, 21502 Geesthacht, Germany

INTRODUCTION: Angiogenesis is a key component of bone repair, in which new blood vessels are formed to bring oxygen and nutrients and bone precursor cells to the injury site. Studies have also indicated the importance of hypoxia in fracture healing, angiogenesis. Magnesium as a bio-degradable material has been reported to influence angiogenesis. The interaction of Mg, hypoxia and angiogenesis still needs to be studied for the development and application of Mg-based biomaterial. Therefore we apply freshly isolated human umbilical cord vein endothelial cells (HUVEC) to investigate the reorganization and migration stages of angiogenesis under impact of Mg degradation and hypoxic conditions.

METHODS: HUVECs were maintained in completed M200 medium (LSGS, Thermo Fisher Scientific, USA) and 10% foetal bovine serum (FBS, PAA Laboratories, Austria). Magnesiumdegradation products were obtained characterised according to and then diluted into 1.5, 2.0, 3.0, 4.0, 8.0, and 16.0 mM. Oxygen concentrations in incubators were 20% and 5%. Isolated HUVECs were characterised with the expression of cluster of differentiation (CD) 31 (platelet endothelial cell adhesion molecule), CD105 and CD45 by S3e flow cytometer and cell (BioRad, Munich, Germany). formation and wound healing assays were performed according to modified methods. All data were acquired from three independent experiments with triplicate observations of three donors. Statistical analysis was performed by one-way ANOVA ( $\alpha$ =0.05).junctions, branches, total length of branches and total length of tubes in controls at 6 h under hypoxic conditions. Cultivation for 24 h under hypoxia resulted in an increased number of extremities and decrease of the total length of tubes in controls. Under impact of Mg degradation products, there were reduced numbers of nodes (at 4, 8 and 16 mM), extremities (16 mM), junctions (4, 8 and 16 mM), branches (2 to 16 mM) and total length of branches (3, 8 and 16 mM) and tubes (3 to 16 mM) observed at 6th hour and 20% O2 when

compared to the control. However, after 6 hours cultured at 5%  $O_2$ , only extremities were significantly reduced in 3 and 4 mM Mg. After one day of incubation under 20%  $O_2$ , there were reduced numbers of nodes (16 mM), junctions (16 mM), branches (3 and 16 mM) and total length of branches (3, 4 and 16 mM) and total length of tubes (3 to 16 mM) observed. The numbers of nodes (8 and 16 mM), extremities (2 to 16 mM), junctions (8 and 16 mM), branches (8 and 16 mM) and total length of tubes (4 to 16 mM) were remarkably decreased after 24 h at 5%  $O_2$ . The wound area of HUVEC was significantly increased under 1.5, 2 and 4 mM Mg at 20%  $O_2$ .

DISCUSSION & CONCLUSIONS: We could confirm the efficient isolation of HUVEC and without hematopoietic contamination based on the high positive ratios of CD105 and CD31 and low expression of CD45. Therefore, the cells can be utilized as model system to study the angiogenesis. Mg-degradation products could decrease the tube formation of HUVEC while hypoxia may have a protective effect on such influence. Wound healing results indicate a stimulation effect of Mg-degradation products on the migration of HUVEC, which may be inhibited by hypoxia.

### Migration assay of human gingival fibroblasts (HGF) on a magnesium surface

R Amberg<sup>1</sup>, A Elad<sup>2</sup>, M Barbeck<sup>2</sup>, F Witte<sup>1</sup>

<sup>1</sup>Julius Wolff Institute, Berlin-Brandenburg Center for Regenerative Therapies, Charité Universitätsmedizin, Berlin, <sup>2</sup>Botiss GmbH, Berlin

INTRODUCTION: Since several years there is a high interest in magnesium as biodegradable metal implants for dentistry due to their excellent biocompatibility and their low elastic moduli, similar to natural bone, which prevent stress shielding. The integration of gingival tissue at the implant abutment plays a crucial role for implant success. The aim of this study was to investigate the migration of human gingival fibroblasts (HGF) on magnesium. Therefore, a migration assay adjusted to the specific requirements of magnesium has be to be developed.

**METHODS:** Primary HGF, labelled with fluorescent dye Cell-Tracker Red were cultivated for 24 h. Cells were seeded in 24-well-plate on plastic as control and pre-corroded magnesium foils by using a silicone insert and were allowed to attach for 24 h to form a confluent monolayer. Before seeding, each slide was "pre-corroded" in 10 mL culture medium for 3 days at 37 °C without CO<sub>2</sub> exchange.

After scratching and washing the monolayer, the slides were placed with the attached cell-site down on silicone half-rings in a new well-plate, then fixed with two glass stones and adding fresh culture medium. After a 4 hour incubation, the plate was tipped sideways to release the formed hydrogen bubbles upon the surface. Imaging was started using an inverted microscope with a live cell imaging system over a period of 50 hours.

**RESULTS:** As shown in **Error! Reference source not found.** and Fig. 2, HGF migrated slower on magnesium compared to plastic. 50 % of the initial area were closed after 13 hours on plastic and after 22 hours on magnesium. Roughness measurements with atomic force microscope indicate a  $S_a$ -value of  $131.6\pm4.43$  nm for pre-corroded magnesium.

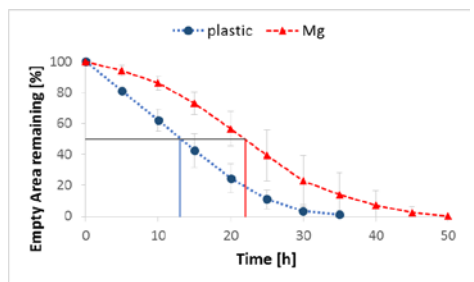


Fig. 1: Wound closure of HGF over time on plastic and magnesium (Mg), n=6.

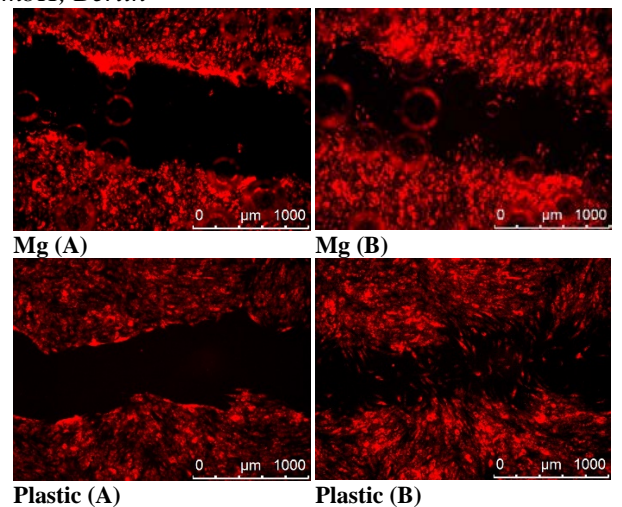


Fig. 2: Images of migrating HGF on plastic and magnesium (Mg) at starting (A) and after 15 hours (B).

**DISCUSSION & CONCLUSIONS:** This study shows the first migration assay developed for magnesium. Pre-corrosion of the magnesium led to an overall increased cell adhesion. The determined  $S_a$ -value of 131.6 nm correlate with cell adhesion tests on titanium alloys at values of 200 nm or less, indicated by Young-Sung et al. who investigate the attachment of HGF on different surface roughnes. Migration of HGF is about 1.7x times slower on magnesium then on tissue culture plastic to reach 50 % scratch are closing. This result is comparable to other migration studies and shows a slightly faster migration on magnesium then on titaniumzirconium surfaces. The manifold impacts, such as hydrophilicity or magnesium concentration, on cell migration behaviour still have to be investigated.

#### **ACKNOWLEDGEMENTS:**

The authors acknowledge the support of the Berlin-Brandenburg Center for Regenerative Therapies (BCRT).

#### In vitro study on degradation behaviour of open porous Mg scaffolds

G Jia<sup>1</sup>, H Huang<sup>1</sup>, R Willumeit-Roemer<sup>2</sup>, F Feyerabend<sup>2</sup>, G Yuan<sup>1</sup>

<sup>1</sup> <u>School of Materials Science and Engineering</u>, Shanghai Jiao Tong University, Shanghai 200240, China. <sup>2</sup> Helmholtz-Zentrum Geesthacht, Geesthacht, Germany

INTRODUCTION: Scaffold is one of the most challenging subjects in tissue engineering, which plays a key role in assisting tissue regeneration. Mg has been considered an osteoconductive and bone growth stimulator material as suggested by many studies, and identified as a promising material for tissue engineering. However, the porous structure of magnesium substrate would deteriorate the structural integrity due to large specific surface area during the contact with aqueous solution. The present study is mainly focused on the degradation behavior of Mg scaffolds under semi-static degradation conditions.

**METHODS:** In order to evaluate the effect of pore characteristics on the degradation behaviour of porous structure. Two groups of Mg scaffolds, one with spherical main pores while the other with irregular polyhedral pores were subjected to static corrosion tests. All degradation tests were conducted on the specimens with dimensions of  $\phi$ 10mm × 2 mm for 2 weeks, 4 weeks and 6 weeks, respectively. The static degradation tests were carried out in 12 wells plates while each sample was immersed in 3 ml of DMEM + 10% FBS under cell culture conditions. The corroded samples were evaluated by micro-computed tomography (µCT) and scanning electron microscope (SEM) equipped with energy dispersive X-ray spectroscopy (EDS).

**RESULTS:** Mg scaffolds were covered with deposits in semi-static corrosion tests after 2 weeks, and it was quite obvious that with the experiment on going the volume of samples were getting smaller and smaller. After 4 weeks, the surface of porous structure of both groups was fully filled with deposits. After 6 weeks, the apparent volume of spherical pore samples was much smaller than the irregular pore group.



Fig. 1 Macroscopic view of Mg scaffolds.

The tomography results showed the inner part of porous structure was still porous even after 6 weeks. However, the interconnected pores were getting blocked after 2 weeks and the interconnectivity was completely lost after 6 weeks. The interconnectivity of irregular pore group was more susceptible during corrosion procedure due to random interconnected pore size distribution which was in the range of  $50 \sim 300$   $\mu m$ . The smaller interconnected pores were more easily blocked by the corrosion deposits at the beginning.

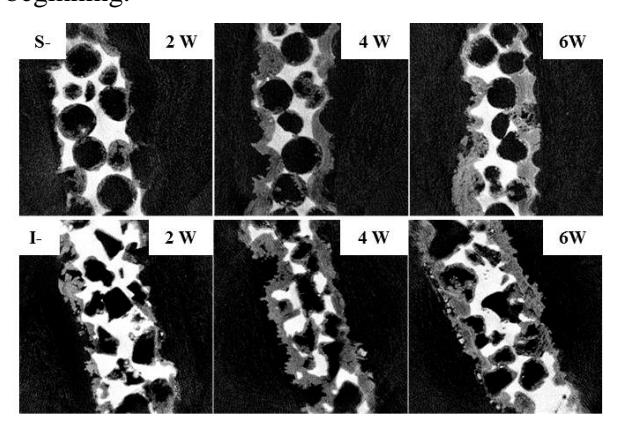


Fig. 2 Micro-CT images of Mg scaffolds after static degradation tests.

**DISCUSSION AND CONCLUSIONS:** Spherical pore structure maintained better interconnectivity during semi-static corrosion test, but the whole structural integrity was not as well as the irregular porous group.

**ACKNOWLEDGEMENTS:** The authors are grateful to the equipments support of Helmholtz-Zentrum Geesthacht and the scholarship given by China Scholarship Council. Frank Feyerabend received funds of the Helmholtz Virtual Institute VH-VI-523 (In vivo studies of biodegradable magnesium based implant materials.)

# Biomaterials *in vivo* microenvironment pH (μe-pH) plays vital role during the bone defects regeneration process

WL Liu<sup>1</sup>, HB Pan<sup>1,\*</sup>

<sup>1</sup> Research Center for Human Tissue and Organs Degeneration, Institute of Biomedicine and Biotechnology, Shenzhen Institutes of Advanced Technology, Chinese Academy of Sciences, Shenzhen, China

**INTRODUCTION:** In scenario of osteoporotic fracture, significantly higher activity of osteoclasts than osteoblasts may lead to continuous loss of bone in fracture/defect site. The key issue for developing biomaterials that specifically tailored for applications in osteoporotic bones is to re-establish normal bone regeneration at the fracture site. Acidbase property could directly influence the behavior of bone cells, thus making it an important factor to modulate the unbalanced activity between osteoclast and osteoblast in osteoporotic conditions; and more importantly, it is adjustable through controlling the release of the alkaline ions. Therefore, a rational strategy to reconstruct the regeneration balance in the fracture site is to regulate the implant microenvironmental pH (µe-pH) application through the and surface modification of biodegradable materials.

**METHODS:** The performance of Akermanite (Ak),  $\beta$ -tricalcium phosphate ( $\beta$ -TCP), calcium silicate (CS), strontium-substituted calcium silicate (Sr-CS) and Hardystone (Har) in healing a 3 mm bone defect on the ovariectomized (OVX) osteoporotic rat model was evaluated. The proliferation, osteoblastic differentiation of bone marrow stromal cell and osteoclastogenesis capability of RAW 264.7 cells that influenced by culture medium pH change was investigated<sup>1,2</sup>.

**RESULTS:** Higher initial μe-pH was associated with more new bone formation, late response of TRAP<sup>+</sup> osteoclast-like cells and the development of an intermediate 'apatitic' layer in vivo. There's more new bone formed in Ak group than in b-TCP or Har group at week 9. The initial μe-pHs of Ak were significantly higher than that of the b-TCP and Blank group, and this weak alkaline condition was maintained till at least 9 weeks post-surgery. increasing deformation. When annealing was performed, full recrystallization was achieved, having equiaxed grains with no twins present inside them. Static immersion tests showed that the degradation rate of the alloy is at least 2 times higher

Increased osteoblastic activity which was indicated by higher osteoid secretion was observed in Ak group at week 4 to week 9. A weak alkaline conditions stimulated osteoporotic rat bone marrow stromal cells (oBMSC) differentiation, while inhibiting the formation of osteoclasts.

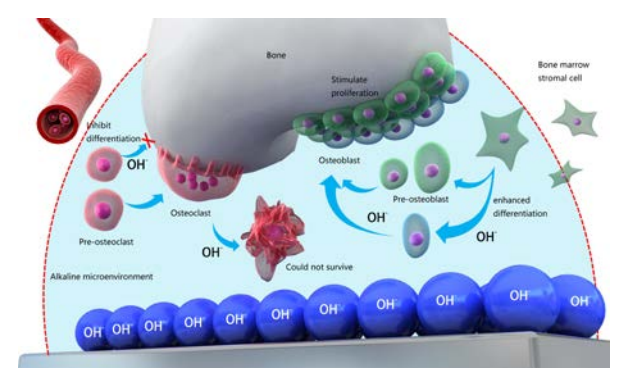


Fig. 1: Sketch map of the  $\mu$ e-pH and the performance of biomaterials

**DISCUSSION & CONCLUSIONS:** We have established the method for *in vivo* biomaterials μepH detection, and demonstrated the important role of μe-pH in guiding the localized bone regeneration. We proposed that an alkaline microenvironment that generated by biodegradable metal alloys is important in the development of orthopaedic biomaterials, in particular for repair of osteoporotic bone fracture /defect.

#### **ACKNOWLEDGEMENTS:**

This work was supported by grants from the National Natural Science Foundation of China (No. 81672227) and Shenzhen Peacock Program (No. 110811003586331).

### In vitro environment influence on magnesium biodegradable materials

J Gonzalez<sup>1</sup>, F Feyerabend<sup>1</sup>, R Willumeit-Römer<sup>1</sup>

<sup>1</sup>Metallic Biomaterials, Helmholtz-Zentrum Geesthacht, Geesthacht, Germany.

**INTRODUCTION:** The difficulty to predict in vivo degradation of magnesium based materials by laboratory testing is mainly related to a non-well degradation understood mechanism conditions. The physiological amount exchange rate of physiological fluid has been postulated as an important factor on the stability of the potentially protective degradation layer. Therefore systematic studies about these influences can help to achieve a better standardization of in vitro testing and to explain differences on degradation behaviour in different implantation sites. The Mg-Ag system combines better mechanical properties than pure Mg with wellknown antibacterial properties of Ag+ ions and an acceptable degradation rate.

**METHODS:** T4 heat treated and extruded Mg-2Ag disks (10 mm x 2 mm) were tested *in vitro* for 30 days under sterile cell culture conditions in different liquid volumes per sample area (V/A ratio = 1, 5, 10 mL/cm²) of MEM-α supplemented with 10% FBS and 1% penicillin-streptomycin. Applying a semi-static methodology, the medium was changed every 2-3 days and at the same time osmolality and pH change were evaluated. Mass loss, degradation morphology and the degradation layer composition were evaluated after 2, 7, 15, 21 and 30 days of immersion.

**RESULTS:** Figure 1 shows how 5 and 10 mL/cm<sup>2</sup> promote higher pH change values than 1 mL/cm<sup>2</sup>. This situation agrees with the higher degradation rate (DR) values measured by mass loss (Table 1) for 5 and 10 mL/cm<sup>2</sup>.

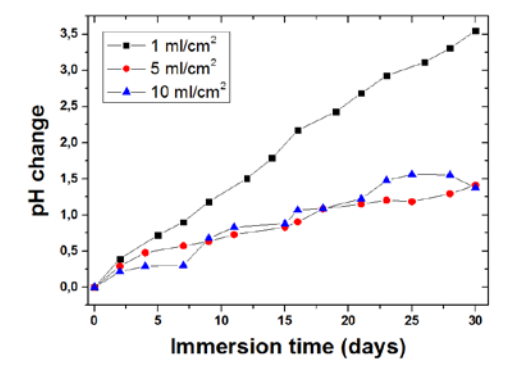


Fig. 1: pH change over the immersion time (30 days) for different V/A ratio applied in semi-static immersion test to extruded Mg-2Ag (T4) disks.

Moreover, high V/A ratios (5 and 10 mL/cm²) promoted higher amounts of phosphorous and calcium deposition on the sample surface from the beginning of the immersion. The precipitation seems to be stabilised after around 15 days of immersion. This stabilisation seems to correlate with the DR consolidation at the same immersion time.

Table 1. Mean degradation depth (MDD) and degradation rate (DR) with the standard deviation evaluated on Mg-2Ag (T4) disks after 30-days immersion test for the different V/A ratio applied.

V/A ratio [mL/cm <sup>2</sup> ]	MDD [μm]	DR [µm/d]
1	$12.0 \pm 0.9$	$0.40 \pm 0.03$
5	$21.0 \pm 0.2$	$0.70 \pm 0.01$
10	$19.0 \pm 0.2$	$0.63 \pm 0.01$

DISCUSSION & **CONCLUSIONS:** The experimental setups evaluated show a minimum V/A ratio below which the degradation rate is significantly decreased. On the other hand, the degradation layer composition obtained for the different experimental setups reveals a correlation between the degradation rate and the degradation layer development. Low V/A ratios promote higher solute concentration coming from the anodic dissolution and contain a lower buffer capacity saturation/passivation generating possible situations that control the rate of the degradation process. However, different V/A ratios provide different amounts of Ca<sup>2+</sup>, and PO<sub>4</sub><sup>3+</sup>, modifying the amount of precipitation that possibly influence the DR developed.

**ACKNOWLEDGEMENTS:** The author whish thanks the support of Helmholtz Virtual Institute VH-VI-523 (in vitro studies of biodegradable magnesium based implant materials).

### Mg-Ag-Gd alloys as biodegradable implant materials

Y. Lu<sup>1</sup>, Z. Liu<sup>1</sup>, Y. Huang<sup>1</sup>, F. Feyerabend<sup>1</sup>, R. Willumeit-Römer<sup>1</sup>, R. Schade<sup>2</sup>, K. Liefeit<sup>2</sup>, K. U. Kainer<sup>1</sup>, N. Hort<sup>1</sup>

<sup>1</sup>Institute of Materials Research, Helmholtz-Zentrum Geesthacht, Max-Planck-Strasse 1, 21502 Geesthacht, DE

<sup>2</sup>Institute for Bioprocess and Analytical Measurement Technology e.V., Rosenhof, 37308 Heilbad Heiligenstadt, DE

**INTRODUCTION:** Mg-Ag alloys were developed as biodegradable implant materials which combine favourable mechanical properties especially with the antibacterial behaviour of silver. The Mg-Gd alloys show promising mechanical and corrosion properties for biomedical application. In this work, the aim was to combine these properties by producing a ternary alloy.

**METHODS:** Pure Mg, Mg-xAg, Mg2Gd-xAg (x=1, 2 wt.%) alloys were prepared by permanent mould casting<sup>1</sup>. *In vitro* degradation experiments for both as-cast and T4 heat treated alloys were performed in cell culture medium (CCM) under cell culture conditions. Degradation rate (DR) was determined by weight loss. The antibacterial assays were carried out in a dynamic bioreactor system by using two types of bacteria, namely S. aureus (DSM no. 20231) and S. epidermidis (DSM no. 3269) at iba e.V. Heiligenstadt, Germany. In order to analyse the living and dead bacteria, Adhered bacteria were counted using a fluorescence microscope after sonification in ultrasonic bath and fluorescence labelling by adopting LIVE/DEAD® BacLight™ Bacterial Viability Kit. After labelling, a confocal laser scanning microscope was utilized to visualize the whole sample surface with local details.

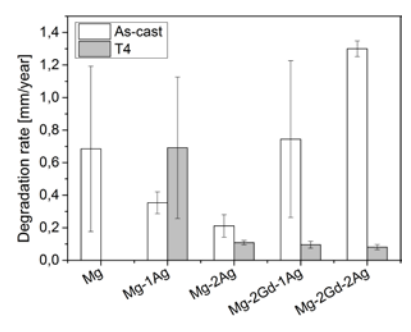


Fig. 1: In vitro degradation rate of the pure Mg, binary Mg-Ag and ternary Mg-2Gd-xAg alloys in the as-cast and T4 conditions after immersion in CCM under cell culture condition for 7 days.

**RESULTS:** As shown in Fig. 1, the addition of 2 wt.% Gd to both Mg-Ag alloys leads to an increase of the DR. With more addition of Ag to the Mg-2Gd alloy, the DR becomes even higher. However, after T4 heat treatment, the DR for both Mg-2Gd-xAg alloys is significantly reduced due to the

dissolution of intermetallic phases. The biofilms of all tested alloys show no obvious difference. The surfaces have a larger number of dead bacteria, while there are still some live bacteria present (Fig. 2). The combination of Gd and Ag with ratio 1:1 (Mg-2Gd-2Ag alloy) leads to a lower viability of bacteria than the negative controls (Ti and B33) and other Ag containing alloys (Fig. 3).

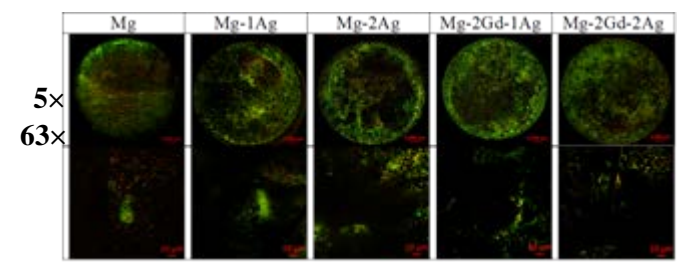


Fig. 2: Surface morphology of formed biofilm on discs of the pure Mg and T4 heat treated alloys after bacteria adhering tests, where live bacteria are labelled in green and dead bacteria in red.

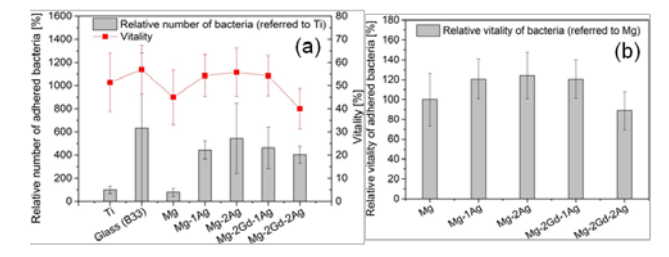


Fig. 3: Comparison of the adhered bacteria number and their vitality on control groups and all tested alloys.

#### **DISCUSSION & CONCLUSIONS:**

Although the Mg-2Gd-2Ag alloy exhibited a slight antibacterial effect, this is far from being effective. This could be due to the very low DR, leading to an insufficient release of silver ions. An increase in the amount of alloying elements may lead to higher antibacterial activity.

**ACKNOWLEDGEMENTS:** This project is funded by the Helmholtz Virtual Institute VH-VI-523 (In vivo studies of biodegradable magnesium based implant materials).

### The effect of surface roughness modification of magnesium alloy by femtosecond laser on cell attachment

Hyejun Kil<sup>1,2</sup>, Hyung-Seop Han<sup>1,3</sup>, Jimin Park<sup>1</sup>, Myoungryul Ok<sup>1</sup>, Hojeong Jeon<sup>1</sup>, Hyun-Kwang Seok<sup>1</sup>, Jin-Woo Park<sup>2</sup>, Yu-Chan Kim<sup>1\*</sup>

<sup>1</sup> <u>Center for Biomaterials</u>, Biomedical Research Institute, Korea Institute of Science and Technology, Seoul, South Korea <sup>2</sup> <u>Laboratory for Materials Interfaces</u>, Department of Materials Science and Engineering, Yonsei University, Seoul, South Korea <sup>3</sup> <u>Nuffield Department of</u> Orthopaedics, Rheumatology and Musculoskeletal Sciences, University of Oxford, Oxford, U.K.

**INTRODUCTION:** The surface treatment of biomaterials is considered as one of the essential parts of material development process since it can have directly impact on the adhesive interaction between cell and the surface of biomaterials. Recently, there has been a significant amount of studies that reported the control of cell adhesion by controlling the surface roughness through the surface treatment methods such as etching, anodizing, laser treatment. Among the various surface treatment methods, laser treatment has attracted tremendous attention due to its simplicity and effectiveness. The femtosecond (fs) laser benefits from a shorter time for the surface to be affected by the heat and thus minimizing the damage from heat while changing the roughness of the surface. In this study, the fs laser was used to the surface of the biodegradable magnesium (Mg) alloy. Variations in the surface roughness of the alloy were measured, and the difference in cell attachment was observed.

**METHODS:** Coin-shaped Mg alloy specimens were prepared (diameter of 8 mm and thickness of 1 mm) for surface modification with fs laser (343 nm wavelength) at a repetition rate of 1 kHz. Scan speed was 2 mm/s and average pulsed power was 35  $\mu$ J. The cell adhesion experiment was performed on the specimens by using the MG63 cells. After one day, specimens were stained with Giemsa stain to show the cell adhesion, and the optical microscope was used.

**RESULTS**: Scanning electron microscope images of Figure 1(a) and 1(b) illustrates the difference in morphology produced by laser ablation, which results in significantly different surface roughness. Laser treated group showed rougher surface in general when compared to the control group without laser treatment. Optical microscope images of Figure 1(c) and 1(d) shows the difference in cell attachment on the laser treatment surface of Mg alloy specimens. There are considerably fewer

cells in the laser treated area when compared to the control area.

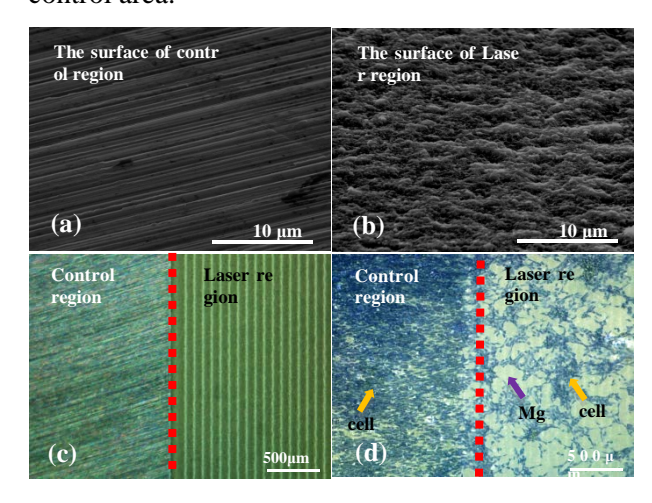


Fig. 1: Surface profile of (a) control and (b) laser treated surface and OM images of samples (c) before the cell experiment and (d) after cell experiment.

**DISCUSSION & CONCLUSIONS:** In this study, we observed the difference in cell adhesion on the surface of Mg alloy depending on the roughness. As reported in the previous studies, the roughness of surface directly affected the attachment of cells [2]. The result from this study can be utilized for various biomaterials to control the adhesion of different cells by changing the roughness of the surface with a laser treatment.

**ACKNOWLEDGEMENTS:** This research was supported by Korea Ministry of Health and Welfare (2M34410) and TRC Project (2V05400).

#### 3D cell culture to test novel implants

N Donohue<sup>1</sup>, B Lohberger<sup>1</sup>, A Weinberg<sup>2</sup>

<sup>1</sup> Medical University of Graz, Department of Orthopaedics Surgery, Austria.

INTRODUCTION: Biodegradable magnesium (Mg) is a promising alternative to steel or titanium implants in orthopaedic surgery. Mg gradually degrades in contact with body fluids, while supporting bone regeneration. However, novel Mg alloys require extensive testing to evaluate their biosafety and capabilities. In this work, 3-dimensional cell culture of human mesenchymal stem cells is used to establish an in vitro model of the interface between bone and Mg implant material. This model allows fundamental research to be conducted on implant safety and Mg-induced bone healing.

**METHODS:** Human mesenchymal stem cells (hMSCs) were isolated from femoral heads collected during hip operations. Following expansion, cells were differentiated osteoblasts, chondrocytes and adipocytes. Successful differentiation was visualized by histological staining, using Alizarin Red, Alcian Blue and Oil Red O dyes, respectively. Fluorescent Assisted Cell Sorting (FACS) was performed to evaluate cell surface markers according to the criteria established by Dominici et al., (2006).

**RESULTS:** Two cell lines were fully characterized as hMSCs by differentiation (Fig. 1 and 2) and FACS, according to which the cell lines were positive for markers CD90, CD105 and CD73 as well as negative for CD14, CD45, CD34 and CD19.

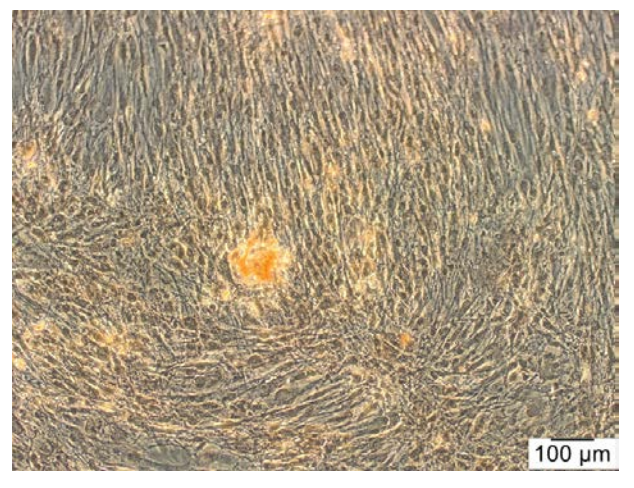


Fig. 1: Osteogenic differentiated hMSCs stained by Alizarin Red.

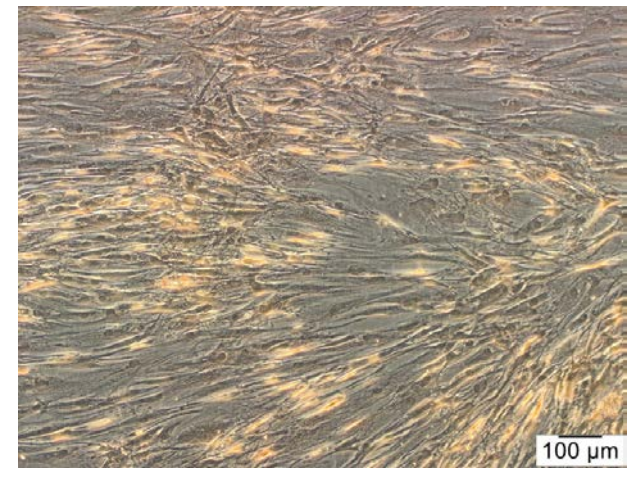


Fig. 2: Undifferentiated hMSCs stained by Alizarin Red.

DISCUSSION & CONCLUSIONS: After successfully characterizing the hMSCs, the next step is to establish the 3D cell culture model and analyse the effects of Mg implants. Degradable Mg pins will be inserted into the 3D culture and the effects on cells will be determined by RNA and protein expression analysis. This work will focus on determining the molecular pathways that are responsible for the bone regeneration properties of Mg and in particular how microRNAs affect major osteogenic regulators such as RUNX2 during this process.

**ACKNOWLEDGEMENTS:** The authors wish to thank Heike Kaltenegger for technical support.

### Mg alloy corrosion by four kinds of cell lines

K Kikuchi, A Kitagawa, K Hanada

Material Processing Group, Advanced Manufacturing Research Institute,

National Institute of Advanced Industrial Science and Technology (AIST), Tsukuba, JAPAN

**INTRODUCTION:** Mg alloy can be used as promising biodegradable grafts for bone, vascular and intestinal tract surgery. Four types of cell lines whose origins were related to these organs were cultured on Mg alloy staples and cell adhesion and proliferation were monitored for 4 weeks. Mg corrosion by cells was accessed by microscopic observations and the tensile testing. Mg content in culture media was also monitored.

METHODS: Mg-2%RE-1%Y (EW21) alloy staples were sterilized with dehydrated ethanol, placed in a 24-well low-bind dish and soaked in DMEM for 60 min before introducing cells. 1.0x10<sup>5</sup> of MC3T3-E1, F-2, CACO-2 and RAW24 were seeded in a well containing 3 staples and cultured for 24 hr in a CO<sub>2</sub> incubator. Cells which had not adhered to staples were removed and cultured for 3, 7, 14, 21 and 28 days, changing media every 3 days. The pH of culture media was measured on media change and changed media were kept at -80 °C until Mg assay.

On the day of observation, staples were transferred to a 96-well white plate containing 50  $\mu$ l DMEM in each well. Cell proliferation was determined by RealTime Glo MT Cell Viability Assay (Promega). 50  $\mu$ l 2X RealTime Glo reagent was added to each well and incubated in a CO<sub>2</sub> incubator for 60 min. Luminescence was monitored at 37 °C with an integration time of 1 sec per well using Synergy HTX (Biotek).

After the cell proliferation assay, staples were transferred to a 24-well dish containing 2  $\mu M$  Calcein AM and 4  $\mu M$  EthD-1 LIVE/DEAD solution. Cells were incubated for 20 min and observed with EVOS FL (ThermoFisher).

**RESULTS:** MC3T3-E1, a murine preosteoblastic cell line showed an excellent cell adhesion on Day 1, propagated to cover the entire staple on Day 3 and formed a thick cell layer on Day 7 (Fig. 1A). F-2, a murine vascular endothelial cell line showed fair cell adhesion on Mg alloy staples on Day 1 and kept growing until Day 7; however, the adhesion was not as strong as MC3T3-E1 and the cell layer easily broke apart by handling (Fig. 1B). CACO-2, a human colorectal epithelial cell line showed very poor cell adhesion on Mg alloy staples on Day 1

and only small part of staples had been covered by Day 7 (Fig. 1C). RAW264, a murine monocyte cell line showed fair cell adhesion on Day 1 and propagated rapidly until Day 3 to form a thick cell layer, but the cell layer began to disintegrate on Day 7. Mg alloy staples with RAW264 seemed to have become fragile and some staples already began to break.

# Corrosion and biological performance of biodegradable magnesium alloys mediated by low copper addition and processing

X D Yan<sup>1,2</sup>, P Wan<sup>2</sup>, L L Tan<sup>2</sup>, M C Zhao<sup>1</sup>, L Qin<sup>3</sup>, K Yang<sup>2</sup>

<sup>1</sup> School of Materials Science and Engineering, Central South University, China. <sup>2</sup> Institute of Metal Research, Chinese Academy of Sciences, China, <sup>3</sup> Department of Orthopaedics and Traumatology, The Chinese University of Hong Kong, Hong Kong SAR, China

INTRODUCTION: The increasing demand for biomaterials with antibacterial property has raised widespread concerns. Magnesium alloys were considered as promising orthopedic implants with of resorption potential in vivo biocompatibility. Additionally, the degradation of magnesium resulted in antibacterial effects which appear to be an alkaline pH. Mg-Cu alloys were designed introducing the well-known by antibacterial property of copper into magnesium alloy to solve the infection problem especially under the neutralized environment in vivo<sub>2</sub>. In this paper the Mg-Cu alloys with gradient composition and further processed by solution and extrusion were studied to optimize the corrosion-related performance for their future application.

**METHODS:** The as-cast Mg-xCu (x = 0.1, 0.2, 0.3 wt.%) alloys were prepared by adding pure copper powders (99.9%) in pure magnesium (99.99%) and smelted in a high purity graphite crucible with the protecting gas mixture of SF<sub>6</sub> (1 vol.%) and CO<sub>2</sub> (balance). The extrusion temperature was 390 °C, the rate was 1.2 m/min and the ratio was 64:1. The as-cast and as-extruded samples were then subjected to the solid solution

treatment at 510  $^{\circ}\text{C}\,$  for 10h and finally cooled in room temperature.

**RESULTS:** Studies on the microstructure have revealed that the alloys retain the original second phases Mg<sub>2</sub>Cu found in the cast condition. However, the second phases can be relieved by solid solution treatment with low Cu contents, and the grain size has significantly been reduced due to the occurrence of extensive recrystallization in the extrusion process. The corrosion behavior is influenced mainly by the second phases present in the alloys. The corrosion resistance of the Mg-Cu alloys has been improved after solution treatment compared with those in the cast, extruded and with

solutionized conditions. The mechanical properties and corrosion behaviors of Mg-Cu alloys could be adjusted by controlling the Cu content and the processing, so Mg-Cu alloys can accommodate specific requirements as biodegradable material. The Mg-0.1Cu alloy did not induce toxicity to rBMSCs cells, and possessed strong antibacterial capability to S. aureus. After solid solution treatment, Mg-0.1Cu alloy with optimal biogood corrosion rate. biocompatibility and antibacterial ability showed promise for biofunctional orthopedic implants.

**DISCUSSION & CONCLUSIONS:** It is shown that the differences in the property profile of Mg-Cu alloys are dependent on different compositions as well as on different microstructures that are obtained by the different processing routes. Galvanic corrosion can be significantly relieved by solution treatment and combination with extrusion due to decrease of cathodic Mg2Cu phases and well distribution for Mg-0.1Cu alloy. Negligible cytotoxicity and sound biocompatibility were observed with rBMSCs incubation. Antibacterial assays proved that the alloys reduced the viability of Staphylococcus aureus by high alkalinity and copper ions releasing, especially in comparison with pure magnesium. In conclusion, the assolutionized Mg-0.1Cu alloy showed the optimal corrosion properties and promising antibacterial activity, which warranted its potentials antibacterial biodegradable implant materials.

ACKNOWLEDGEMENTS: This work was financially supported by National Natural Science Foundation of China (No. 31500777, No. 51631009 and No. 81501859), National High Technology Research and Development Program of China (863 Program, No. 2015AA033701), Hong Kong Scholar Program and CAS-Croucher Founding Scheme for Joint Laboratories (Ref. CAS14303).

## Effect of magnesium on the crosstalk between human umbilical cord perivascular cells and monocytes

Qian Wang, Regine Willumeit-Römer, Bérengère Luthringer

Helmholtz-Zentrum Geesthacht Centre for Materials and Coastal Research Institute of Materials Research, Division of Metallic Biomaterials,

Max-Planck-Street 1, 21502 Geesthacht, Germany

INTRODUCTION: Human mesenchymal stem cells (hMSCs) interact with a wide range of immune cells and processes like macrophages polarisation. Biomaterials has been indicated to influence such interactions during fracture healing. Human umbilical cord perivascular cells (HUCPV) has been reported as a prolific source of mesenchymal stem cells. We hypothesised that the cross-talk between HUCPV and the immune system may be specifically impacted by Magnesium-based biomaterials. In order to elucidate the mode of action we developed and applied an indirect co-culture model.

**METHODS:** HUCPV were isolated from human umbilical cords and cultured in Eagle's minimum essential medium, alpha modification (α-MEM; Life Technologies GmbH, Karlsruhe, Germany) supplemented with 15% foetal bovine serum for human mesenchymal stem cells (hMSC-FBS; Biological Industries, Israel) and 1% penicillinstreptomycin (P/S, Gibco, USA). Monocytes were isolated via the CD14 marker by Pluribead system (pluriBead®, Germany) from peripheral blood mononuclear cells (PBMC), which were isolated from fresh whole blood by Ficoll Paque 400 (Ge Healthcare, USA). Pure Mg discs (52 mm thick, 165 mm in diameter) were cleaned and sterilised, then incubated in α-MEM with 10% plasma (obtained from blood) and 1% P/S (culture medium) for 24 hours. For the coculture, CD14+ Monocyte and HUCPV were respectively seeded on incubated Mg discs on upper chambers and lower wells of transwell microtiter plates in culture medium. The proliferation was monitored by Live/Dead Staining (Invitrogen, Thermo Fisher Scientific, USA). The RNA was isolated with QIAshredder and RNeasy Mini kit and cDNA was synthesized by Omniscript RT Kit (QIAGEN, Germany). Then quantification reverse transcription polymerase chain reaction (qRT-PCR) was performed.

**RESULTS:** Live/dead staining revealed that more vital HUCPV at day 7 in both treatments. CD14+ monocyte (in co-culture) survived on Mg discs at day 1 and 4, however appeared almost dead at day Osteoblastic related genes, like morphogenetic protein 6 (BMP6), Osteoprotegerin (OPG) and matrix metalloproteinase (MMP13) were upregulated from day 1 to 7 in both groups. At the same time points, this gene expression was lower in co-culture than in the control group at day 1 and 4. However, at day 7 the expression level of osteoblastic genes of HUCPV were almost the same in both groups. Besides, The expression of the transient receptor potential melastatin 6 (TRPM6) was apparently up-regulated in co-culture from day 1 to 7.

**DISCUSSION & CONCLUSIONS:** Cultivation on Mg-discs may alter the CD14+ monocytes viability in co-culture, more than HUCPV cells. Immune cells like macrophages should be the first biomaterials-induced responder modulation, usually for 5 to 7 days. Our results indicate that CD14+ monocytes may have a negative effect on the gene expression of osteogenesis marker at the early stage and Mg may be involved because of TRPM6 upregulation. To ensure the role of Mg, we will investigate genes expression of indicator proteins and cytokines of HUCPV and CD14+ monocytes, and the polarization of CD14+ monocytes.

#### In vitro study on degradation and biocompatibility of Zn-HA composites

H.T. Yang<sup>1</sup>, Y.F. Zheng<sup>1,\*</sup>

<sup>1</sup> Department of Materials Science and Engineering, College of Engineering, Peking University, No.5 Yi-He-Yuan Road, Hai-Dian District, Beijing 100871, China

**INTRODUCTION:** Zn, as an essential element with osteogenic potential of human body, is regarded and studied as a new kind of biodegradable metal recently. Through alloying with Mg, Ca and Sr, Zn alloys show promotion effects on the formation of new bone (Li *et al.*, 2015). In this study, Zn-HA composites were fabricated by using spark plasma sintering. Their degradation property and biocompatibility to MC3T3-E1 cells were investigated.

**METHODS:** Pure zinc powders hydroxyapatite (HA) powders were used as raw materials to fabricate Zn-XHA (X=1, 5 and 10 wt.%) composites via a SPS-1050 system. The degradation properties were characterized by immersion test and electrochemical measurement. Immersion tests were carried out in Hank's solution at 37°C. The electrochemical tests were conducted with a three-electrode cell in an electrochemical working station temperature in Hank's solution. The cytotoxicity test was carried out by culturing MC3T3-E1 cells in the extracts of samples for 1, 2 and 4 days.

**RESULTS:** Degradation properties of Zn-HA composites were shown in Fig. 1. The corrosion potentials of Zn- HA composites shifted to more negative ones compared to that of pure Zn. In addition, the corrosion current density increased with increasing contents of HA. The current plateaus emerged in the anodic part of curves indicated the formation of a passive film. In addition, according to the degradation rates calculated from weight loss, addition of HA accelerated the corrosion rates of Zn in Hank's solution as well. The cell cytotoxicity of Zn-HA composites was performed in Fig. 2. An obvious toxicity was observed in the extract of pure zinc group. However, the addition of HA showed a significant promotion in the cell viability at all

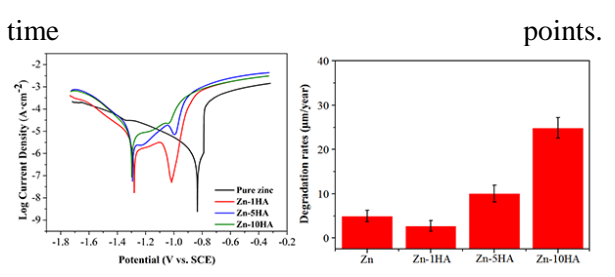


Fig. 1: Polarization curves and degradation rates of pure Zn and Zn-HA composites.

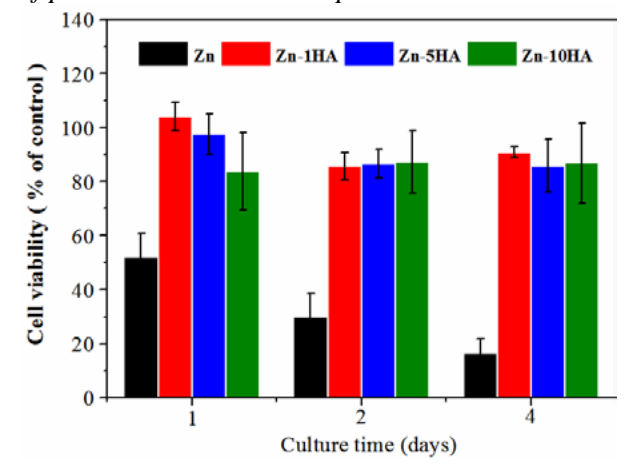


Fig. 1: Viability of MC3T3-E1 cells after culturing in abstracts of samples for 1,2 and 4 days

**DISCUSSION & CONCLUSIONS:** The increased degradation rates of Zn-HA composites can be derived from the increased contact surface areas with solution after adding HA. In contrast to pure Zn, Zn-HA composites show an increased degradation rates and improved biocompatibility.

#### **ACKNOWLEDGEMENTS:**

This work was supported by National Key Research and Development Program of China (Grant No. 2016YFC1102400 and 2016YFC1102402) and National Natural Science Foundation of China (Grant No. 51431002).

## Effects of bovine serum albumin (BSA) and fetal bovine serum (FBS) on Mg degradation under cell culture conditions

RQ Hou<sup>1</sup>, F Feyerabend<sup>1</sup>, R Willumeit-Römer<sup>1</sup>

<sup>1</sup> <u>Helmholtz-Zentrum Geesthacht</u>, Institute of Material Research, Max-Planck-Str. 1, 21502 Geesthacht, Germany

**INTRODUCTION:** Bovine serum (BSA) or fetal bovine serum (FBS) are usually added to cell culture media to study the effects of proteins on Mg degradation. However, the composition of FBS is very complex, which leads to the different degradation performance of Mg in media with BSA and with FBS. For example, N.T. Kirkland et al. reported that FBS decreased the degradation rate of MgCa alloys in minimum essential medium (MEM), while J. Walker et al. (2012) reported that BSA promoted the mass loss of Mg0.8Ca alloy in MEM. Therefore, the aim of this study is to investigate the difference between the influence of BSA and FBS on Mg degradation under cell culture conditions.

**METHODS:** The immersion tests were performed for pure Mg (99.94%) at a ratio of 0.2 g/mL (sample/medium) in Hank's balance salt solution (HBSS) and Dulbecco's modified eagle medium Glutamax-I (DMEM) with or without 3.4 mg/mL BSA or 10% FBS under cell culture conditions (37 °C, 5% CO<sub>2</sub>, 20% O<sub>2</sub>, 95% rel. humidity). The degradation rate (*DR*) in μm/year was calculated by mass loss as following:

$$DR = 8.76 \times 10^4 \, \Delta m / (A \, \rho \, t) \tag{1}$$

where A is the surface area (cm<sup>2</sup>),  $\rho$  is the density of pure Mg (g/cm<sup>3</sup>), t is immersion time (hour),  $\Delta m$  is the mass loss (gram). The degradation products were characterized by SEM, EDS and XRD.

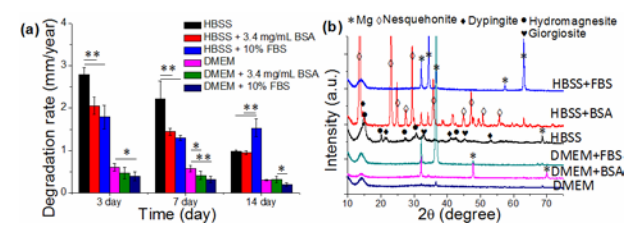


Fig. 1 (a) Degradation rates of pure Mg and (b) XRD patterns for degradation products formed in different media after different immersion time.

**RESULTS:** The presence of FBS resulted in lower degradation rate than BSA for Mg degradation during 7 days of immersion (Fig. 1a). However, after 14 days of immersion the degradation rate of Mg in HBSS+FBS was higher than in HBSS, while it still kept the lowest value

in DMEM. Moreover, the formation of precipitates in HBSS was largely affected by BSA and FBS (Fig. 1b and 2). More important, the addition of BSA/FBS significantly promotes the formation of Mg/Ca-PO<sub>4</sub> on Mg surface.

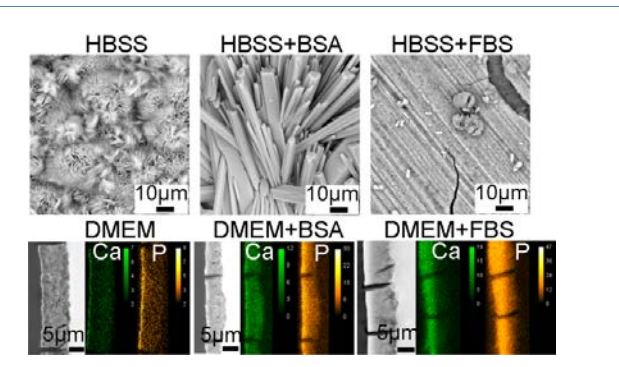


Fig. 2 Degradation products and the distributions of P and Ca in degradation layers formed in different immersion media after 3 days' immersion

**DISCUSSION & CONCLUSIONS: BSA and** present different influence on degradation in HBSS and DMEM. Generally, FBS is more protective than BSA for Mg degradation during the initial exposure. However, after a relatively long immersion time, the effects of other components in FBS or the interaction between organic molecules should be taken into consideration. Moreover, BSA and FBS also show obviously different impacts on the formation of precipitates in HBSS, while both of them promotes the formation of Ca-P salts on Mg surface in DMEM, suggesting the addition of proteins to test media is necessary and the effects of proteins on Mg degradation should be studied under more physiological conditions to get a comparable results to in vivo experiments.

**ACKNOWLEDGEMENTS:** This work was supported by the Helmholtz Virtual Institute "In vivo studies of biodegradable magnesium based implant materials (MetBioMat)" (grant number: VH-VI-523). The first author received the financial support from China Scholarship Council (CSC).

# Novel bio-functional magnesium coating on porous Ti6Al4V orthopaedic implants: *in vitro* and *in vivo* studies

K Yang<sup>1</sup>, X K Li<sup>2</sup>, , P Gao<sup>2</sup>

<sup>1</sup> Institute of Metal Research, Chinese Academy of Science, Shenyang 110016, China <sup>2</sup> Department of Orthopaedics, Xijing Hospital, Fourth Military Medical University, Xi'an, China

**INTRODUCTION:** The lack of osteo-conduction and integration into the bone for long-term survival often occurs and leads to titanium alloy implant failure. Studies on magnesium-based metals have found that magnesium could influence bone tissue growth positively, improving the bone healing and reconstruction. Thus, biodegradable magnesium employed as a coating is possible to be appropriate for medical implants, which is expected to promote the osteo-integration after implantation.

**METHODS:** In this study, pure magnesium (Mg) was fabricated as coating instead of substrate for the first time. The bio-functional Mg coating was fabricated by arc ion plating technique, which was proved with fine grain size and high film/substrate adhesion in comparison with other PVD methods. Microstructure, morphology and composition of the Mg coating were investigated by means of SEM, EDS and XRD. In vitro degradation and ions releasing were measured after immersion in simulated body fluids. Furthermore. cytocompatibility and animal implantation tests were performed to evaluate the related cell attachment, viability, bone response and vessel growth in vivo.

**RESULTS:** The surface composition and were characterized by morphology diffraction and SEM equipped with energy dispersive spectroscopy. Furthermore, the in vitro study of cytotoxicity and proliferation of MC3T3-E1 cells showed that the Mg coated porous Ti6Al4V alloy had suitable degradation rate and good biocompatibility. Moreover, the in vivo studies including fluorescent labelling, microcomputed tomography analysis scan and Van-Gieson staining of histological sections indicated that the Mg coated porous Ti6Al4V implant could significantly promote bone regeneration in rabbit femoral condylar defects after implantation for 4 and 8 weeks, and had better osteogenesis and osteo-integration than the bare porous Ti6Al4V implant. There are more new vessels observed around the Mg coated porous Ti6Al4V implant compared with the bare porous Ti6Al4V implant.

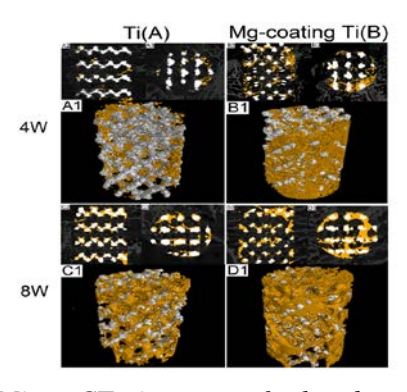


Fig.1 Micro-CT images of the bare porous Ti6Al4V (group A) and Mg coated porous Ti6Al4V (group B) at 4 weeks and 8 weeks after implantation.

DISCUSSION & CONCLUSIONS: In this study, bioactive Mg coating was successfully fabricated on porous Ti6Al4V alloy, which was proved with fine grain size and high film/substrate adhesion. Furthermore, the *in vitro* study showed that the Mg coated porous Ti6Al4V had suitable corrosion rate and good biocompatibility. Moreover, *in vivo* studies indicated that the Mg coated porous Ti6Al4V implant had better osteogenesis, osteo-integration properties and more new vessels formation than the bare porous Ti6Al4V implant. It is expected that this bioactive Mg coating on porous Ti6Al4V scaffolds with improved osteo-integration and osteogenesis functions can serve as an alternative for orthopedic applications.

**ACKNOWLEDGEMENTS:** This template was modified with kind permission from eCM Journal.

# Response of bone cells and bone tissues towards magnesium-implants monitored at the proteome level

Hartmut Schlüter<sup>1</sup>, Maryam Omidi<sup>1</sup>, Marcus Wurlitzer<sup>1</sup>, Berengere Luthringer<sup>2</sup>, Regine Willumeit<sup>2</sup> Eric Hesse<sup>3</sup>

<sup>1</sup> <u>Mass Spectrometric Proteomics,</u> Department of Clinical Chemistry & Laboratory Medicine, University Medical Center Hamburg-Eppendorf, Hamburg, Germany, <sup>2</sup> <u>Centre for Materials and</u> <u>Coastal Research, Helmholtz-Zentrum Geesthacht</u>, <sup>3</sup> Department of Trauma, Hand and Reconstructive Surgery, University Medical Center Hamburg-Eppendorf

**INTRODUCTION:** Biodegradable implants for bone healing are giving the advantage of disappearing during the regeneration process of the bone tissue thereby circumventing a second surgery for removing the implant. Magnesium (Mg) implants are belonging to biodegradable implants because they are degraded in the body by corrosion. During the corrosion process of Mgimplants hydrogen, hydroxyl-ions and Mg<sup>2+</sup> - ions and further alloy metal ions are generated, which may have an impact on the surrounding bone tissue and on the healing process. Thus, it was the aim of our study to investigate the response of bone cells from cell culture and bone tissue in mice to Mgimplants on the molecular level via proteomics.

METHODS: Protein extracts from diverse cultured bone cells (osteoblast) and bone tissue sections from mice in the absence (control) the presence of steel implants or titanium implants (control) and Mg-implants and their corrosion products were analyzed by differential proteomics using label-free quantification. Protein extracts were digested with trypsin and resulting tryptic peptides subjected to liquid chromatography (reversed-phase-nano-UPLC-column) coupled to a spectrometer (Orbitrap-Fusion, mass Thermo Fisher scientific). Data processing and data analysis for relative quantification of proteins was performed with MaxQuant. Statistical analysis and interpretation was performed with PERSEUS.

**RESULTS:** In each of the differential proteomic experiments several thousand proteins were identified. Many of the proteins, which were regulated in response to Mg-implants, are bonecell specific proteins including up-regulated extracellular proteins. Furthermore the levels of proteins belonging to the functional group of energy metabolism were increase whereas levels of proteins associated with apoptosis were decreased.

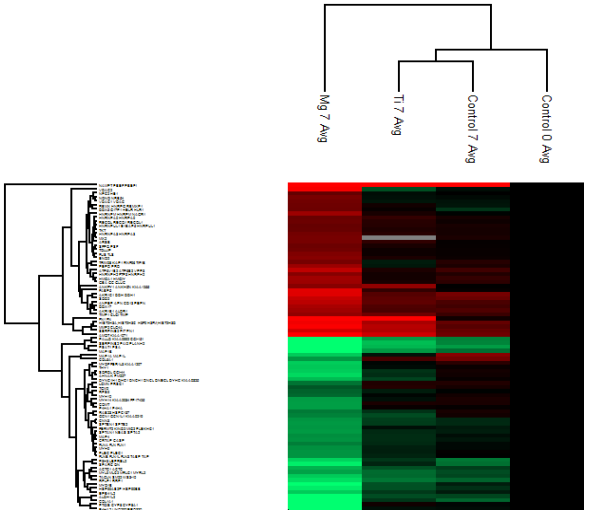


Fig. 1: Typical heat-map & hierarchical clustering of up (red)- and down-(green)-regulated proteins (FDR= 0.01; S0= 0.1, min. fold-change of 2) in cultured osteoblasts after 7 days of incubation with Mg-implant materials compared to control.

**DISCUSSION & CONCLUSIONS:** The results of this study correlate well with the findings about changes of the phenotypes in response to Mgimplants observed and described by Jähn et al. showing that "bone histomorphometry revealed a significant increase in callus size due to an augmented bone formation rate and a reduced bone resorption in fractures supported by Mg2Ag nails, thereby improving bone healing".

**ACKNOWLEDGEMENTS:** Financial support by the Helmholtz Virtual Institute MetBioMat is gratefully acknowledged.

## Bioresorbable rare—earth-free magnesium screws used for osteosynthesis in a sheep model

J Eichler <sup>1</sup>, P Holweg<sup>2</sup>, L Berger<sup>3</sup>, M Cihova<sup>3</sup>, N Grün<sup>1</sup>, N Donohue<sup>1</sup>, JF Löffler<sup>3</sup>, A Weinberg<sup>1</sup>.

<sup>1</sup>Department of Orthopaedics and Traumatology, Medical University Graz, Graz, AT. <sup>2</sup>Department of Trauma Surgery, Medical University Graz, Graz, AT. <sup>3</sup>Laboratory of Metal Physics and Technology, Department of Materials, ETH Zurich, Zurich, CH.

#### INTRODUCTION

Osteosynthesis of small and medium size bone fragments represents the gold standard indication for a treatment with surgical screws. Corresponding fragments are fixated with screws made of stainless steel or titanium (Ti). However, complications such as loosening, inflammatory reactions and discomfort may necessitate a secondary operation for screw removal. Biodegradable magnesium (Mg) offers adequate mechanical properties close to human bone, renders a removal intervention unnecessary and may also support the healing process. Rapid degradation rates of Mg alloys have represented a substantial challenge in recent years. In previous work, addition of rare-earth (RE) elements to Mg alloys successfully retarded the degradation rate. Nevertheless, the reaction of the human body to RE elements and their long-term effect after degradation remain unclear.

A first RE-free Mg-Zn-Ca alloy with 5 wt.% Zn (ZX50) degraded rapidly and produced high amounts of hydrogen gas [2]. Another Mg-Zn-Ca-poor alloy with a decreased Zn content of only 1 wt.%, ZX10, showed promising characteristics and hydrogen gas production in [3]. This study aimed to evaluate fracture healing under presence of the degrading implant. Furthermore, degradation, gas evolution and bone-implant interface reaction to the employed Zn-poor Mg-Zn-Ca (ZX00) screws in an *in vivo* sheep model were investigated.

METHODS: RE-free Mg screws with a diameter of 3.5 mm and a length of 29 mm and 26 mm were manufactured from the alloy ZX00 (Mg-0.45Zn-0.45Ca) and machined with a custom-made diamond thread cutting tool to ensure a smooth and impurity-free surface condition. All implants were cleaned with ethanol, packaged and gamma sterilized. Under general anesthesia, an incision was made medial from the trochanter of the right proximal tibiae of n=5 female lambs. Tissue was carefully mobilized to avoid any harm. A wedge osteotomy was performed with an oscillating saw and stabilized with one transcortical 26 mm screw and one retrograde 29 mm screw crossing the epiphyseal plate. Before insertion bicortical drilling and thread tapping was performed and 6 further 26 mm screws were implanted along the tibia, in order to evaluate degradation behavior and bone incorporation. Control animals (n=4) were treated with Ti screws at the same sites with and without wedge osteotomy. After insertion of the screws, the wounds were closed in layers. All surgical interventions were performed under sterile clinical conditions. All animal trials were accredited by the Austrian Ministry of Science, Research and Economy, accreditation number

BMWFW-66.010/0073-WF/V/3b/2015. The *in vivo* fracture healing and degradation behavior was evaluated

by clinical CT imaging (Siemens Somatom Force) at 2, 6 and 12 weeks after implantation. Control and experimental group animals were euthanized at 6 and 12 weeks. Tibiae were harvested for micro-CT evaluation (Siemens Inveon micro CT). Implant volume and surface as well as gas volume were quantified with Materialise MIMICS, ver. 17.

**RESULTS:** The wedge osteotomy was properly stabilized using the ZX00 screws, no dislocation of the fragment was detected at any time. Initial callus formation was observed after 2 weeks. After 6 weeks the callus was stable and after 12 weeks progressed callus resorption was noticed on radiological observations. No qualitative differences were found in comparison to the conventional Ti implant. After week 12, all 29 mm Mg implants crossing the physis were broken, which was not the case for the Ti control group. Consequentially, differences in bone lengths were observed between the Ti and the Mg groups. Slow and homogenous degradation could be observed for all ZX00 screws and the production of hydrogen gas was considered as moderate. ZX00 screws exhibited a tight and stable bone-implant interface, as well as increased periosteal bone incorporation, especially in the region of the screw heads.

DISCUSSION AND CONCLUSION: stabilization and healing properties were comparable to gold standard Ti osteosynthesis in the present study. Within 12 weeks of application, the use of the biodegradable screw within the physis led to implant breakage which may have been caused by the growth process of the tibia. However, tibiae treated with the Ti screws were shorter than tibiae within the Mg group. For transepiphyseal application, the Mg implants may therefore be beneficial for a growing skeleton. The increased bone mass found at the very tight boneimplant interface may lead to elevated mechanical stability for the Mg screws, which will be evaluated by mechanical testing in further experiments. The homogenous degradation and moderate hydrogen formation of the material did not cause any harm to the surrounding tissue or disturb the healing process.

#### Do magnesium implants support osteogenesis in osteoporotic bone?

NG Grün<sup>1</sup>, D Hirzberger<sup>1</sup>, J Eichler<sup>1</sup>, N Donohue<sup>1</sup> and AM Weinberg<sup>1</sup>

<sup>1</sup> Department of Orthopaedics and Traumatology, Medical University of Graz, Austria

**INTRODUCTION:** The World Health Organization predicts a doubling of the number of people aged over 60 and a tripling of those older than 80 by 2050. The strong increase in age and the associated chance to suffer not only from one but from multiple fractures present a new challenge to orthopaedic surgeons. Conventional alloys currently used in the treatment of fractures include titanium (Ti) and stainless steel, which are more rigid, but cause so-called "stress-shielding" by reducing loading-induced bone remodeling that leads to bone loss and increased risk of periimplant fractures. Under osteoporotic conditions, each individual fracture requires its own stabilization, which limits the space and, therefore, the option of incorporating any further material is available. Due not to biodegradability, biocompatibility and mechanical properties, magnesium (Mg)-based alloys may induce and support appropriate osteoporotic fracture healing.

**METHODS:** Twelve-month old Spraque Dawley rats underwent bilateral ovariectomy to induce osteoporosis or sham-operation to serve as healthy controls. Micro-computed tomography ( $\mu$ CT) was performed 2, 4, 8 and 12 weeks after ovariectomy to observe osteoporosis progression. Twelve weeks after ovariectomy, Mg-based pins (consisting of Mg, calcium and zinc) were transcortically implanted into the metaphyseal area of proximal tibiae and compared to sham operated controls.  $\mu$ CT analysis was performed 2 weeks after Mg implantation and will be further assessed 6, 9 and 12 weeks post-implantation.

**RESULTS:** To evaluate, whether Mg-based implants will induce and support adequate osteogenesis in osteoporotic bone, ovariectomy-induced osteoporotic rats were transcortically implanted with Mg-based pins.

Two weeks after implantation into proximal tibiae, hydrogen gas formation indicated degradation of Mg implants (Fig. 1).

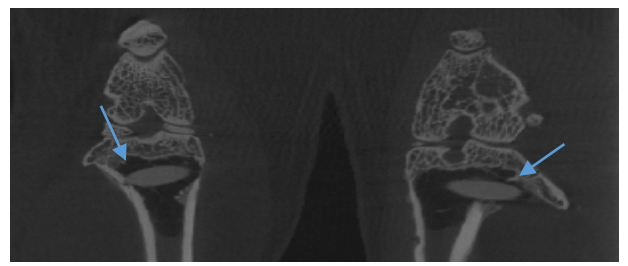


Fig. 1: Mg-implant degradation two weeks after implantation in osteoporotic tibiae of rats. Blue arrows indicate Mg-implants; black the implant indicate hydrogen gas evolution

**DISCUSSION & CONCLUSIONS:** The strong increase in age of the population is closely linked with increasing prevalence and incidence of osteoporosis-associated bone fractures. Osteosynthesis with more rigid materials including Ti and stainless steel provides the state-of-the-art technique. Several disadvantages are associated with Ti and stainless steel implants, including bone loss and peri-implant fractures. The FDA has already described possible metallic sensitivity or allergic reactions linked to Ti-based alloys. Mgbased implants are biodegradable, biocompatible and Mg has already demonstrated its active role in osteoblastogenesis. Here, we demonstrated biodegradability of the Mg-based pins in osteoporotic rats 2 weeks after implantation. Further µCT analysis after 6, 9 and 12 weeks will be performed to demonstrate appropriate bone ingrowth and decreased hydrogen gas formation.

**ACKNOWLEDGEMENTS:** This template was modified with kind permission from eCM Journal.

### Magnesium materials inhibit tumor, a myth or a chance?

Yigang Chen<sup>1</sup>, Shaoxiang Zhang<sup>2</sup>

<sup>1</sup> Wuxi Second Hospital, Nanjing Medical University, Jiangsu <sup>2</sup> School of Materials Science and Engineering, Shanghai Jiao Tong University, Shanghai

**INTRODUCTION:** Magnesium is considered to be a biologically active metal. Studies have shown that magnesium can promote tissue healing and anti-inflammatory. At present, it has become another research hotspot whether the magnesium material has the anti-tumor effect. In the background of the increasing complexity of cancer treatment, does magnesium provide a new therapeutic approach, or does it make the problem more complicated?

METHODS: In the in vitro experiments, extraction was prepared by high pure magnesium (HP Mg) rods (99.99 wt.% Mg). The human osteosarcoma cells (MG-63), human colonic adenocarcinoma cells (LS174T), human neuroblastoma cells (NBL-WS and SH-SY5Y), and human lung cancer cell line (MSTO-211H and Calu-3) were cultured in the high pure magnesium extraction. The CCK-8 method was performed, and the cell relative growth rate (RGR) was calculated.

In the in vivo experiments, the HP Mg wire (diameter 0.3 mm and length 2 cm) is wound into a circle shape (Fig.1A). Subcutaneous tumor xenograft models were performed to evaluate the in vivo function of HP Mg wires. The tumor cells above were injected subcutaneously into the left flank of a nude mouse, respectively. Two weeks after subcutaneous tumor formed, all animals were sacrificed and tumor tissue was moved. The tumor tissue was cut into numerous equal parts (each volume is 3 mm<sub>3</sub>) (Fig.1A), and together with a Ti wire or a HP Mg wire implanted subcutaneously into the left flank of 4-week-old female BALB/c nude mice (n = 5) (Fig.1B). Three weeks after implantation, tumor weight was measured and proliferating cell nuclear antigen (PCNA) was performed.

**RESULTS:** The extract of HP Mg has inhibitory effect on both above tumor cells when the concentration of magnesium ion was larger than 120 mmol. At 24 h, the decline trend of RGR is the

most obvious in the LS174T cells group than that of other cancer cells. In the in vivo experiments, tissue necrosis, which direct contact with HP Mg wire

occurred at the surface of all tumor tissues (Fig 1C). However, only the weight of colonic tumor significantly changed, no significant differences were found in other tumors. The weights of colonic tumor were  $0.52\pm0.11g$  and  $1.63\pm0.32g$  in the HP Mg wire and Ti wire group at 3 weeks postoperation, respectively (P=0.005). The expression levels of PCNA significantly decreased in the HP Mg wire group than those in the Ti group.

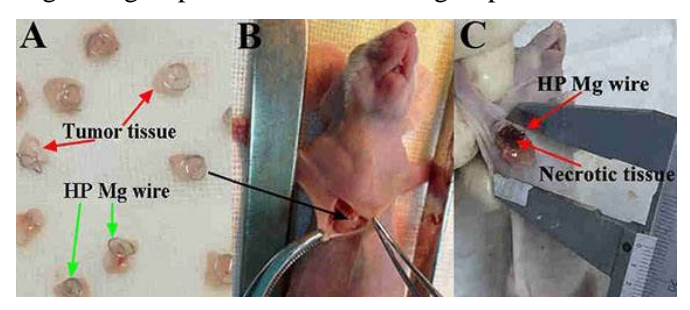


Fig. 1: The magnesium wire was covered on the surface of the tumor, and then implanted subcutaneously in nude mice. (A)The magnesium wire and tumor tissues.(B) An incision in the left flank that is used to place the tumor. At 3 weeks post-operation, the colonic tumor in the Ti group (C).

DISCUSSION & CONCLUSIONS: In the in vitro environment, extracts with a concentration larger than 120 mmol can inhibit the growth of tumor cells. In the in vivo environment, the sensitivity of tumor tissues, which from different cancer cells, to HP Mg is different. HP Mg can induce tumor necrosis of contact surface, and inhibit the growth of colon cancer cells. Therefore, we suggest that magnesium has different sensitivity to different tumors. Mg materials may provide a new therapeutic idea for sensitive cancers.

**ACKNOWLEDGEMENTS:** We thank Changli Zhao and Jiahua Li for advice regarding in vitro studies.

### The effect of Ti on biodegradation behaviour of Mg in vitro and in vivo

W.H. Wang<sup>1</sup>, Peng Hou<sup>2</sup>, H.L.Wu<sup>1</sup>, Pei Han<sup>2</sup>, S.X. Zhang<sup>3</sup>, J.H.Ni<sup>1</sup>, Yimin Chai<sup>2</sup>, X.N. Zhang<sup>1,3</sup>

<sup>1</sup> School of Materials Science and Engineering, Shanghai Jiao Tong University

<sup>2</sup>Orthopaedic Department, Shanghai Jiao Tong University Affiliated Sixth People's Hospital <sup>3</sup>Suzhou Origin Medical Technology Co., Ltd.

**INTRODUCTION:** Magnesium has a low potential, and is prone to produce galvanic corrosion. In the present study, the corrosion behaviour which produced by co-implement with titanium was investigated in high purity magnesium (HP Mg) in vitro and in vivo.

METHODS: The HP Mg and Ti disc samples with a diameter of 7.5 mm and a thickness of 1 mm were used for the immersion experiments in PBS solution at 37 °C in 3 days, and they fixed at a distance of 5 and 10 mm. Surface morphology was analyzed by scanning electron microscopy (SEM, JEOL 7600) In the in vivo experiments, the HP Mg and Ti screws with an outer diameter of 2.0 mm, inner diameter of 1.6 mm, screw pitch of 0.6 mm and a length of 10.0 mm were prepared. They were co-implanted into Sprague-Dawley rat' femur, spacing 5 and 10 mm in 8 weeks. Micro CT scan and 3D reconstruction were used to observe the corrosion morphology of HP Mg screws.

**RESULTS:** Fig.1 shows the effect of Ti on the corrosion behaviour, including hydrogen evolution and corrosion topography of HP Mg in vitro experiment. Form the data of H<sub>2</sub> gas volume, it seem that the existence of Ti in medium system may slightly accelerate the corrosion of Mg. Moreover, from the SEM results, various corrosion pits in Mg nearby Ti can be observed.

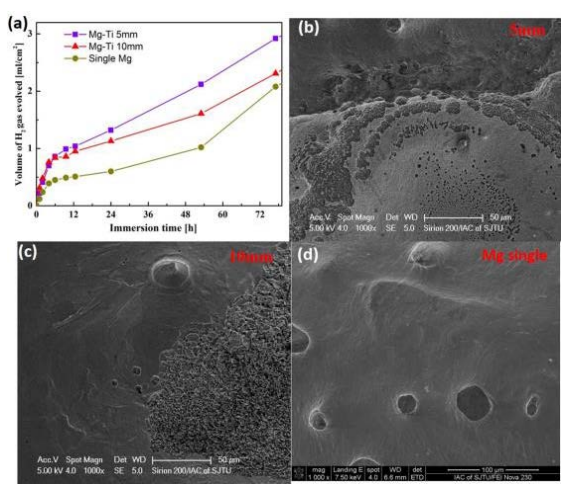


Fig. 1: Hydrogen evolution volumes and SEM morphologies of HP Mg disc.

Fig.2 shows the corrosion behaviour of HP Mg affected by Ti after 8 weeks in vivo experiment. However, the serious corrosion behaviour can be found in HP Mg screws close to Ti with 5mm when compared to the groups with a longer distance and without Ti existence. The results confirmed hastening corrosion of HP Mg screws when they were co-implanted with Ti screws. Besides, the HP Mg screws in different region of bone tissue were with marked difference discrepancy in corrosion. For magnesium, the corrosion potential is sensitive with the surrounding medium. The galvanic corrosion may also happen by itself, since the two parts of Mg are at different solutions environment.

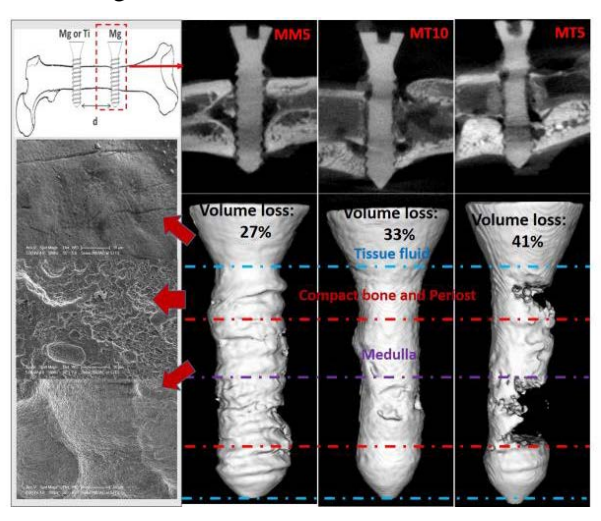


Fig.2 CT, SEM image and 3D reconstruction of HP Mg screw in different distance with Ti.

DISCUSSION & CONCLUSIONS: The mechanism of galvanic corrosion in Mg co-implanted with Ti under same environment is the different potential in them and will increase the corrosion rate of Mg, and in Mg self with different solutions is different corrosion potential but may cause non-uniform corrosion instead of changing corrosion rate. Therefore, a certain distance is critical to maintain the mechanical and biological property of Mg when it is co-implanted with Ti.

**ACKNOWLEDGEMENTS:** This work was supported by the Natural Science Foundation of China (NO. 51571142 and No. 51271117).

#### The effect of biodegradable metals degradation on the foreign body response

S Krummsdorf <sup>1,2</sup>, A Schreiber <sup>1,2</sup>, C Beutler <sup>1,2</sup>, T Schmidt <sup>1,2</sup>, F Witte <sup>1,2</sup>

<sup>1</sup> Julius Wolff Institute, Charité- Universitätsmedizin Berlin, <sup>2</sup> Berlin Brandenburg Center for Regenerative Therapies (BCRT), Charité- Universitätsmedizin Berlin

INTRODUCTION: Due to their degradation properties, magnesium alloys play a significant role in the growing field of biomaterials. Being a natural component of the body, the involvement of magnesium in various biochemical processes reflects the promising potential as a suitable implant material. In this study, the local inflammatory response to biodegradable implants was characterized using a newly established FACS immune cell panel which allows for quantitative single cell analysis. To verify the correlation of degradation and cellular response the corrosion rate was determined for each explanted material.

**METHODS:** Round shaped implants (8mm) made of MgGd10%, MgGd5% and pure magnesium with 150 ppm Fe (MgFe) were implanted intramuscular (i.m.) and subcutaneously (s.c.) in the back of 108 female Lewis rats, all 12 weeks old. After 1, 3, 7, 14, 21 or 28 days animals were sacrificed (each material n=6) and the capsules formed around the implants were prepared. Tissue was digested with collagenase buffer (1h, 37°C). Samples were stained for CD45, CD3, CD4, CD8, HIS48, CD68 and CD163 following the instructions of the manufacturer. FACS analysis was performed on MACS-Quant. Values are presented as percentage (%) of living CD45+ cells (all leukocytes). The corrosion rate (CR) was calculated via the weight loss method as below:

$$CR = \frac{8,76*10000*\Delta GV}{A*t*\rho}.$$

Statistics: two-way ANOVA,  $p \le 0.05$ .

#### **RESULTS:**

Regardless of the location, a direct relationship between the corrosion rate and the number of living leukocytes could be determined. If the corrosion rate is high, the number of living leukocytes in the capsule increases around the implant. A characteristic progression of the foreign body response to magnesium implants was observed according to an initial peak of granulocytes at day 1 and subsequent regression. M1-macrophages (CD68+CD163-) increases from day 7 to day 28. M2-macrophages

(CD68+CD163+) increases from day 1 till day 7 and decreases slowly afterwards.

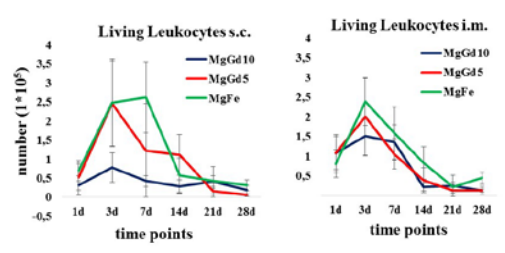


Fig. 3: Means of Living Leukocytes with standard deviation s.c. and i.m. in the capsule

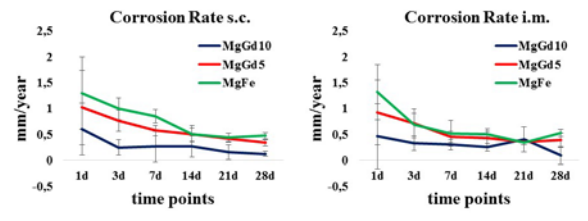


Fig. 4: Means of the Corrosion Rate with standard deviation s.c. and i.m. in mm/year

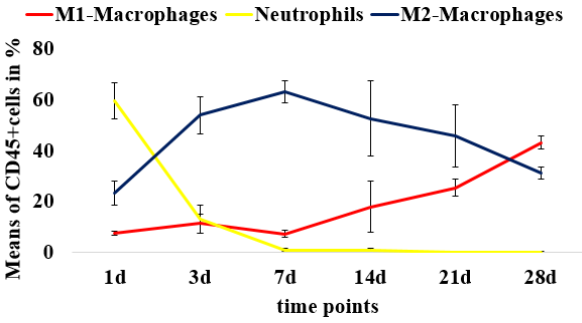


Fig. 5: Means of CD45+cells in % with standard deviation of neutrophils and macrophages in i.m. capsule of MgGd5 depending on time points.

**DISCUSSION & CONCLUSIONS:** The established FACS panel is a good tool to quantify the inflammatory response to implants in rats. Our results show a comparable moderate local foreign body response to the implants with more leucocytes accompanying faster corrosion. We saw an early immigration of granulocytes to the implant site followed by an appearance of M2 at day 3 followed by a slow M1-immigration, indicating an early anti-inflammatory effect.

#### **ACKNOWLEDGEMENTS:**

Dr. Désirée Kunkel, FACS Core Unit BCRT